

**FIELD INVESTIGATION AND FINITE ELEMENT
ANALYSIS OF SOIL CEMENT COLUMNS IN
FOUNDATION AND EXCAVATION APPLICATIONS
IN SOFT BANGKOK CLAY**

Chayanon Srijaroen



**A Thesis Submitted in Partial Fulfillment of the Requirements for the
Degree of Doctor of Philosophy in Civil Engineering
Suranaree University of Technology**

Academic Year 2020

การศึกษาในสนามและการวิเคราะห์ทางไฟฟ้าในต์เอ็ดิเมนต์ของการประกยุคต์ใช้
เสาเข็มดินซีเมนต์ในงานฐานรากและงานขุดในพื้นที่ดินเหนียวอ่อนกรุงเทพฯ




วิทยานิพนธ์นี้เป็นส่วนหนึ่งของการศึกษาตามหลักสูตรปริญญาวิศวกรรมศาสตรดุษฎีบัณฑิต
สาขาวิชาวิศวกรรมโยธา
มหาวิทยาลัยเทคโนโลยีสุรนารี
ปีการศึกษา 2563

**FIELD INVESTIGATION AND FINITE ELEMENT ANALYSIS OF
SOIL CEMENT COLUMNS IN FOUNDATION AND
EXCAVATION APPLICATIONS IN SOFT BANGKOK CLAY**


Suranaree University of Technology has approved this thesis submitted in partial fulfillment of the requirements for the Degree of Doctor of Philosophy.

Thesis Examining Committee



(Prof. Dr. Panich Voottripruex)

Chairperson



(Prof. Dr. Suksun Horpibulsuk)

Member (Thesis Advisor)




(Assoc. Prof. Dr. Chatchai Jothityangkoon)

Member



(Prof. Dr. Avirut Chinkulkijniwat)

Member



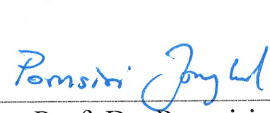
(Asst. Prof. Dr. Runglawan Rachan)

Member

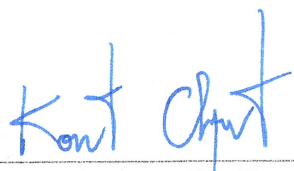


(Dr. Menglim Hoy)

Member



(Assoc. Prof. Dr. Pomsiri Jongkol)



(Assoc. Prof. Ft. Lt. Dr. Kontorn Chamniprasart)

Vice Rector for Academic Affairs
and Internationalization

Dean of Institute of Engineering

ชยานนท์ ศรีเจริญ : การศึกษาในสนามและการวิเคราะห์ทางไฟไนต์เอลิเมนต์ของ
การประยุกต์ใช้เสาเข็มดินซีเมนต์ในงานฐานรากและงานขุดในพื้นที่ดินเหนียวอ่อน
กรุงเทพฯ (FIELD INVESTIGATION AND FINITE ELEMENT ANALYSIS OF SOIL
CEMENT COLUMNS IN FOUNDATION AND EXCAVATION APPLICATIONS IN SOFT
BANGKOK CLAY) อาจารย์ที่ปรึกษา : ศาสตราจารย์ ดร.สุขสันต์ หอพิบูลสุข, 162 หน้า.

วิทยานิพนธ์นี้ประกอบด้วยห้าบทหลัก บทแรกอธิบายความเป็นมาของปัญหาในการวิจัย
บทที่ สองเป็นการศึกษางานวิจัยในอดีต 2 เรื่อง คือการประยุกต์ใช้เสาเข็มดินซีเมนต์ร่วมกับเสาเข็ม
เหล็กเพื่อเป็นเสาเข็มรับน้ำหนักอาคารขนาดเล็กถึงปานกลางในพื้นที่ดินเหนียวอ่อนกรุงเทพ และการ
ประยุกต์ใช้เสาเข็มดินซีเมนต์เป็นกำแพงกันดินชั่วคราวในงานขุดลึกระดับปานกลาง บทที่สาม
ศึกษากำลัสน้ำหนักบรรทุกของเสาเข็ม 4 รูปแบบ รูปแบบที่ 1 เป็นเสาเข็มดินซีเมนต์เส้นผ่าน
ศูนย์กลาง 60 เซนติเมตร ยาว 17.00 เมตร, รูปแบบที่ 2 เป็นเสาเข็มเหล็กขนาดเส้นผ่านศูนย์กลาง
20 เซนติเมตร ยาว 17.00 เชื่อมติดเป็นเกลียวเส้นผ่านศูนย์กลาง 40 เซนติเมตรหนา 5 มิลลิเมตร
ระยะห่าง 1.50 เมตร, รูปแบบที่ 3 เป็นเสาเข็มดินซีเมนต์เส้นผ่านศูนย์กลาง 60 เซนติเมตร ยาว 13.00
เมตร โดยมีเสาเข็มเหล็กเหมือนรูปแบบที่สองยาว 17.00 เมตร ฝังอยู่ตรงกลาง และรูปแบบที่ 4 คล้าย
รูปแบบที่สาม แต่เสาเข็มดินซีเมนต์ยาว 17.00 เมตร ผลการศึกษาพบว่าเสาเข็มเหล็ก (รูปแบบที่ 2)
มีค่าการก่อสร้าง (ราคาต่อกำลัสน้ำหนัก) ที่แพงที่สุด เสาเข็มเหล็กดินซีเมนต์ (รูปแบบที่ 4)
มีค่าการก่อสร้างถูกที่สุดและใกล้เคียงกับเสาเข็มเจาะ ขณะที่เสาเข็มเหล็กดินซีเมนต์รูปแบบที่ 3 มี
ค่าการก่อสร้างปานกลาง เมื่อพิจารณาในเรื่องเวลาของการก่อสร้างพบว่าเสาเข็มเหล็ก รูปแบบที่ 2
และ 3 ใช้เวลาในการก่อสร้างที่รวดเร็วกว่าเสาเข็มเหล็กดินซีเมนต์รูปแบบที่ 4 และเสาเข็มเจาะใช้
เวลานานที่สุด บทที่สี่ศึกษาในโครงการก่อสร้างจริงด้วยระบบกำแพงกันดินซีเมนต์ป้องกันดินพังใน
งานขุดวางบ่อบำบัดน้ำเสียใต้ดิน 2 รูปแบบ, รูปแบบที่ 1 เป็นเสาเข็มดินซีเมนต์เส้นผ่านศูนย์กลาง
60 เซนติเมตร ยาว 12.00 เมตร เรียงติดกัน 3 แถว และรูปแบบที่ 2 เป็นเสาเข็มดินซีเมนต์ขนาดและ
ความยาวเท่ากัน เรียงติดกัน 1 แถว มีเสาเข็มเหล็กยาว 9.00 เมตร ฝังอยู่ตรงกลางทุกต้น ผลการ
ตรวจวัดพฤติกรรมในสนามถูกนำมาสอบเทียบความถูกต้องของแบบจำลองทางไฟไนต์เอลิเมนต์โดย
โปรแกรม Plaxis 2D แบบจำลองที่ได้รับการสอบเทียบแล้วถูกนำไปจำลองพฤติกรรมของเสาเข็ม
อีก 3 รูปแบบ คือ รูปแบบที่ 3 เป็นเสาเข็มดินซีเมนต์ 2 แถว รูปแบบที่ 4 เป็นเสาเข็มดินซีเมนต์เรียง
ติดกัน 1 แถว มีเสาเข็มเหล็กยาว 9.00 เมตร ฝังอยู่ตรงกลางต้นเว้นต้น พร้อมระบบค้ำยัน และ
รูปแบบที่ 5 เป็นระบบเข็มพีคเหล็กยาว 12 เมตร พร้อมระบบค้ำยัน ความลึกของเสาเข็มดินซีเมนต์
ถูกแปรผันจาก 5.00-13.00 เมตร ผลการวิเคราะห์พบว่าระบบเข็มพีคเหล็กพร้อมระบบค้ำยันเหมาะ
สำหรับพื้นที่ที่เครื่องจักรสามารถขนย้ายเข้าหน่วยงานได้สะดวก เนื่องจากมีราคาต่ำก่อสร้างที่ต่ำ

และมีอัตราส่วนปลอดภัยที่สูง ในขณะที่ ระบบกำแพงเสาเข็มดินซีเมนต์ จำนวน 2 แถว ที่ความลึกของกำแพง 7.0 เมตร หรือลึกประมาณ 1.5 เท่าของความลึกของการขุดที่ 4.5 เมตร เหมาะสมทั้งพื้นที่ที่สะดวกและพื้นที่ที่ค่อนข้างจำกัด เนื่องจากมีราคาค่าก่อสร้างที่ต่ำและมีอัตราส่วนปลอดภัยที่สูง เมื่อพิจารณาที่เกณฑ์อัตราส่วนความปลอดภัยตามเกณฑ์ของกรมโยธาธิการและผังเมืองที่กำหนดอัตราส่วนความปลอดภัยต่ำสุดที่ 1.30 และบทที่ 5 แสดงบทสรุปและประโยชน์ที่ได้รับจากการศึกษาวิจัยในครั้งนี้



สาขาวิชา วิศวกรรมโยธา

ปีการศึกษา 2563

ลายมือชื่อนักศึกษา

ลายมือชื่ออาจารย์ที่ปรึกษา

CHAYANON SRIJAROEN : FIELD INVESTIGATION AND FINITE
ELEMENT ANALYSIS OF SOIL CEMENT COLUMNS IN FOUNDATION AND
EXCAVATION APPLICATIONS IN SOFT BANGKOK CLAY . THESIS
ADVISOR : PROF. SUKSUN HORPIBULSUK, Ph.D., 162 PP.

SOIL CEMENT COLUMN/SCREW PILE, PILE FOUNDATION/SOIL CEMENT
RETAINING WALL/GROUND IMPROVEMENT/SOFT BANGKOK CLAY

This thesis consists of five main chapters. Chapter 1 is introduction, describing the statement of the problems. Chapter 2 reviewed 2 topics related to this research: the application of soil-cement columns (SCCs) combined with screw pile to be a foundation of low to medium rise buildings in soft Bangkok clay and the application of SCCs as retaining wall for moderate deep excavation. The load capacity of four different types of pile was investigated and presented in Chapter 3. All piles were installed at a fixed depth of 17.0 m. Pile no 1 was a SCC with a diameter of 0.6 m (without screw pile) and Pile no 2 was SP. Pile no 3 and 4 were partial SCSP and full SCSP, respectively where the SP was installed in the SCC. A partial SCSP is a combination of SP (17.0 m length) and SCC with a diameter of 0.6 m and a length of 13 m from the ground surface. A full SCSP comprises SP (17.0 m length) and the SCC with a diameter of 0.6 m and a length of 17.0 m. The unit cost of the SP was found to be the highest, and the unit cost of the SCSP and bored pile was found to be the lowest and almost similar. As a result, the application of the full SCSP and bored pile is more economical than the partial SCSP and SP under the same ultimate load design. However, the partial SCSP and SP have more advantages in term of

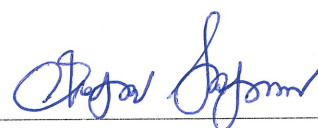
construction time and are suitable for a time-constrained project. The SCSP has higher efficiency, productivity, and competitiveness than the traditional dry-process bored pile. The SCC application as a retaining wall in the real project was investigated and presented in Chapter 4. Two types of soil cement column wall were studied, namely soil cement column (SCC) wall and stiffened soil cement column (SSCC) wall. SCC wall consisted of 3 rows of SCC with 0.60 m diameter and 12.00 m length, the SSCC consisted of a pipe (0.2 m in diameter and 9.0 m length), which embedded in the middle of SCC 1 row. The calibration of finite element model was first carried out by comparing the simulation result with the field measurement data. The parametric studies including types of retaining structures, length of pile (L), row number of SCC, and bracing system were then performed to investigate the advantages and disadvantages of the studied walls for short-term condition with $FS > 1.3$. The low construction cost of sheet pile wall had advantage over other types of wall only for the project in an accessible construction site with the standard length of pile ($L = 12$ m). SCC and SSCC Walls can be effectively designed to maximize stability and economic performance by varying the studied parameters, which had more advantages than conventional sheet pile system. SCC-2Row Wall at 7 m where $L = 1.5$ times longer than excavation depth (4.5 m) was found to be the most effective wall in term of time and cost at the same $FS > 1.3$ criterion (minimum requirement specified by local authorities) among the studied walls in both accessible and confined construction sites. Chapter 5 concluded the outcome of this research such as method of design, optimization of time and cost of construction.

School of Civil Engineering

Academic Year 2020

Student's Signature

Advisor's Signature



ACKNOWLEDGEMENTS

The author would like to express his deepest sincere and gratitude to Professor Dr. Suksun Horpibulsuk for his guidance valuable advices, endless kindness, encouragement and enthusiasm throughout my studies. He always advice and support every time that the author consult him. It has been a very pleasure to work under guidance of him, who has a great consultant, leadership character and philosophical through.

The author would like to sincerely thank Professor Dr. Avirut Chinkulkijniwat and Assistant Professor Dr. Pornpot Tangseng, School of Civil Engineering, Suranaree University of Technology, for influential lectures, enlightening the Geomechanics and Advance Foundation Engineering teach students with kindness.

The author would like to sincerely thank Associate Professor Dr. Chatchai Jothityangkoon, School of Civil Engineering, Suranaree University of Technology, Professor Dr. Panich Voottopruex, King Mongkut's University Of Technology North Bangkok and Assistant Professor Dr. Rungrawan Rachan, Mahanakorn University Of Technology who are the exam committee for the many advice in research with kindness.

I wish to thank all the staff and faculty members of the School of Civil Engineering, Suranaree University of Technology, for the academic, administrative and technical support during my study.

I acknowledge Dr. Hoy meng Lim for his discussion, encouragement and advice in this research. Dr. Teerasak Yaowarat, and Mr. Arthit Udomchai for their discussions and encouragement. I would like to thank Suranaree University of Technology for facilities, equipment and financial support. I also would like to acknowledge Thai piling rig company limited (TPR) and TPR staff, especially Mr. Surasak Sahasakmontri, the president who support and empower for this study.

Finally, I would like to appreciate my family for their love and kind support on my graduate studies.

Chayanon Srijaroen

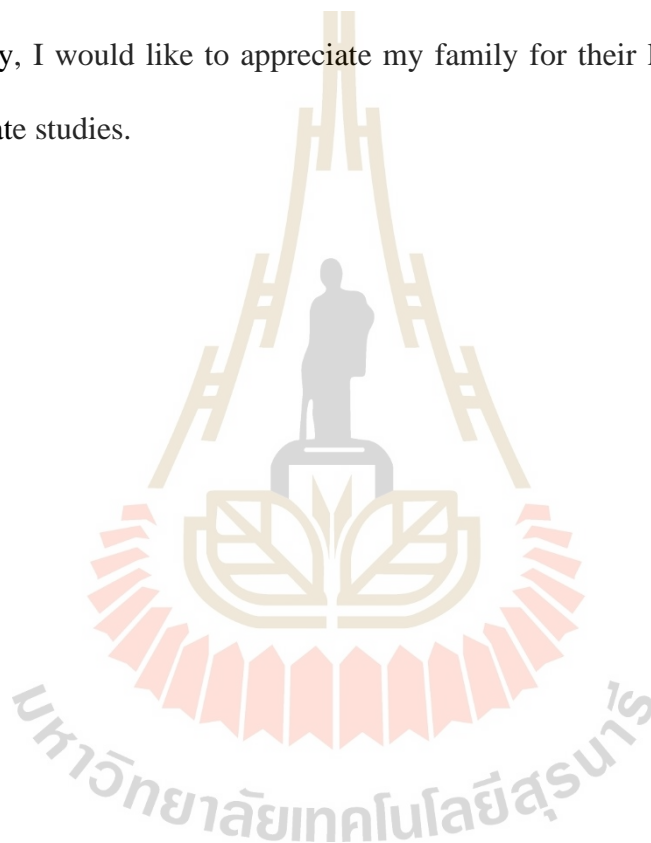


TABLE OF CONTENTS

	Page
ABSTRACT (THAI)	I
ABSTRACT (ENGLISH).....	III
ACKNOWLEDGEMENTS	V
TABLE OF CONTENTS.....	VII
LIST OF TABLES	XII
LIST OF FIGURES	XIII
SYMBOLS AND ABBREVIATIONS.....	XVIII
CHAPTER	
I INTRODUCTION	1
1.1 Statement of the problem	1
1.1.1 Deep cement mixing background.....	1
1.1.2 Screw pile background	2
1.1.3 Excavation in soft Bangkok clay.....	4
1.2 Objectives of the study.....	4
1.3 Organization of the dissertation.....	5
1.4 References	6
II LITERATURE REVIEW	9
2.1 Introduction	9

TABLE OF CONTENTS (Continued)

	Page
2.2	The ultimate bearing capacity of pile by..... 10
	load settlement curve 12
2.2.1	Davission (1972) Mothod 10
2.2.2	Chin (1970) Mothod..... 11
2.2.3	Derbeer (1967) Mothod 13
2.2.4	Standard 90 percent of Brinch Hansen (1963) Method 13
2.2.5	Standard 80 percent of Brinch Hansen (1963) Method 14
2.2.6	Mazurkiewicz (1972) Method..... 15
2.2.7	Fuller & Hoy (1970) Method..... 16
2.2.8	Vander Veen (1953) Method..... 18
2.3	The study of ultimate bearing capacity of pile in the past 18
2.3.1	Screw pile failure models 18
2.3.2	Cylindrical shear method.....21
2.3.3	Individual bearing method..... 23
2.4	Deep cement mixing (DCM) pile 39
2.4.1	Installation of deep cement mixing technique 39
	2.4.1.1 Wet mixing low pressure method..... 39
	2.4.1.2 Jet grouting method 39

TABLE OF CONTENTS (Continued)

	Page
2.4.1.3 Dry Mixing method	40
2.5 Ultimate bearing capacity of deep cement mixing (DCM) pile	40
2.6 Application of DCM pile.....	41
2.6.1 DCM for foundation work	41
2.6.2 DCM for excavation work	49
2.7 References	60
III SOIL-CEMENT SCREW PILE: ALTERNATIVE PILE FOR LOW- AND MEDIUM-RISE BUILDINGS IN SOFT BANGKOK CLAY	65
3.1 Introduction	65
3.2 Methodology.....	69
3.2.1 Detail of studied piles	69
3.2.2 Determination of ultimate bearing capacity.....	73
3.3 Results	81
3.4 Ultimate load, time and cost analysis	87
3.4.1 Screw pile	88
3.4.2 Soil cement screw pile.....	89
3.5 Conclusion.....	97
3.6 References	99

TABLE OF CONTENTS (Continued)

	Page
IV APPLICATION OF SOIL CEMENT COLUMN AS A TEMPORARY RETAINING WALL FOR EXCAVATION IN SOFT BANGKOK CLAY	104
4.1 Introduction.....	104
4.2 Field case study.....	107
4.2.1 Project description.....	107
4.2.2 Soil and SCC properties	111
4.2.3 Finite element analysis	113
4.3 Parametric study	117
4.4 Finite element analysis results.....	120
4.5 Result of parametric study.....	122
4.6 Advantages and disadvantages of the studied walls	130
4.6.1 For an accessible construction site.....	130
4.6.2 For a confined construction site.....	131
4.6.3 Summary and Recommendation	132
4.7 Conclusion.....	133
4.8 References	134
V CONCLUSION	140
5.1 Conclusion.....	140
5.2 Recommendation	142
APPENDIX A.....	143

TABLE OF CONTENTS (Continued)

	Page
APPENDIX B.	147
BIOGRAPHY	162



LIST OF TABLES

Table	Page
2.1	Summary of pile installation 29
2.2	Summary of axial compression test results 29
2.3	Summary of axial tension (uplift) test results..... 29
2.4	Comparison of Measured and Calculated Ultimate Pile Resistances 36
2.5	Rank of degree of influence on maximum lateral movement 60
3.1	Summary of ultimate bearing capacity of all types of studied piles 87
3.2	Cost and time analysis of SP and SCSP execution..... 95
4.1	Soil parameters for finite element analysis 115
4.2	Parameter of steel pipe and sheet pile (Plate) for finite element analysis..... 116
4.3	Parameter of strut (Anchor) for finite element analysis..... 119

LIST OF FIGURES

Figure	Page
2.1	The ultimate bearing capacity by Davission (1972) method..... 11
2.2	The ultimate bearing capacity by Chin (1970) method 12
2.3	The ultimate bearing capacity by De Beer (1967) method 13
2.4	The ultimate bearing capacity by 90% of Brinch Hansen (1963) method 14
2.5	The ultimate bearing capacity by 80% of Brinch Hansen (1963) method 15
2.6	The ultimate bearing capacity by Mazurkiewicz (1972) method 16
2.7	The ultimate bearing capacity by Fuller & Hoy and Butler & Hoy (1970) method 17
2.8	The ultimate bearing capacity by Vander Veen (1953) method..... 18
2.9	Helical Pile Failure Models: (a) Individual Plate Bearing Model under compression, and (b) uplift (after Mooney et al. 1985); (c) Cylindrical Shear Model under compression, and (d) uplift (after Narasimha Rao et al. 1991)..... 21
2.10	Ratio of predicted to measured ultimate axial screw pile capacities 24
2.11	Schematic of a typical pile lead section 25
2.12	Typical helical pile installation..... 26
2.13	Typical axial compression test setup 28
2.14	Load test results 31
2.15	The model of screw pile..... 33

LIST OF FIGURES (Continued)

Figure	Page
2.16 The geometry of screw pile	37
2.17 Different types of screw piles that were used in this study	38
2.18 Schematic for Bangna-Bangpakong Highway using DCM	42
2.19 Mixing energy and number of wing rotation relationship of the columns.....	43
2.20 Suggested procedure of wet mixing method for soft Bangkok clay	44
2.21 Plan view of test embankment on DCM and SDCM pile (a); Crossection of test embankment on DCM and SDCM pile (b).....	45
2.22 Schematic diagram of SDCM pile (a); details of prestress concrete core piles (dimensions in m.).....	46
2.23 The curve of axial load plotted against settlement from field tests	46
2.24 Axial and lateral pile load test simulation model	47
2.25 Comparisons between observed and simulated axial compression load –settlement curves for DCM-C1 and DCM-C2	48
2.26 Comparisons between observed and simulated axial compression load – settlement curves for SDCM	48
2.27 Load Settlement curve of DCM pile and SDCM pile	49
2.28 Lateral movement of DCM pile and SDCM pile.....	50
2.29 Layout of soil protection system and mat footing	51
2.30 Typical cross section of SCW type 2.....	51
2.31 Performance of SCW after excavate to final depth	52

LIST OF FIGURES (Continued)

Figure	Page
2.32 Canal and roadway cross-section with DCM column configuration. (a) Initial DCM column configuration, (b) Remedial DCM column configuration	53
2.33 Five patterns of soil cement wall	55
2.34 Relationship between excavation depth to effective thickness ratio and horizontal displacement	55
2.35 Horizontal lateral movement of soil cement wall at excavation depth of 5.0 m	56
2.36 Layout of compound DCM wall: (a) plan view, (b) section view	57
2.37 Effects of stabilized mat, nonexistence of front DCM wall, and DCM column pattern	58
2.38 Effect of modulus of elasticity of DCM column	59
2.39 Effect of thickness of soft clay	59
3.1 A schematic of screw piles	70
3.2 Types of studied piles: a) SCC, b) SP, c) Partial SCSP and d) Full SCSP	71
3.3 The soil profile at the construction site, Nongchok District, Thailand	72
3.4 The installation process of SP and SCSP	73
3.5 Static load test apparatus	76
3.6 Cylindrical shear model for screw pile under compression load	79
3.7 Individual bearing model for screw pile under compressive load	80

LIST OF FIGURES (Continued)

Figure	Page
3.8 A relationship between the depth of SCC and its unconfined compressive strength.....	82
3.9 Load-settlement curve of SCC (Pile no 1)	83
3.10 Load-settlement curve of SP (Pile no 2)	84
3.11 Load-settlement curve of a partially SCSP (Pile no 3)	85
3.12 Load-settlement curve of a fully SCSP (Pile no 4).....	86
3.13 A relationship between ultimate load and length of screw pile.....	89
3.14 Relationships between length of screw pile versus ultimate load of SCSP at various lengths of SCC.....	91
3.15 Relationships between SCC friction versus unconfined compressive strength of SCC	93
3.16 Relationships between cost versus ultimate load of SP and SCSP.....	94
4.1 (a) Site geometry, and types of retaining wall that construction: (b) SCC-3Row Wall and (c) SSCC-1Row Wall.....	110
4.2 Construction sequence.	111
4.3 The soil profile at the construction site, Bangkok-Noi District, Thailand....	112
4.4 A relationship between depth and undrained shear strength of SCC.....	113
4.5 FE mesh used for the back-analysis soil stiffness: a) SCC-3Row Wall and b) SSCC-1Row Wall	116

LIST OF FIGURES (Continued)

Figure	Page
4.6	Layout and section of retaining wall: a) SCC-2Row, b) SSCC-1Row with bracing, and c) sheet pile 118
4.7	FE mesh: a) SCC-2Row wall, b) SSCC-1Row Wall with bracing, and c) Sheet pile wall 120
4.8	Soil movement a) SCC-3Row Wall and b) SSCC-1Row Wall 121
4.9	Correlation between maximum lateral movement and factor of safety of various walls..... 123
4.10	The relationship between factor of safety and lateral movement varied with lengths of piles..... 125
4.11	The relationship between factor of safety and cost of construction varied with lengths of piles..... 127
4.12	The relationship between time and cost of construction varied with lengths of piles..... 128

SYMBOLS AND ABBREVIATIONS

DCM	=	Deep Cement Mixing Piles
W/C	=	Water to cement ratio
PR	=	Penetration Rate
WR	=	Withdrawal Rate
SDCM	=	Stiffened Deep Cement Mixing Piles
S_u	=	Undrain Shear Strength
Q_{ult}	=	Ultimate Bearing Capacity
α	=	Adhesion factor between pile and soil
A_s	=	Area around the pile
N_c	=	Endbearing factor in clay
A_b	=	Aea at the end of pile
K	=	Lateral earth pressure factor
σ'_{vs}	=	Vertical effective stress along pile
δ'	=	Friction angle
N_q	=	Endbearing factor in sand
P	=	Load value
Δ	=	Movement value
C_1	=	Constant value
C_2	=	Constant value
P_{ult}	=	Ultimate load
$Q_{ult,soil}$	=	Bearing capacity of single column at soil failure

SYMBOLS AND ABBREVIATIONS (Continued)

$Q_{ult,column}$	=	Bearing capacity of single column at column failure
WRN	=	Wing Rotation Number
E_m	=	Mixing energy
W/C	=	Clay-water to cement ratio
SP	=	Screw pile
SCSP	=	Soil cement screw pile
FEM	=	Finite element method
C'	=	Effective shear strength parameter
Φ'	=	Effective friction angle parameter
E'	=	Effective young modulus parameter
γ_{dry}	=	Dry density
γ_{wet}	=	Wet density
ν'	=	Poisson's Ratio
Q_{helix}	=	shearing resistance along the cylindrical failure surface
$Q_{bearing}$	=	end bearing capacity
Q_{shaft}	=	resistance developed along the steel shaft
S_f	=	spacing ratio factor
D	=	diameter of pile helix
L_c	=	distance between top and bottom helical plates
A_H	=	area of the helix
c_u	=	undrained shear strength of soil
d	=	diameter of pile shaft

SYMBOLS AND ABBREVIATIONS (Continued)

H_{eff}	=	effective length of pile above top helix
A_{col}	=	The cross sectional area of the column
q_{uf}	=	The field strength of the column.
SCW	=	Soil cement column wall
SSCC	=	Stiffened soil cement column
H/T _{eff}	=	Excavation depth to effective thickness ratio
λ^*	=	Modified compression index
K^*	=	Modified swelling index
δ_{max}	=	Lateral movement of wall

CHAPTER I

INTRODUCTION

1.1 Statement of the problem

1.1.1 Deep cement mixing background

Currently, the infrastructure development in urban area such as shopping center, low and medium rise buildings is increasing. Due to the limitation of property area, the deep cement mixing (DCM) technique can be applied for the pile foundation and the retaining wall of the infrastructure. In the deep mixing process, the ground is mixed in place while a binder is injected with the help of a mixing tool. After hardening, soil mix elements with improved mechanical and hydraulic characteristics are realized. DCM was first developed in Japan where first field tests began in 1970. Originally granular quicklime was used as a binder to stabilize the underlying soil, but soon better results were obtained using cement slurry and cement mortar. Until the end of the 1980s, DCM was used only in Japan and Scandinavia. Since then, it has gained popularity also in the United States and Europe. The DCM in Thailand has been investigated by many researchers, the factors controlling in-situ strength of soil cement columns have been investigated via a full-scale test (Horpibulsuk et al., 2000). The laboratory investigation on the strength development in cement admixed clay at various conditions of cement content and water content was presented by Miura et al. (2001) and Horpibulsuk and Miura (2001). Horpibulsuk et al. (2001) have proposed interrelationship among water content, cement content,

curing time and strength of cement admixed clays. Based on the proposed relationship, the strength of the cement admixed clays can be predicted by a single trial test. The application of deep mixing technique to reduce settlement of an embankment in Thailand was successfully done by Bergado et al. (1999). Moreover, the application of using DCM in earth work have been investigated by many researchers (Petchgate et al., 2003a, Jamsawang et al., 2008, Horpibulsuk et al., 2011, Horpibulsuk et al., 2012, Jamsawang et al., 2011, Vootipruex et al., 2011a, Jamsawang et al., 2015, Tanseng et al., 2015).

1.1.2 Screw pile background

Screw pile or Helical piles, also known as screw anchors or screw piles, is deep foundation elements comprised of one or more circular helical plates affixed to a central shaft of smaller diameter. The shaft of the helical pile is frequently manufactured from standard sizes of hollow steel pipe, typically ranging from about 114 mm to 320 mm in diameter; helical piles fabricated from hollow circular shafts are typically fitted with steel helical plates having a diameter of 2 to 3 times of the shaft diameter. Helical piles are embedded into the ground by applying a turning moment to the head of the pile shaft, which causes the helix or helices to penetrate the soil in a screwing motion, without producing any spoil. Installation of helical piles can be accomplished using relatively light weight equipment, such as a torque head affixed to the arm of a backhoe or to a trailer-mounted hydraulic boom.

Screw piles can be also referred to as steel screw-in foundations, screw piers, helical piles, helical anchors, screw anchors, screw foundations and helical piers. Screw foundations first appeared in the 1800s as pile foundations for lighthouses and were extensively used for piers in harbors. Between the 1850s

through 1890s, more than 100 light houses were erected on the east coast of the United States using screw piles. Made originally from cast or wrought iron, they had limited bearing and tension capacities. Modern screw pile load capacities are in excess of 2,000 kN (220 tons-force). Large load capacity screw piles may have various components such as flat half helices, cutting tips and helices, cap plates or re-bar interfaces for connection to various concrete or steel structures. More recently, composite technology has been developed and patented for use in small screw piles. Composites offer significant advantages over steel in small screw pile manufacture and installed performance.

Screw pile design is based on standard structural and geotechnical principles. Screw pile designers typically use their own design software, which has been developed through field testing of differing compression pile and tension anchor configurations in various soil profiles. Corrosion is addressed based on extended field trials, combined with worldwide databases on steel in ground corrosion. Screw pile foundations are still used extensively, and their usage has extended from lighthouses to rail, telecommunications, roads, and numerous other industries where fast installation is required, or building work takes place close to existing structures. Most industries use screw pile foundations due to the cost efficiencies and increasingly the reduced environmental impact. 'Screwing' the foundations in the ground means that there is less soil displacement so excess soil does not need to be transported from the site, saving on transportation costs and reducing the carbon footprint of the project. The main benefits of screw pile foundations include: shorter project times, ease of installation, ease of access, reduction of the carbon footprint, ease of removal when the foundations are no longer required, reduced risk to the workforce, and reduced

costs. They are also suitable for both tensile and compression loads, so they are also used for masts, signs, and retaining structures.

1.1.3 Excavation in soft Bangkok clay

For the excavation work with 3-5 m depth in soft Bangkok clay, the retaining structure and supporting system must be stable enough to prevent large soil movement which may cause damage to the neighboring structure. For the wide and convenience of construction site to transportation of materials into the site, the standard 12-m long steel sheet pile with bracing system is commonly used due to easy installation and cost-effectiveness. On the other hand, in narrow of construction site that is unable to transport and install the steel sheet pile, the DCM is an alternative. The advantage of DCM is easy and quick installation by a small machine, low noise and vibration during installation.

In this study, the DCM application for foundation of low and medium rise building and for retaining wall in soft Bangkok clay is investigated.

1.2 Objectives of the study

1.2.1 To study the ultimate capacity of SCC, SP, and SCSP.

1.2.2 To study and compare the cost and time of construction of SCC, SP, SCSP and bored pile.

1.2.3 To suggest a stepwise procedure for designing the ultimate bearing capacity of SCSP at optimal time and cost.

1.2.4 To study the time cost and stability of of SCC wall, SSCC wall without bracing, SSCC wall with bracing and sheet pile system as a temporary retaining wall.

1.2.5 To suggest a stepwise for design and construction the SCC wall, SSCC wall and sheet pile at optimal time and cost of construction.

1.3 Organization of the dissertation

This thesis consists of five chapters and outlines of each chapter are presented as follows:

Chapter I presents the introduction part, describing the statement of the problems, the objectives of the study and the organization of the dissertation.

Chapter II presents the literature review of screw pile (SP) and application of using deep cement mixing (DCM) in foundation and excavation work.

Chapter III presents the ultimate load, time and cost analysis and suggested effective design method for soft Bangkok clay. The cost and time of executing SCSP were also compared with those of traditional dry-process bored pile to illustrate the advantage of SCSP. Four different types of studied all piles were installed at a fixed depth of 17.0 m. Pile no 1 was a SCC with a diameter of 0.6 m (without screw pile) and Pile no 2 was SP. Pile no 3 and 4 were partial SCSP and full SCSP, respectively where the SP was installed in the SCC. A partial SCSP is a combination of SP (17.0 m length) and SCC with a diameter of 0.6 m and a length of 13 m from the ground surface. A full SCSP comprises SP (17.0 m length) and the SCC with a diameter of 0.6 m and a length of 17.0 m. The construction site was located at Nongchok District, Bangkok, Thailand. The SCC (Pile no 1) was installed by the wet mixing method. The cement content of 200 kg/m³ of soil and the water to cement (w/c) ratio of 1.0 were used for SCC execution. The installation (both for penetration and withdrawal) rate is 1.0 m/min. The SP (Pile no 2) was installed to the depth of 17.0 m by the installation

machine. The execution process of the partial SCSP (Pile no 3) and full SCSP (Pile no 4) was similar. First, the SCC with 0.6 m diameter was installed by the wet mixing method of deep mixing machine to the designed depths of 13.0 m and 17.0 m for pile no 3 and pile no 4, respectively. The 17.0 m length of SP was then immediately installed at the center of the SCC for both partial and full SCSP. The hollow steel pile was next filled with concrete.

Chapter IV presents the application of soil cement column as a temporary retaining wall using deep mixing technique for deep excavation in soft Bangkok clay. Due to the limitation of the property line of the construction site, two types of soil cement column wall were studied, namely Soil Cement Column (SCC) wall and Stiffened Soil Cement Column (SSCC) wall. SCC of 0.6 in diameter and 12 m length was used in this study. SSCC was the SCC strengthened with a steel pipe diameter of 0.2 m in the middle. The wall movement and factor of safety of SCC and SSCC walls were calculated by finite element method using Plaxis 2D V.8.2. The construction cost and time and factor of safety of SCC and SSCC walls were compared with the conventional sheet pile wall studied.

Chapter V present conclusion and recommendation.

1.4 References

Bergado, D.T, Anderson, L.R, Miura, N., & Balasubramaniam, A.S. (1996). **“Soft Ground Improvement in Lowland and Other Environment.”** ASCE Press, New York.

- Bergado, D.T, Ruenkairergsa, T., Taesiri, Y., & Balasubramaniam, A.S. (1999). **“Deep soil mixing used to reduce embankment settlement.”** Ground Improvement, 3, 145-162.
- Chen, C.H. (1990), **“Behavior of the improved ground by deep cement mixing method underembankment loading.”** M. Eng. Thesis, AIT, Thailand.
- Horpibulsuk, S., & Miura, N. (2001). **A new approach for studying behavior of cement stabilized clays.** Paper presented at the International Conference on soil mechanics and geotechnical engineering.
- Horpibulsuk, S., Shibuya, S., Fuenkajorn, K., & Katkan, W. (2007). **“Assessment of engineering properties of Bangkok clay.”** Canadian Geotechnical Journal, 44(2), 173-187.
- Horpibulsuk, S., Rachan, R., Suddeepong, A., & Chinkulkijniwat, A. (2011). **“Strength development in cement admixed Bangkok clay: laboratory and field investigations.”** Soil and Foundations, 51(2), 239-251.
- Jamsawang, P., Bergado, D.T., & Voottipruex, P. (2010). **“Field behaviour of stiffened deep cement mixing piles.”** Proceedings of the Institution of Civil Engineers, 164, 33-49.
- Lai, Y.P., Bergado, D. T., Lorenzo, G. A. & Duangchan, T. (2006), **“Full-scale reinforced embankment on deep jet mixing improved ground .”** Ground improvement Journal, 10(4), 153-164.
- Lin, K. Q., & Wong, I. H. (1999), **“Use of deep mixing to reduce settlement at bridge approaches.”** ASCE Journal of geotechnical and Geoenvironmental Engineering, 125(4), 309-320.

- Monkaew, S., & Nawalerspunya, T. (2012). **Productivity of bored piles dry process**, the research in funded by faculty of engineering Rajamangala University of Technology Phra Nakhon.
- Petchgate, K., Jongpradit, P., & Panmanajaroenphol, S. (2003a). **Field pile load test of soil cement column in soft clay**. Proceeding of the International Symposium 2003 on Soil/Ground Improvement and Geosynthetics in Waste Containment and Erosion Control Applications. Asian Institute of Technology, Bangkok, Thailand 175-184.
- Poonlappanish, C., & Buasri, P. (2006). **Capacity of dry-process bored piles in Bangkok**, The 22nd National Convention on Civil Engineering, Thailand.
- Tand, K.E., & Vipulandan, C. (2008). **“Comparison of computed vs measured lateral load/deflection response of ACIP piles.”** PLAXIS Bulletin, 23, 10-13.
- Tanseng, P. (2011). **“Soil-Cement Wall without Bracing for Mat Foundation Construction in Bangkok Sub-Soils.”** the 14th asian regional conference on soil mechanics and geotechnical engineering, Hongkong.
- Voottipruex, P., Bergado, D. T., Suksawat, T., Jamsawang, P., & Cheang, W. (2011). **“Behavior and simulation of deep cement mixing (DCM) and stiffened deep cement mixing (SDCM) piles under full scale loading.”** Soil and foundations., 5(2), 307-320.
- Wonglert, A., Jongpradist, P., Jamsawang, P., & Petchgate, W. (2015). **“Efficiency of using eucalyptus wood to reinforce deep cement mixing piles in field: Pile load and embankment tests.”** KMUTT Research & Development Journal., 38(3), 225-242 (In Thai).

CHAPTER II

LITERATURE REVIEW

2.1 Introduction

Many researchers have studied the ultimate bearing capacity of a single pile either driven pile or bored pile. The empirical equation of ultimate bearing capacity of single pile was suggested. In clay layer, the bearing capacity of a single pile can be calculated using the following relationship.

$$Q_{ult} = \alpha S_u A_s + N_c S_u A_b \quad (2.1)$$

where:

α is the adhesion factor between pile and soil

S_u is the undrained shear strength of soil around pile

A_s is area around the pile

N_c is end bearing factor (can be taken as 9.0)

A_b is section area at end of pile

In sand layer, the bearing capacity of single pile can be calculated using the following relationship.

$$Q_{ult} = K \sigma'_{vs} \tan \delta A_s + N_q \sigma'_{vb} A_b \quad (2.2)$$

where:

K	is	the lateral earth pressure factor
σ'_{vs}	is	vertical effective stress along pile
σ'_{vb}	is	vertical effective stress at the end of pile
δ'	is	friction angle
N_q	is	end bearing factor
A_s	is	area around the pile
A_b	is	section area at end of pile

2.2 The ultimate bearing capacity of pile by load settlement curve

The pile failure due to soil failure is the state of large settlement of pile under little increment of load. In the past, the definition of the ultimate bearing capacity of pile was the load that settlement of pile over 10 percent of end of pile diameter, but this definition did not consider about pile length that the long pile has more compressibility than the short pile. The ultimate bearing capacity of pile was also defined as the intersection between the first curve and final curve, but the obtained value is strongly dependent on interpretation and scale. Therefore many researchers have proposed methods of determining the ultimate bearing capacity of pile.

2.2.1 Davission (1972) Method

Davission's limit value is defined as the load corresponding to the movement which exceeds the elastic compression of the pile by value of 0.15 inch (4mm) plus a factor equal to the diameter of the pile divided by 120. For example, the 12 inches of diameter, the value is 0.25 inch (6mm). Draw the line from origin with slope equal to AE/L and draw the line with the same slope having distance from first

line equal to 0.25 inch to intersect the relationship graph. The point is the ultimate bearing capacity of pile as shown in Figure 2.1. The Davisson limit was developed in conjunction with the wave equation analysis of driven piles and has widely used.

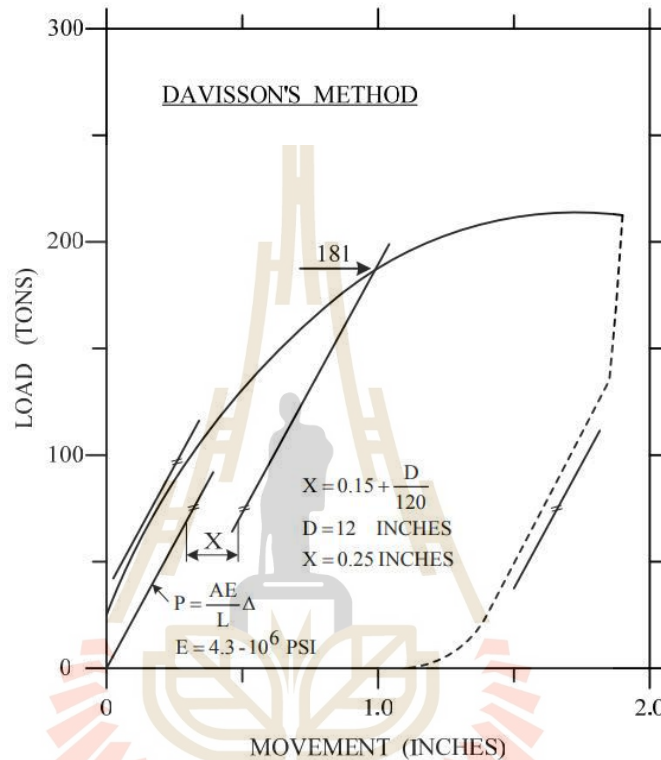


Figure 2.1 The ultimate bearing capacity by Davisson (1972) method.

2.2.2 Chin (1970) Method

Figure 2.2 presents the method was proposed by Chin (1970 and 1971) for piles in applying the general work by Kondner (1963). The method assumes that the load-movement curve when the load approaches the failure load is of hyperbolic shape. Each load value is divided with its corresponding movement value and the resulting value is plotted against the movement. After some initial variation, the

plotted values fall on a straight line. The inverse slope of this line is the Chin failure load.

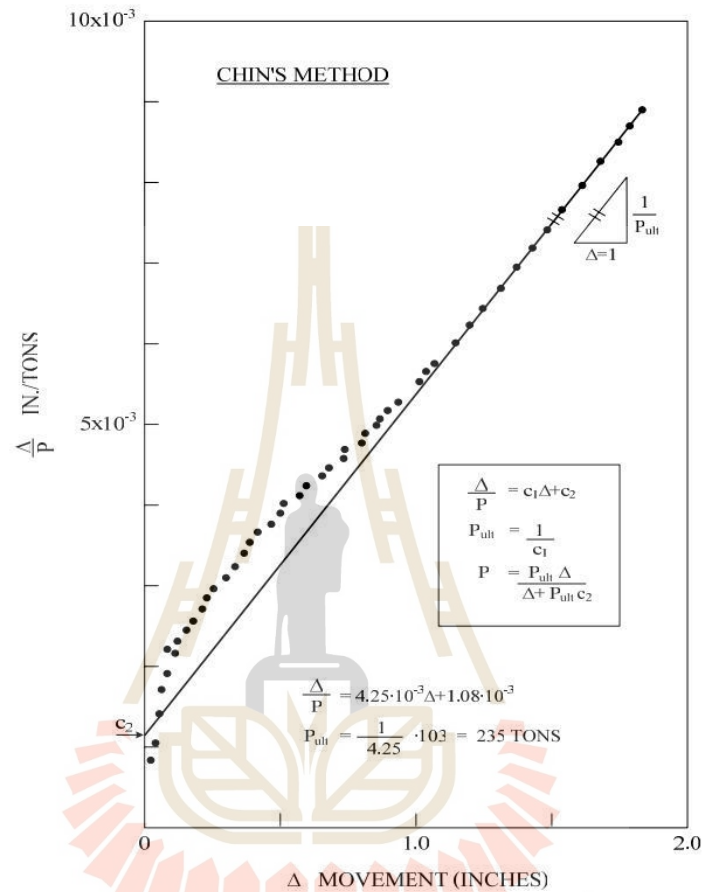


Figure 2.2 The ultimate bearing capacity by Chin (1970) method.

The bearing capacity of single pile can be calculated using the following relationship.

$$\Delta/P = c_1\Delta + c_2 \quad (2.3)$$

where: P is the load value Δ is the movement value c_1 and c_2 is constant value

2.2.3 De Beer (1967) Method

Figure 2.3 presents a method was proposed by De Beer (1967), where the load movement values are plotted in a double logarithmic diagram. When the values fall on two approximately straight lines, the intersection of these point is defined as the failure value.

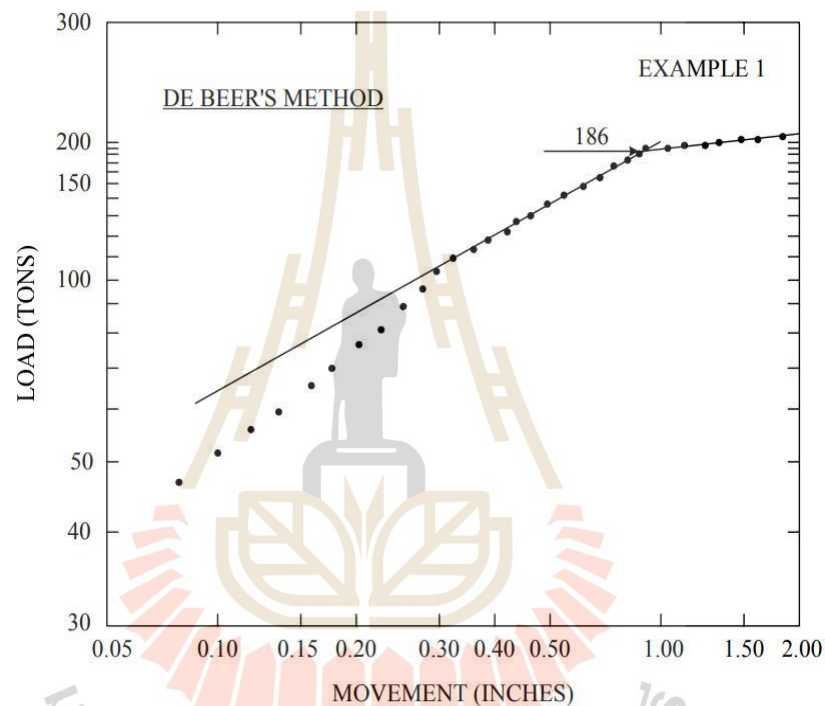


Figure 2.3 The ultimate bearing capacity by De Beer (1967) method.

2.2.4 Standard 90 percent of Brinch Hansen (1963) Method

Figure 2.4 presents a method proposed by Brinch Hansen (1963). The failure is defined as the load that gives twice the movement of the pile head as obtained for 90% of that load. This method also called the 90% criterion, and has widely used in Scandinavia (Swedish Pile Commission, 1970).

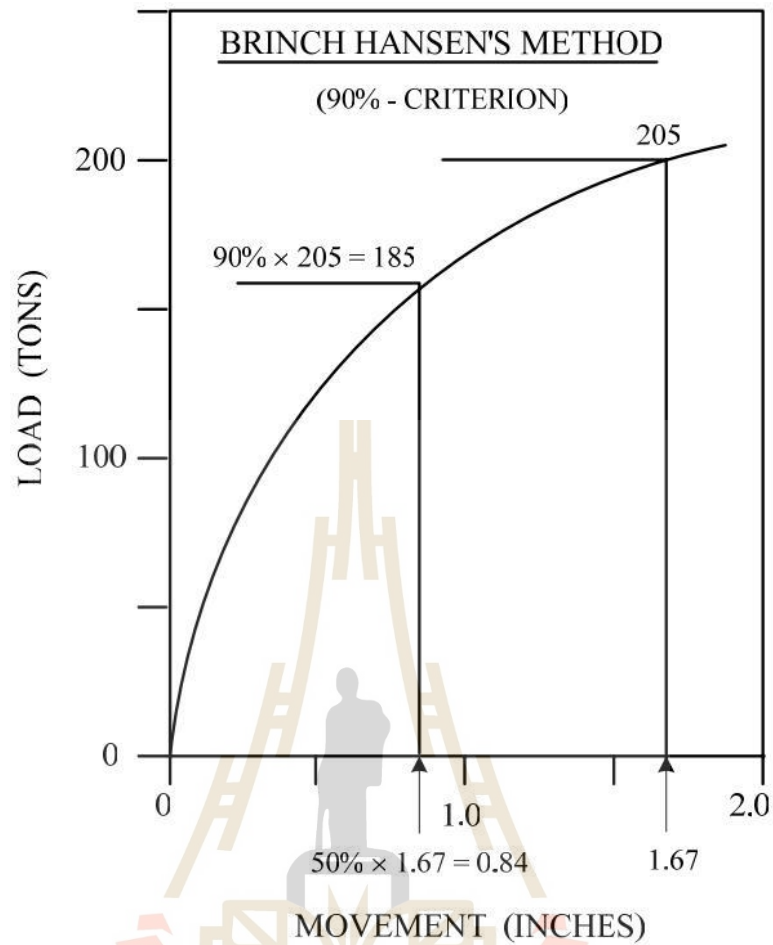


Figure 2.4 The ultimate bearing capacity by 90% of Brinch Hansen (1963) method.

2.2.5 Standard 80 percent of Brinch Hansen (1963) Method

Figure 2.5 presents the method by Brinch Hansen's 80% criterion. A definition for pile capacity as the load that gives four times the movement of the pile head as obtained for 80 % of that load. This '80%- criterion' can be estimated directly from the load movement curve, but it is more accurately determined in a plot of the square root of each movement value divided by its load value and plotted against the movement. Normally, the 80%-criterion agrees well with the intuitively perceived "plunging failure" of the pile. The following simple relations can be derived for

computing the capacity or ultimate resistance. The criterion gives the following simple relationships to use in calculating the ultimate failure, P_u :

$$P_u = 1/(2\sqrt{C_1 C_2}) \quad (2.4)$$

$$\Delta_u = C_2/C_1 \quad (2.5)$$

where: C_1 is the slope of the straight line, C_2 is the y-intercept in the \sqrt{P}/Δ_u plotted.

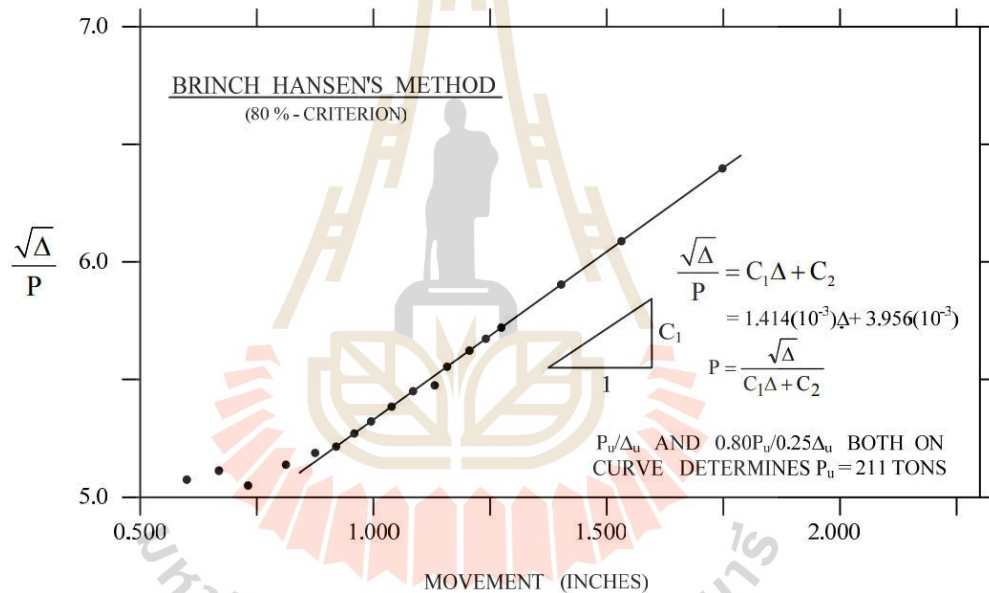


Figure 2.5 The ultimate bearing capacity by 80% of Brinch Hansen (1963) method.

2.2.6 Mazurkiewicz (1972) Method

Figure 2.6 presents the method put forward by Mazurkiewicz (1972). A series of equal pile head movement lines are arbitrarily chosen and the corresponding load lines are constructed from the intersections of the movement lines with the load-movement curve. From the intersection of each load line with the load

axis, a 45-degree line is drawn to intersect with the next load line. These intersections fall, approximately, on a straight line, the intersection of which with the load axis defines the failure load. This method is based on the assumption that the load movement curve is approximately parabolic. Consequently, the interpreted failure load of Mazurkiewicz's method is close to that of Brinch Hansen's 80% criterion. However, when drawing the line through the intersections according to Mazurkiewicz, some disturbing freedom of choice is usually found.

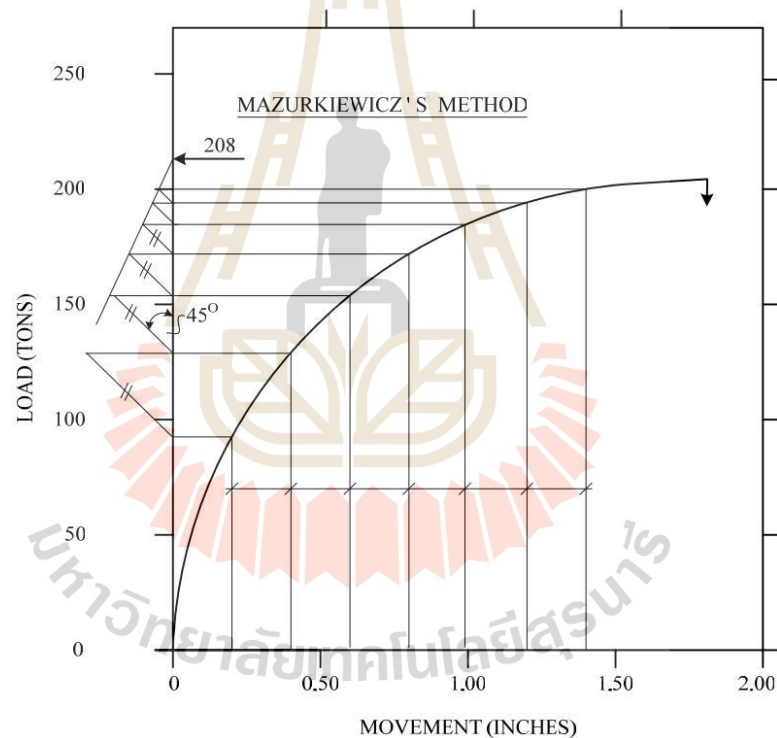


Figure 2.6 The ultimate bearing capacity by Mazurkiewicz (1972) method.

2.2.7 Fuller and Hoy (1970) Method

Figure 2.7 shows a simple definition proposed by Fuller & Hoy (1970). The failure load is equal to the test load for where the load movement curve is

sloping 0.05 inch/ton (0.14mm/kN). Figure 2.7 also shows a development of the above definition proposed by Butler & Hoy (1977) defining the failure load as the load at the intersection of the tangent sloping 0.05 inch/ton, and the tangent to the initial straight portion of the curve, or to a line that is parallel to the rebound portion of the curve.

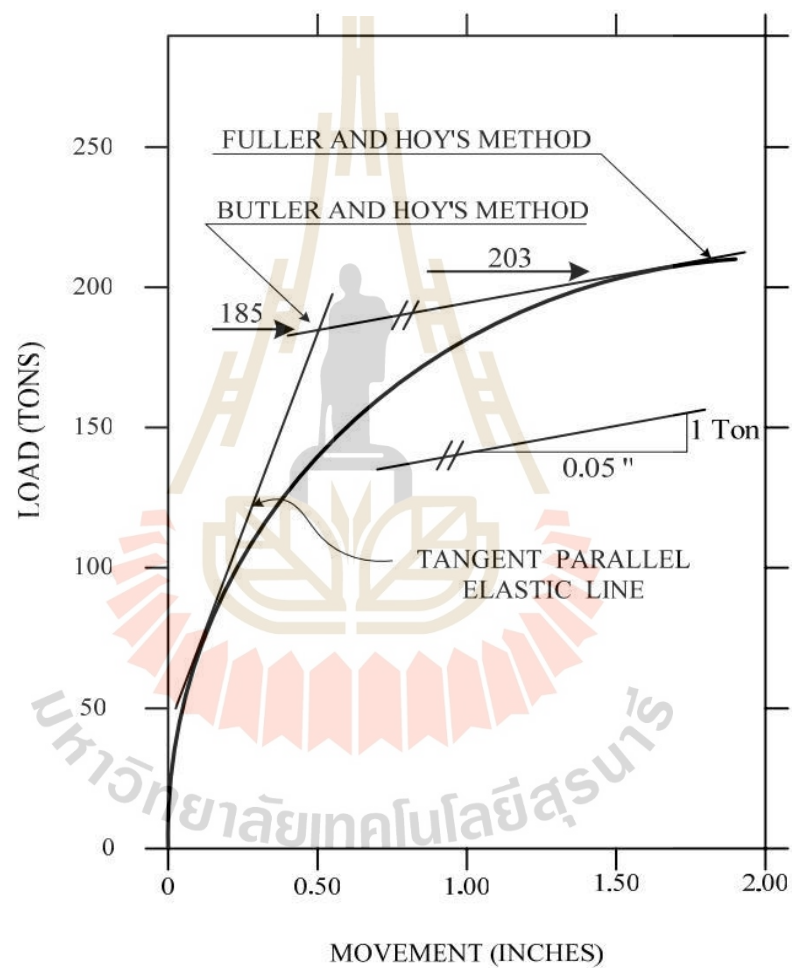


Figure 2.7 The ultimate bearing capacity by Fuller & Hoy and Butler & Hoy (1970) method.

2.2.8 Vander Veen (1953) Method

Figure 2.8 presents the determination of the failure load as proposed by Vander Veen (1953). A value of the failure load, P_{ult} is chosen and values calculated from $\ln(1 - P/P_{ult})$ are plotted against the movement. When the plot becomes a straight line, the correct P_{ult} has been chosen.

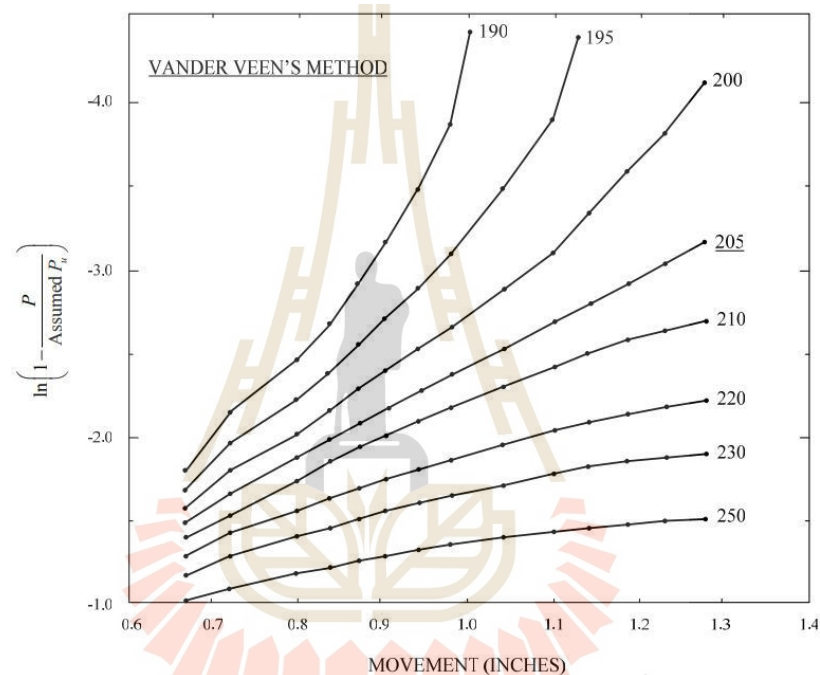


Figure 2.8 The ultimate bearing capacity by Vander Veen (1953) method.

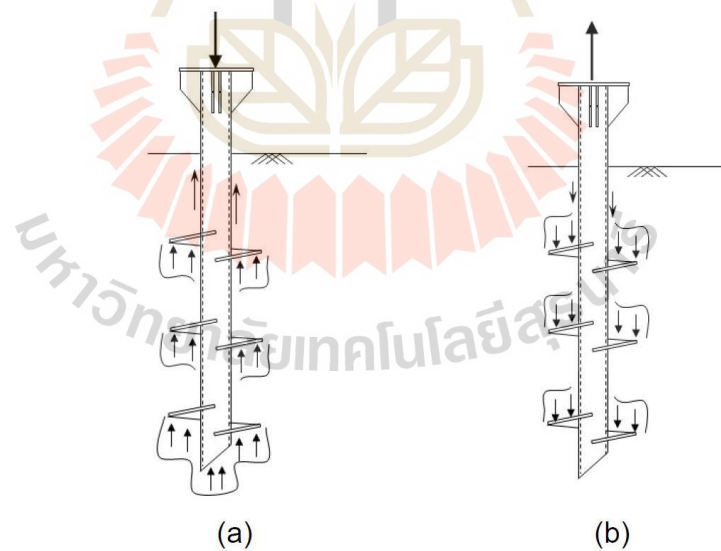
2.3 Ultimate load capacity of screw pile or helical pile

2.3.1 Screw pile failure models.

Two primary failure models have been proposed in the literature for describing the behavior of helical piles under axial loading these are the individual plate bearing model (Adams and Klym 1972, Narasimha Rao et al. 1993) and the cylindrical shear model (Mitsch and Clemence 1985, Mooney et al. 1985, Narasimha

Rao and Prasad 1991). The individual plate-bearing model assumes the helical pile behaves as a series of independent plates, whereby each helix acts independently of the others in bearing or uplift. The pile's axial capacity is therefore taken as the sum of the bearing capacities of the individual helices in compression or tension (Figure 2.9a and b). The cylindrical shear model assumes the formation of a cylindrical failure surface, circumscribed between the uppermost and lowermost helices of the pile, during axial loading. The axial capacity of the helical pile is presumed to consist of shear resistance along this cylindrical surface and bearing resistance above the top helix (in tension) or below the bottom helix (in compression) (Figure 2.9c and d). Skin friction acting along the section of the pile shaft between the uppermost helix and the ground surface may also be considered to contribute to the axial capacity, in both the cylindrical shear and the individual plate bearing models. This shaft friction component may be of considerable importance for deeply installed piles. It is generally concluded, however, that under tensile loading, skin friction should be neglected along the portion of the pile shaft contained within the zone of bearing failure above the uppermost helix. This bearing zone may be considered to extend a distance approximately equal to the diameter of the uppermost helix for deeply embedded piles (Zhang 1999). For shallow helical piles in uplift, the zone of bearing failure above the top helix extends to the ground surface, and the skin friction component along the entire shaft length should therefore be neglected (Mitsch and Clemence 1985). The choice of the most representative failure model to describe the behavior of helical piles under axial loading is considered to be a function of the pile geometry. It is well established that the failure zone at the tip of a pile extends over a depth of almost twice the pile diameter (Zeevaert 1983). For this reason, the

assumption that the helical plates behave independently of one another (as per the individual plate bearing model) is only considered valid for multi-helix piles with inter-helix spacing ratios greater than 2.0 (Narasimha Rao et al. 1993). For multi-helix piles with spacing ratios of less than 2.0, interaction between the closely spaced helical plates under axial loading is generally considered to create a failure surface better represented by the cylindrical shear model. The cylindrical shear model has been primarily established on the basis of laboratory uplift tests performed on model helical piles installed in sand, silt, and clay (Mitsch and Clemence 1985; Mooney et al. 1985; Narasimha Rao et al. 1993; Narasimha Rao et al. 1989), and has also been applied to laboratory compression tests performed on model helical piles installed in clay (Narasimha Rao et al. 1991).



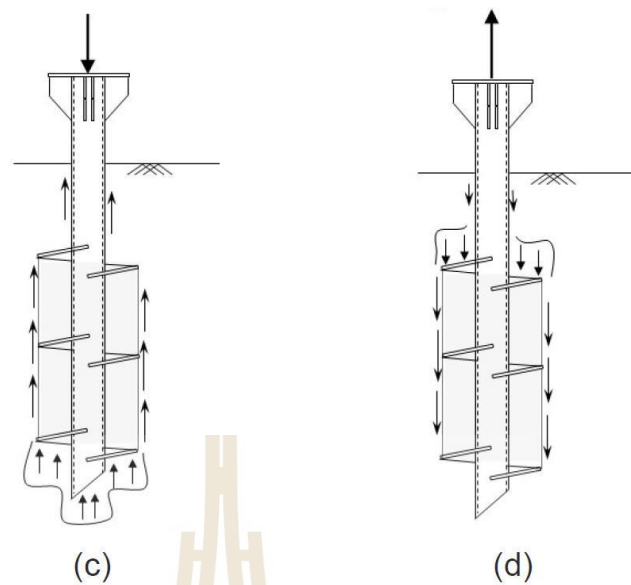


Figure 2.9 Helical Pile Failure Models: (a) Individual Plate Bearing Model under compression, and (b) uplift (after Mooney et al. 1985); (c) Cylindrical Shear Model under compression, and (d) uplift (after Narasimha Rao et al. 1991).

2.3.2 Cylindrical shear method

The cylindrical shear method was pioneered by Mitsch and Clemence (1985) and Mooney et al. (1985) to estimate the axial capacity of SP in sand and clay/silt, respectively. The cylindrical shear model assuming that the cylindrical shear failure is formed in the connection between the top and bottom helices. Nasr (2004, 2009) concluded that the ultimate load capacity is influenced by the number of helices, the pile geometry, the soil condition and the helical spacing. The ultimate load capacity is the sum of the end bearing resistance below the bottom helix, the sum of shear resistance along the cylindrical shear surface and the shaft friction above the

top helix as shown in Eq. (2.6) (Hawkins & Thorsten, 2009; Livneh & El Naggar, 2008; Sakr, 2009, 2011; Tappenden et al., 2009; Zhang et al., 1998):

$$Q_{ult} = Q_{helix} + Q_{bearing} + Q_{shaft} \quad (2.6)$$

where Q_{ult} = ultimate load capacity; Q_{helix} = shearing resistance mobilized along the cylindrical failure surface; $Q_{bearing}$ = end bearing capacity; and Q_{shaft} = resistance developed along the steel shaft.

The ultimate load capacity of SP in cohesive soil is therefore derived from Eq. (2.7) as follows (Mooney et al. 1985):

$$Q_{ult} = S_f(\pi DL_c)c_u + A_H c_u N_c + \pi d H_{eff} \alpha c_u \quad (2.7)$$

where S_f = spacing ratio factor; D = diameter of pile helix; L_c = distance between top and bottom helical plates; A_H = area of the helix; c_u = undrained shear strength of soil; N_c = bearing capacity factor for cohesive soils; d = diameter of pile shaft; H_{eff} = effective length of pile above top helix; and α = adhesion factor.

Rao and Prasad (1993) reported that the spacing to diameter (S/D) ratio of pile helix significantly affects the ultimate load capacity. Increasing S/D ratio results in reduction of the ultimate load capacity. Rao and Prasad (1993) proposed equations to determine the spacing ratio factor (S_f) as follows:

$$\text{For } S/D < 1.5 \quad S_f = 1.00 \quad (2.8)$$

$$\text{For } 1.5 \leq S/D \leq 3.5 \quad S_f = 0.683 + 0.069(3.5 - S/D) \quad (2.9)$$

$$\text{For } 3.5 \leq S/D \leq 4.6 \quad S_f = 0.700 + 0.148(4.6 - S/D) \quad (2.10)$$

2.3.3 Individual bearing method

Adams and Klym (1972) reported that the load capacity of SP can be estimated individually, where the spacing distance between each plate is large enough. The individual bearing method. The parameters affecting the load capacity are screw plate bearing area and the undisturbed surrounding soil. Furthermore, the equations for individual bearing method involves both the resistance from each individual helix and the shaft resistance. Therefore, the overall ultimate load capacity of the SP can be calculated by the sum of all the individual helical capacities along with the shaft resistance as presented in Eq. (2.11) (Hawkins & Thorsten, 2009; Livneh & El Naggar, 2008; Sakr, 2009, 2011; Zhang et al., 1998).

$$Q_{ult} = \sum A_H c_u N_c \quad (2.11)$$

where A_H is the area of helix, c_u = undrained shear strength of soil, and N_c = bearing capacity factor for cohesive soils.

Moreover, Kristen M. Tappenden and David C. Seago (2007) present the predicting the axial capacity of screw piles installed in Canadian soils. The results of 26 full-scale static axial load tests are presented for screw piles installed in Alberta and British Columbia since 1998, and the effectiveness of three design methods are evaluated for predicting the axial capacity of screw piles in cohesive and cohesionless soils. Theoretical formulations for capacity calculation are examined alongside the LCPC direct pile design method, and an empirical relationship correlating the

installation torque to the ultimate screw pile capacity. The results are shown in Figure 2.10.

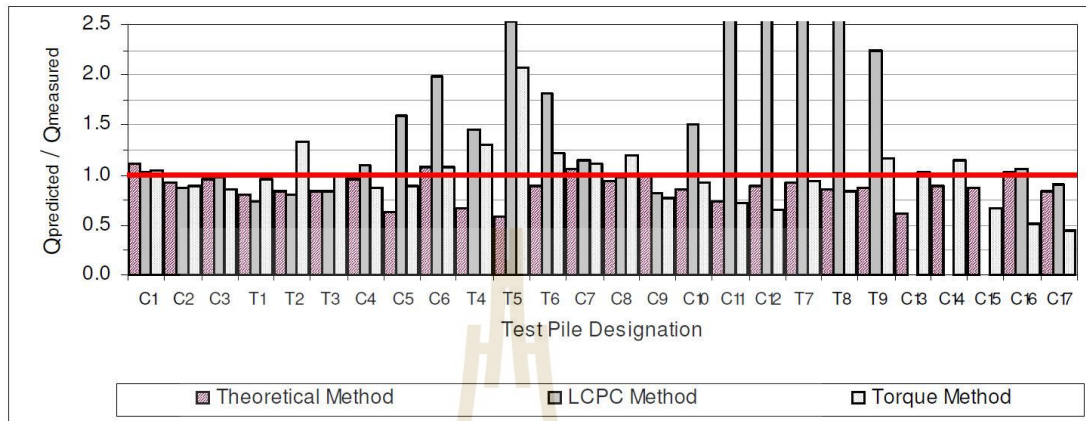


Figure. 2.10 Ratio of predicted to measured ultimate axial screw pile capacities.

The axial capacities of 26 full-scale screw piles installed in Alberta and British Columbia since 1998 were interpreted on the basis of static load test results. The effectiveness of three design methods were evaluated for predicting the ultimate axial capacity of the test piles, installed in cohesive and cohesionless soils. The failure surfaces were approximated by the cylindrical shear model for multi-helix screw piles having an inter-helix spacing ratio (S/D) less than 3.0, and by the individual plate bearing model for single-helix screw piles and multi helix piles with S/D rather than 3.0. Good predictions of the ultimate screw pile capacities in uplift and compression were obtained using theoretical formulations for appropriate components of bearing capacity and friction. Most of the capacity predictions made by the theoretical method fell within 20 percent of the measured capacities, with a small number of predictions outside the 20 percent range erring on the side of conservatism. Capacity predictions based on the LCPC direct pile design method, using the results of static cone

penetration tests, were good for screw piles under uplift and compression in clay, but significant deviations from the measured capacities occurred for piles installed in sand and glacial till materials. A direct empirical relationship between the installation torque and the ultimate axial screw pile capacity was applied using a K_t factor of 9.2 m^{-1} derived by linear regression of the data set. Capacity predictions made using the torque method typically fell within 30 percent of the measured capacities for deep screw piles in uplift and compression. The torque relationship significantly over-predicted the uplift capacity of a shallow screw pile installed in sand.

Ben Livneh and Hesham El Naggar (2008) presented a detailed investigation into the axial performance of helical piles. The study encompassed 19 full-scale load tests in different soils. It consisted of three helical bearing plates (diameters 300 mm, 250 mm, and 200 mm – decreasing with depth) welded to a central shaft (44.5 mm) and it was defined as a segmented deep foundation system as shown in Figure 2.11.

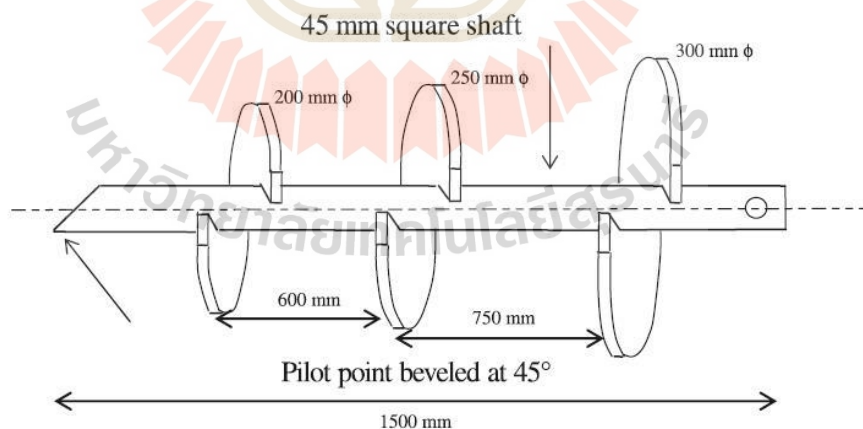


Figure. 2.11 Schematic of a typical pile lead section.

The load transfer mechanism for all piles tested was found to be predominantly through a tapered cylindrical shear failure surface and bearing of the “lead helix” in the direction of loading. To avoid overlapping between the influence zones of adjacent helical piles, a minimum spacing of $4D$ and $5D$ was proposed for piles loaded in compression and tension, respectively.

Mohammed Sakr (2010) presented the full-scale axial compression and tension (uplift) testing program executed on large capacity helical piles. Figure 2.12 shows a typical installation of a helical pile. Helical piles were typically installed through the use of mechanical torque applied at the pile head. Due to frozen soil conditions near ground surface and hard installation conditions between depths of about 1 and 3 m, pilot holes with size less than or equal to shaft size were predrilled to penetrate frozen and very hard soils.



Figure 2.12 Typical helical pile installation.

Figure 2.13 shows a typical load test setup using six reaction piles. Each axial compression or tension test setup included a total of seven piles including the test pile and six reaction piles. The reaction piles were installed to provide sufficient load reaction at a clear distance from the test pile of at least about 2.3 m. The 400-ton test beam was centered over test pile and supported on four 100-ton reaction beams, which in turn were supported on three reaction piles per beam. The arrangements for applying loads to the test piles involved the use of a hydraulic jack acting against the test beam. The connections were designed to adequately transfer the applied loads to the reaction piles and to prevent slippage, rupture or excessive elongation of the connections under the maximum load. The axial loads were applied at the pile head using two 1800-kN hydraulic jacks situated at the pile head for the case of compression test and situated on the top of test beam between the test pile head and test beam for the case of tension test. The test pile is connected to the load cell through a loading frame consisting of four 50.8 mm diameter all-thread Grade 8 steel bars and 51 mm thick steel plate. The load at pile head was measured using a 7400 kN strain gauge load cell that was calibrated up to 4500 kN. A redundant hydraulic pressure transducer (10,000 psi capacity and 0.25%FS accuracy) was also attached to the hydraulic jack to measure the pressure applied at pile head. Pile head axial movements were monitored at four points during the test, using two independently supported Linear Displacement Transducer (LDT) gauges (0.05 mm accuracy- 150 mm travel) and two mechanical dial gauges (0.05 mm accuracy- 50 mm travel). The LTDs, oriented in orthogonal directions and mounted with their stems perpendicular to the vertical axis of the test pile cap, were bearing against glass plate affixed to the pile cap. All LDTs, load cell and pressure transducer readings were recorded

automatically using a Flex Data Logger system at intervals of 30 seconds throughout the test duration.



Figure. 2.13. Typical axial compression test setup.

Table 2.1 provides a summary of the pile installations at test Sites 1 and 2, including the maximum torque recorded, predrill depth, thickness of soil plug and depth of embedment. A total of twelve tests were carried out, including eight axial compression tests and four tension (uplift) tests as shown in Table 2.2 and Table 2.3 respectively.

Table 2.1 Summary of pile installation.

	Test ID	Pile type	Shaft diameter mm	Installation torque at end of installation kN.m (ft.lbs)	Embedment depth m	Soil Plug thickness m	Predrill depth m
Site 1	ST1	4	324	211.5 (156,000)	9.0	5.1	7.6
	ST2	3	324	211.5 (156,000)	9.5	4.1	6.1
	ST3	4	324	211.5 (156,000)	9.5	4.4	6.1
	ST20	5	406	338.3 (249,500)	6.1	3.8	4.5
	ST21	5	406	338.3 (249,500)	5.7	1.9	4.0
	ST22	7	508	338.3 (249,500)	5.75	2.9	4.0
Site 2	ST5	4	324	211.5 (156,000)	5.9	1.7	5.2
	ST6	4	324	211.5 (156,000)	5.7	1.8	4.8
	ST7	3	324	211.5 (156,000)	5.7	2.0	5.0
	ST13	5	406	338.3 (249,500)	5.8	-	4.1
	ST14	5	406	338.3 (249,500)	5.6	-	3.9
	ST15	7	508	338.3 (249,500)	5.4	2.8	4.1

Table 2.2 Summary of axial compression test results.

Test ID	Pile Type	Shaft Dia. (mm)	Helix Dia. (mm)	Ultimate Capacity (5%)	
				Load (kN)	Displacement (mm)
Site 1					
ST1	4	324	762	2030	38
ST2	3	324	762	1892	38
ST20	5	406	914	2533	46
ST22	7	508	1016	2200	51
Site 2					
ST6	4	324	762	1912	38
ST7	3	324	762	1540	38
ST13	5	406	914	2292	46
ST15	7	508	1016	2400	51

Table 2.3 Summary of axial tension (uplift) test results.

Site	Test ID	Pile Type	Shaft Dia. (mm)	Helix Dia. (mm)	Ultimate Capacity (5%)	
					Load (kN)	Displacement (mm)
Site 1	ST3	4	324	762	1993	38
	ST21	5	406	914	1497	46
Site 2	ST5	4	324	762	1195	38
	ST14	5	406	914	1680	46

He investigated the axial compressive capacities of helical piles estimated using 5% failure criterion varied between about 1500 kN and 2500 kN. Therefore,

helical piles could be used successfully to resist high compressive loads. The uplift capacity of helical piles tested on site was also relatively high and varied between about 1500 kN and 2000 kN. The axial uplift capacities of helical piles were typically at least 60% to 70% of the axial compressive capacities. The high compressive and tensile capacities of helical piles were likely to reduce the number of piles required to support the loads for bridges, which generally reduced the foundation costs. The speed of helical pile installation with minimal level of noise was really another differentiating factor for use of helical piles for bridge applications. Helical pile installation was typically performed by screwing the pile into ground without a predrilling process. However, if a predrilling process was used during pile installation, the depth of predrilling should be limited to about 1 helix diameter above the top helix to avoid disturbing the bearing stratum for the most top helix. The use of double helixes was recommended at this site to increase the axial capacities of large diameter helical piles.

Weech et. al. (2012) presented a field study of disturbance effect on pile capacity using 2 types of helical piles with $S/D = 1.5$ and $S/D = 3.0$. Plots of total pile load versus pile head displacement are presented in Fig. 2.14.

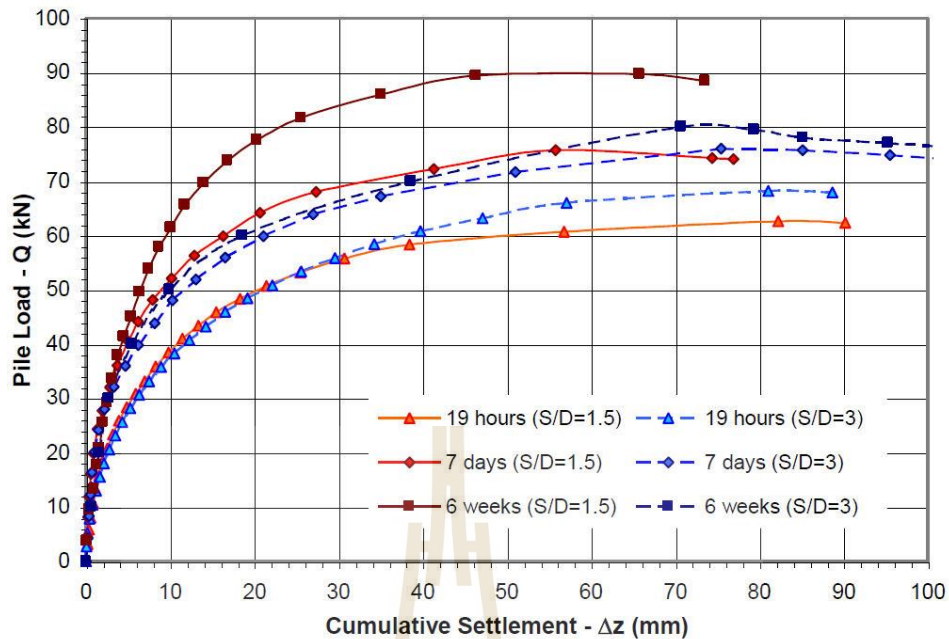


Figure 2.14 Load test results.

They found that helical piles with $S/D = 1.5$ had higher capacities than for $S/D=3$ in soft clays. The results have confirmed the applicability of the design approach that assumes that the failure mechanism changes as the S/D ratio of the helices reduces. In this case study, it appeared that the failure mechanism for piles with $S/D = 3$ was by individual bearing failure at each helix, whereas for piles with $S/D=1.5$, it was by individual bearing failure for the bottom helix and by shearing along a cylindrical failure surface of the same diameter as the helices for the remainder of the lead section. The results also showed that the undrained shear strength mobilized by helical piles in fine-grained soils was unlikely to be equivalent to the shear strength of the soil prior to pile installation, unless the soil was normally consolidated and unstructured prior to pile installation. The installation of the helical piles used in this study caused significant disturbance of the soil. However, the soil below the pile tip, which was loaded by the bottom helix, was essentially intact after

pile installation. The capacity mobilized by the $S/D = 1.5$ helices increased substantially with time as the shear strength of the soil surrounding the piles recovered after pile installation. This was because the cylindrical failure surface induced by the $S/D = 1.5$ helices passed through soil that had been softened and destructured by pile installation. Consequently, care should be taken to load test such piles after dissipation of excess pore pressure is substantially complete. Conversely, the capacity of the $S/D = 3$ helices did not appear to increase significantly with time after installation and so the effect of installation disturbance was less. This was believed to be due to the bearing-type failures induced by the $S/D = 3$ helices which mobilized resistance from a significant volume of soil beyond the edge of the helices, much of which did not appear to have experienced any significant softening or structural breakdown during installation.

Javad Khazaie and Abolfazl Eslami (2016) presented the behavior of helicle piles as a geoenvironmental choice by frustum confining vessel. They presented the performance assessment of screw piles embedded in sand in laboratory test. For testing, first the sand prepared and placed in FCV-AUT in loose state by air raining method and leveled by a wooden pallet in each 50 mm depth. In this filling method relative density was about 20% to 25%. In the second state, which relative density was about 45% to 50%, the sand placed in FCV and each 50 mm layers height compacted by body vibration. Hammer compaction in layers was used to achieve 65% to 70% relative density. The tests were applied on short rigid model piles in vertical compressive and pullout tests in the FCV-AUT. All fourteen model piles tested in this study had 750 mm embedment depth and were made from 4 mm thick steel plate. Shaft diameters of three usual and eleven helical model piles were 89 mm and 32 mm,

respectively. Helix diameters varied from 64 to 89 mm and spacing ratios were assumed 1 to 5. Some of model screw piles are shown in Figure 2.15.

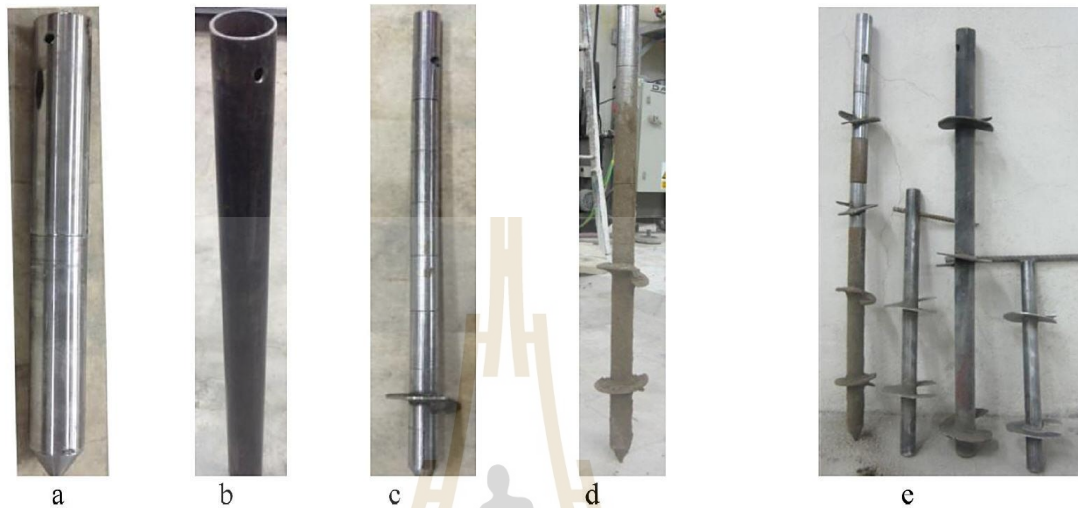


Figure 2.15 The model of screw pile.

They found that helical piles had some advantages that had made them very reasonable choice for using in offshore structures, building supports and crowded urban sites. Some of these advantages include ease of installation, safety piling because of pre-drilling elimination, short installation time. Helical piles also are economical and environment-friendly pile types that the pile applications reduce carbon dioxide, noise, raw material, fuel and manpower. FCV-AUT was used to test small scale model piles due to its configuration (lateral stresses vary almost linear from zero at the top soil to system applied pressure at the bottom). The FCV device presented a practical and economical alternative to chambers and centrifuge devices. Furthermore, the most limitations associated with simple 1g and CC devices can be eliminated when model piles were tested in FCV. The results of stress tests have

shown clearly that FCV could simulate the stress gradient in reality where the full scale piles were instrumented. According to test results, displacement of 5% pile diameter in loose and medium, and 10% in dense conditions were assumed as criteria in usual piles. In helical piles, 15% of pile diameter was proposed as a criterion if structural movements allowed. Helical piles had a suitable performance to bear tension loads. A helical pile with two helixes could function approximately, equal to a steel pile when the steel pile diameter was the same as the helix diameter. The helical pile weight was less than 45% of steel pile in these conditions. In compression, helical piles with two helixes could bear about 47% to 65% of a common steel pile capacity with the helixes diameter. Therefore, helical piles were reasonable choices in where there were uplift loads, especially in marine projects. Adding a helix to a single helix pile in tension was more effective than compression loading. Uplift load could be enhanced about 30% and higher. However, it was limited to 20% in compression. If two helixes used in one helical pile, had various sizes, better results could be achieved when the larger helix is put on top. When the number of helixes were up to three, helical piles behavior was close to common piles behavior. Uplift loads in this state were equal to ordinary piles or more. Compressive loads increment was about 10-15% in comparison with two helixes piles. Helical piles with three or more helixes had a better performance when the spacing ratio in down was larger than the pile top, i.e. S/D be 2 in top and 3 in down.

Based on the results, helical piles had a better performance when the relative density of site soil increases; this is because of more restraint between soil and pile helixes.

Tappenden and Segoo (2018) conducted a load testing program of full-scale instrumented helical piles to investigate the load transfer mechanism between multi-helix piles and the surrounding soil during axial loading. Five circular shaft, triple-helix piles were instrumented with strain gauges and installed at two separate test sites, comprising glaciolacustrine clay and aeolian sand soils. At each test site, the helical piles were loaded to failure in compression and tension in accordance with the ASTM “quick test” procedures for static pile load testing (ASTM D 1143-81 and D 3689-90). The resulting load distribution curves determined at various stages of applied compressive or tensile load were presented in Table 2.4 for each of the five test piles. The measured load distributions at the ultimate compressive or tensile capacities were compared to the theoretical ultimate load distributions calculated using the cylindrical shear and individual plate bearing models. The pile capacities calculated using the individual plate bearing model were particularly sensitive to the value chosen for N_c (in cohesive soils) and N_q (in cohesionless soils). At the Bruderheim (sand) site, a conservative N_q value of 20 was used in both compression and uplift, based on Das (1990) and Vesic (1963), for the inferred soil friction angle of 28 degrees. With the exception of pile C1, the individual plate bearing model provided very good estimates (within approximately 6 percent) of the ultimate axial helical pile capacities, and reasonably captured the shape of the measured ultimate load distributions along the piles at failure. Perhaps due to the close spacing between the helical plates ($S/D = 1.5$), at the Edmonton (clay) site, the behavior of the helical piles in cohesive soils was better represented by the cylindrical shear model. However, at the Bruderheim (sand) site, the behavior of the helical piles in

cohesionless soils was more accurately captured using the individual plate bearing model.

Table 2.4 Comparison of Measured and Calculated Ultimate Pile Resistances.

Test Pile	Applied Load at Failure (kN)	Calculated Axial Resistance (kN)	
		Cylindrical Shear Model	Individual Plate Bearing Model
C1	190 ^a	207	248
T1	215 ^b	227	221
T2	145 ^b	157	149
C2	480 ^b	292	450
T3	365 ^a	199	378

Notes: a) axial load at 35 mm displacement
b) axial load at onset of plunging failure

Ali and Abbas (2019) presented the performance of screw piles embedded in soft clay in laboratory test. The behavior of screw piles in soft clay soils has focused predominantly on the behavior of multi-helix screw piles loaded in axial compression with varying embedment depth, number of helix plates, helical plate spacing ratio, S/D_h , and pile length, L , as defined in Figure 2.16.

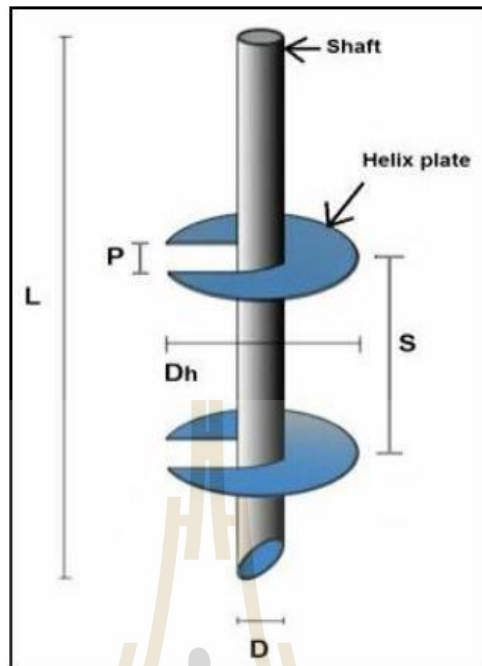


Figure 2.16 The geometry of screw pile.

Twelve steel screw piles with a length of 300, 350 and 400 mm and a circular solid section with a diameter of 10 mm were made of high-strength steel. The diameter of helix plate (D_h) was 30mm with thickness of 2 mm and a helical plate pitch (p) of 10 mm. The helix plate was manufactured from steel and welded firmly and accurately to the pile shaft. Two spacing values were studied: 30 mm ($S=D_h$) and 50 mm ($S=1.6D_h$). Figure 2.17 shows screw pile geometry. The termination of the shaft was a 45° to aid keying during installation. The experimental program was carried out on a single pile with different lengths, helical plate spacings and number of helical plates.

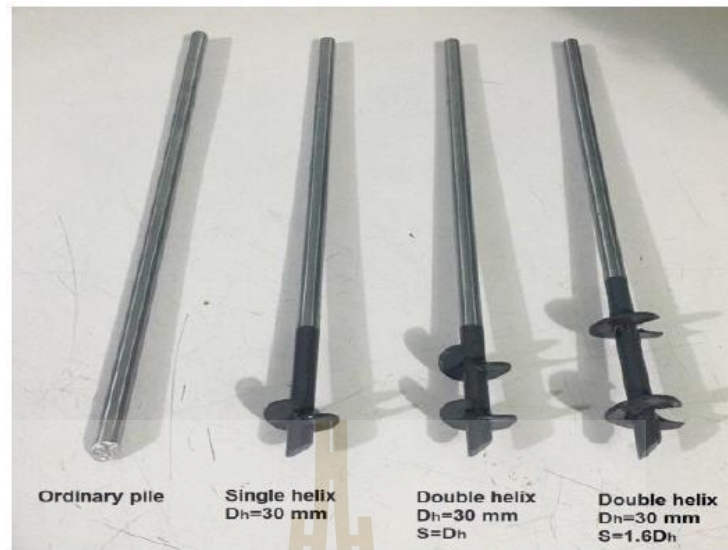


Figure 2.17 Different types of screw piles that were used in this study.

They found that the screw pile were quick and easy installation, immediate use and other advantages over the conventional pile system have expanded the use of screw piles as a deep foundation for various structures. The ultimate compressive capacity of screw piles increased with the increasing the number of helices. The ultimate compressive capacity of screw piles increased with increasing the depth of embedment in sandy soil. The most effective spacing ratio “ S/D_h ” was found to be equal to 1. Laboratory results showed that the ultimate compression capacity of screw piles was (4–8) times higher than that of ordinary piles depending upon the number of helices. The ultimate compressive capacity of screw piles of $S/D_h = 1.6$ less than for screw pile of $S/D_h = 1$.

2.4 Deep cement mixing (DCM) pile

2.4.1 Installation of deep cement mixing technique

The type of installation of deep cement mixing technique can be classified to three methods.

2.4.1.1 Wet mixing low pressure method

Wet mixing process is soil improvement by jetting slurry with low pressure into the soil. The equipment consists of base machine, low pressure pump, generator, mixing plant, silo and water tank. The ground is drilled by an auger having a head diameter equal to that of deep cement mixing pile. The auger has a hole at the end to jet slurry with a low pressure (around 10-20 bars) into the soil. The soil is then mixed with cement slurry by blade mixing. During penetration, the penetration rate and the quantity of slurry are controlled by the computer system until the tip of required depth. The jetting of slurry is stopped and the auger head is rotated with the reverse direction of penetration to the ground surface. In Thailand, this method has been widely used in many governmental projects such as Department of irrigation, Department of highways and Department of marine.

2.4.1.2 Jet grouting method

Jet grouting process is soil improvement by jetting slurry with high pressure into the soil. The equipment consists of base machine, high pressure pump, generator, mixing plant, silo and water tank. The auger head with a nozzle at the end is used to drill the soil ground. The soil was pre-cut by high pressure (around 150-250 bars) of air and water during penetration to become the mud until the tip of required depth. Then jetting slurry is started while the auger head is withdrawn to the ground surface. During withdrawing of the auger, the withdrawal rate and the quantity

of slurry are controlled by the computer system. In Bangkok, this method has been researched by many researchers such as Petchgate et. al (1998) and Bergado et al. (1999).

2.4.1.3 Dry mixing method

This process is similar to the wet mixing of low pressure process but only cement powder is used instead of slurry. The auger head with a hole at the end is used to drill the soil ground. The equipment consists of base machine, high pressure pump, generator and cement tank. During penetration, the penetration rate and the quantity of cement powder are controlled by the computer system until the tip of required depth. Then injection of cement powder is stopped and the auger head is lift up to the ground elevation. In Thailand, this method was employed in many projects such as Bangna-Bangpakong road no. 34 (Bergado et al., 1999).

2.5 Ultimate bearing capacity of deep cement mixing (DCM) pile

The bearing capacity of a single column is either governed by the shear strength of the surrounding soft clay (soil failure) or by the shear strength of the column material (column failure). The former mode of failure depends on both the skin friction resistance along the surface of the column and on the point resistance, while the later is dependent on the shear strength of the column material. The short-term bearing capacity of single column in the soft clay at soil failure can be calculated from the given expression (Bergado et al., 1996):

$$Q_{ult,soil} = (\pi dH + 2.25\pi d^2) S_u \quad (2.12)$$

where $Q_{ult,soil}$ is the bearing capacity of single column at soil failure; d is the diameter of the column, H is the column length and S_u is the average undrained shear strength of the surrounding soft clay. It has been assumed that the skin resistance is equal to the undrained shear strength of the surrounding clay and that the point resistance corresponds to $9S_u$. Due to the strength of the cement admixed clays is insignificantly influenced with the increase in effective stress at pre-yield state (Horpibulsuk, 2001), the short-term ultimate bearing capacity due to column failure is estimated from the relationship:

$$Q_{ult,col} = A_{col} (q_{uf}) \quad (2.13)$$

where $Q_{ult,col}$ is the bearing capacity due to column failure; A_{col} is the cross sectional area of the column and q_{uf} is the field strength of the column.

2.6 Application of DCM pile

2.6.1 DCM for Foundation Work

Bergado et al. (1999) used DCM piles used to reduce embankment settlement. The studied site was at the Bangna-Bangpakong road, Department of Highways in Thailand to mitigate the severe settlement and stability problems. The DCM piles using ordinary Portland cement has been utilized for foundation improvement (Figure 2.18). They found the DCM piles could reduce the settlement of road as well as the predicted vertical and horizontal deformations were comparable with the observed values.

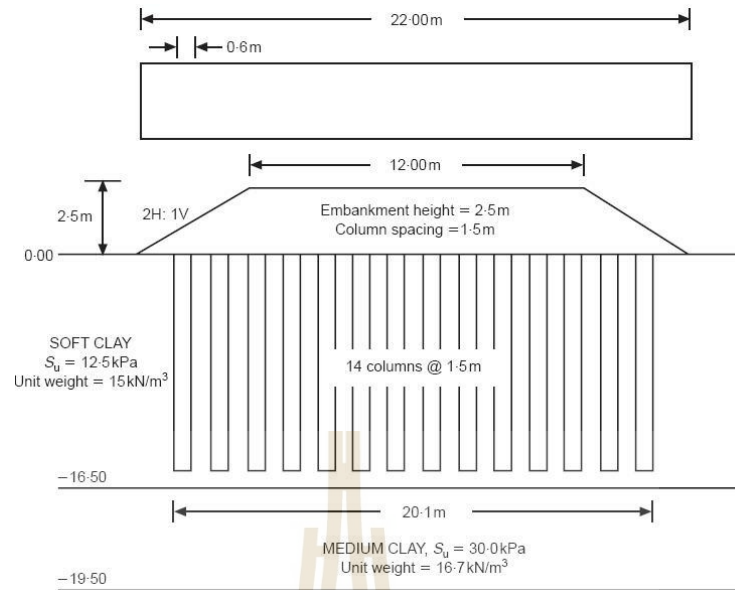


Figure 2.18 Schematic for Bangna-Bangpakong Highway using DCM.

Miura et al. (2001) studied engineering behavior of cement stabilized clay at high water content. The soil was collected in Saga, Japan in the experimental investigation and its water content was varied in the range of liquidity index between 1.0 and 2.0. The clay water to cement ratio, w/c was proposed as the prime parameter governing the engineering behaviour of cement stabilized clay both in compressibility and shear behavior.

Horpibulsuk et al. (2002) studied the strength improvement of soft marine clays by deep mixing technique at Saga Airport, Saga, Japan. It was effective to execute the columns at the number of wing rotation, WRN of 90 to 120 N/min to attain the Zone 3 of mixing zones as shown in Figure 2.19. Geotechnical engineers can achieve this range of WRN by varying the installation (penetration and withdrawal) rates and speed of rotation of mixing wings consistent with the construction period and construction cost.

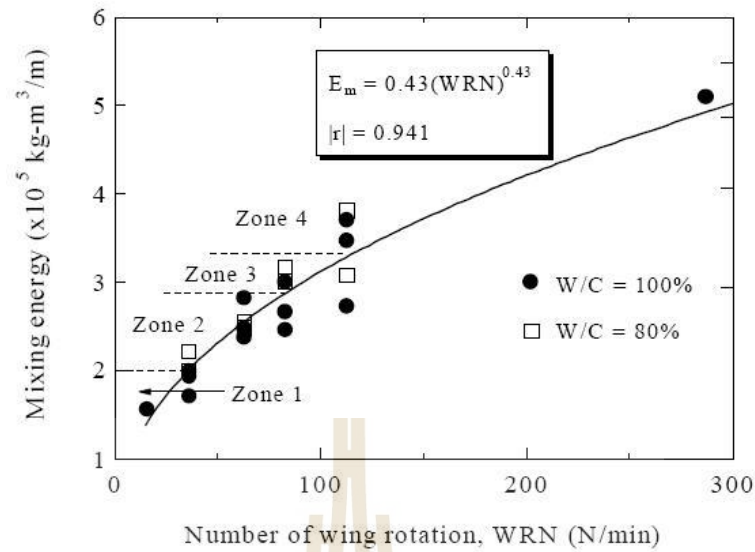


Figure 2.19 Mixing energy and number of wing rotation relationship of the columns.

Horpibulsuk et al. (2011) found that for the cement stabilization of soft Bangkok clay in the range of liquidity index 1.0-2.0, the w_c/C is the prime parameter governing the strength and the compressibility at the pre-yield state. The cementation bond strength increased, as the clay-water/cement ratio w_c/C , decreased. A water to cement ratio, W/C of 1.0 was recommend for the wet mixing improvement of soft Bangkok clay. They also suggested the procedure for the wet mixing improvement for soft Bangkok clay that was useful both an engineering and economical viewpoint shown in Figure 2.20.

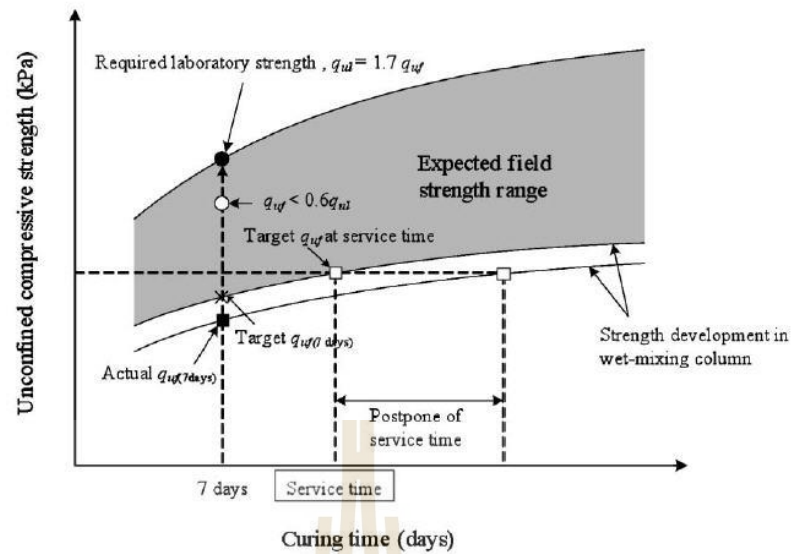
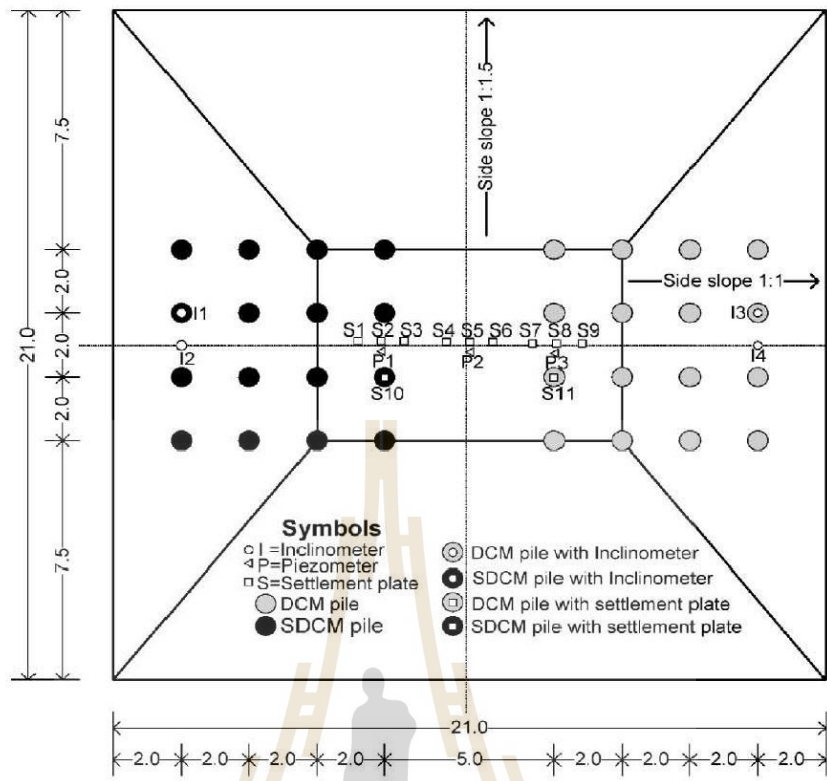
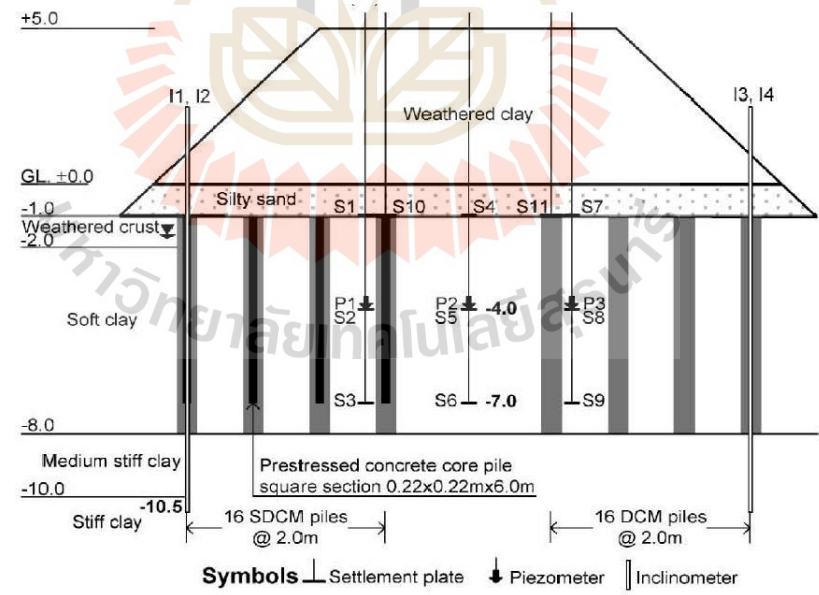


Figure 2.20 Suggested procedure of wet mixing method for soft Bangkok clay.

Field behavior of stiffened deep cement mixing piles were investigated by Jamsawang et al. (2010). They have studied the ultimate load capacity of DCM pile with diameter of 60 cm and 7.0 m of length and the concrete cored piles of 0.18x0.18 m and 0.22x0.22 m with 4.0 m and 6.0 m at the middle of DCM pile designated as stiffened deep cement mixing (SDCM). The plan view of test embankment on DCM and SDCM piles is shown in Figure 2.21 at the campus of the Asian Institute of Technology (AIT) Bangkok, Thailand. The schematic of SDCM pile is shown in Figure 2.22. The maximum of ultimate bearing capacity of SDCM piles was equal to 320 kN (32.6 tons), which was 2.2 times higher than DCM piles. The axial load against settlement plots for all test pilea were shown in Figure 2.23.



(a)



(b)

Figure 2.21 (a) Plan view of test embankment on DCM and SDCM pile; (b) Cross section of test embankment on DCM and SDCM pile.

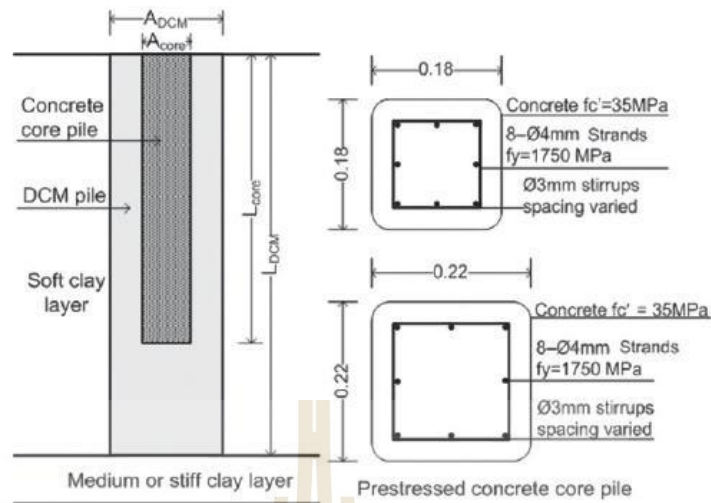


Figure 2.22 (a) Schematic diagram of SDCM pile; (b) details of prestress concrete core piles (dimensions in m.).

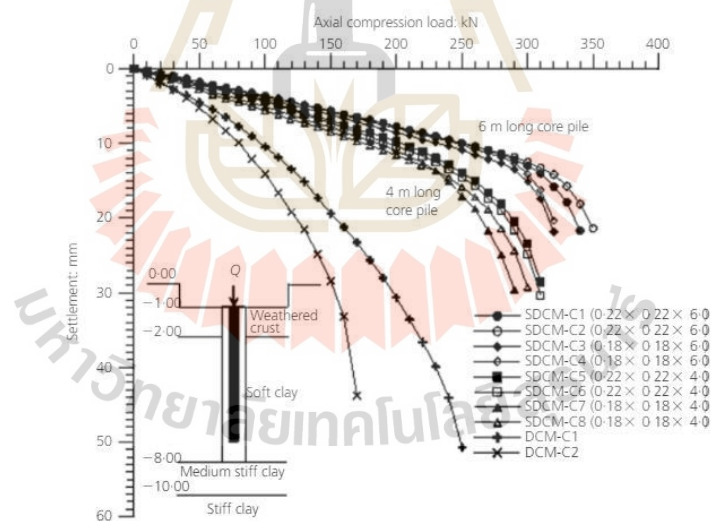


Figure 2.23 The curve of axial load plotted against settlement from field tests.

Numerical simulation and parametric study of SDCM and DCM piles under full scale axial and lateral load as well as under embankment load were studied by Bergado et al., (2010). The embankment was supported by two types of piles: 16-

SDCM piles and 16-DCM piles. For the purpose of simulation, the length of concrete core piles in SDCM piles were varied from 3.00 to 7.00 m with varied sectional dimension from 0.22x0.22 to 0.30x0.30 m. The embankment discretization model using Plaxis Foundation 3D software is shown in Figure 2.24.

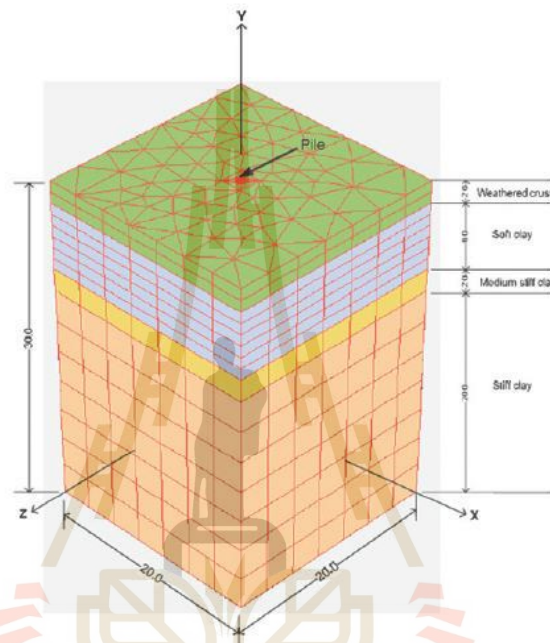


Figure 2.24 Axial and lateral pile load test simulation model.

They found the appropriate parameters from back analysis of cohesion of cement-clay in the DCM and SDCM piles, obtained from the 3D finite element simulations were 300 kPa and 200 kPa, respectively, as shown in Figure 2.25. However, the cement-clay modulus, E_{DCM} , were obtained as 60,000 kPa and 40,000 kPa for DCM C-1 and DCM C-2, respectively. Moreover, for the SDCM pile, the corresponding value for SDCM and E_{DCM} were 200 kPa and 30,000 kPa, respectively, as shown in Fig 2.26. The slightly different results reflect the construction quality control in the field tests.

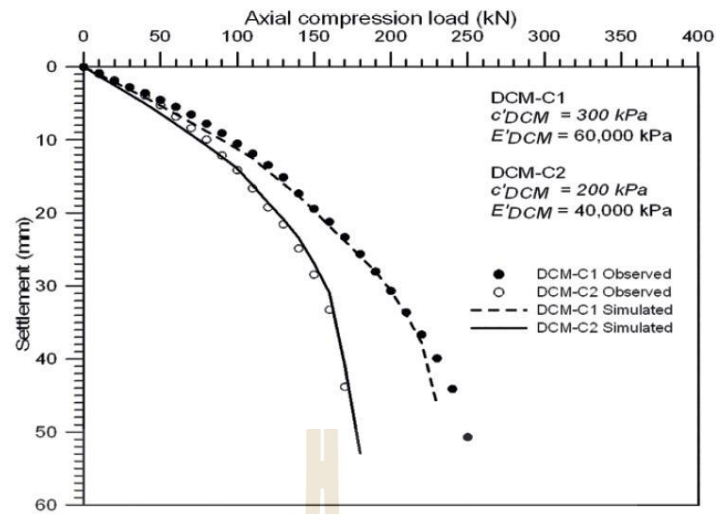


Figure 2.25 Comparisons between observed and simulated axial compression load – settlement curves for DCM-C1 and DCM-C2.

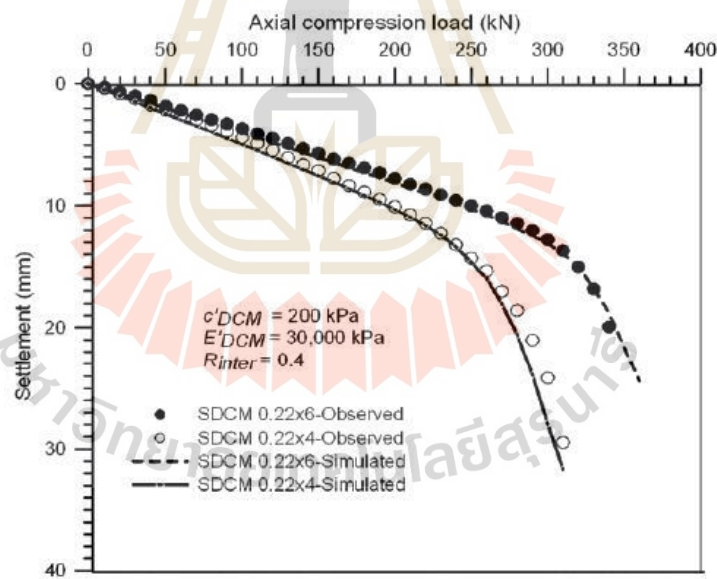


Figure 2.26 Comparisons between observed and simulated axial compression load – settlement curves for SDCM

Jongpradist et al. (2015) investigated an efficiency of using eucalyptus wood to reinforce deep cement mixing piles in field: pile Load and embankment tests. The

studied DCM pile was 0.50 m in diameter and 10.0 m in length with eucalyptus wood of 15 cm diameter and 6.0 m length at the middle at Rama hospital Bangplee Samutprakarn. The ultimate load capacity of SDCM pile was equal to 250 kN, which was greater than that of DCM pile of 190 kN as shown in Figure 2.27.

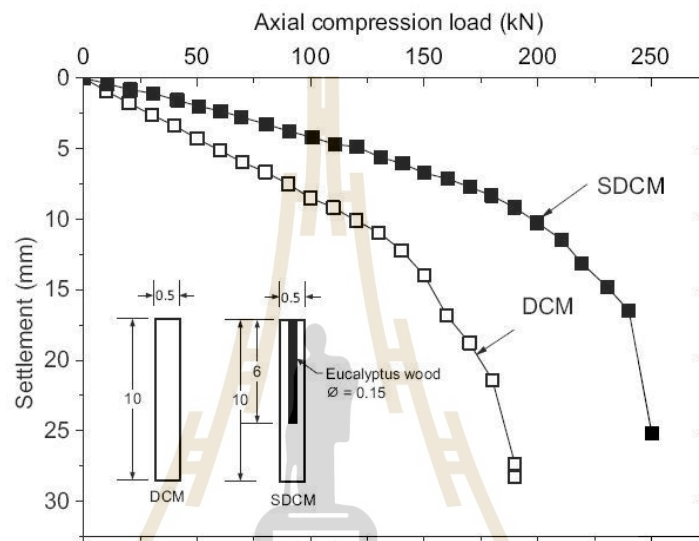


Figure 2.27 Load Settlement curve of DCM pile and SDCM pile.

2.6.2 DCM for excavation work

The field lateral movement of DCM and SDCM has been investigated by Jamsawang et al. (2010) in Figure 2.21. The lateral movement of SDCM was reduced to 60% of DCM movement as shown in Figure 2.28. The lateral movement of SDCM and DCM piles in Figure 2.28a was 65% and 55% of the total lateral movements occurred immediately after construction of the test embankment respectively. Due to its higher flexural stiffness, the lateral movement in the SDCM piles was 60% that of the DCM pile. The lateral movement of adjacent soil of SDCM pile and adjacent soil of DCM pile in Figure 2.28b was 65% and 50% of the total

lateral movements occurred immediately after construction of the test embankment respectively. This indicated that the SDCM pile was capable of reducing the magnitude of lateral movement by 60%. Therefore, the SDCM and DCM piles were confirmed to move laterally together with their adjacent ground.

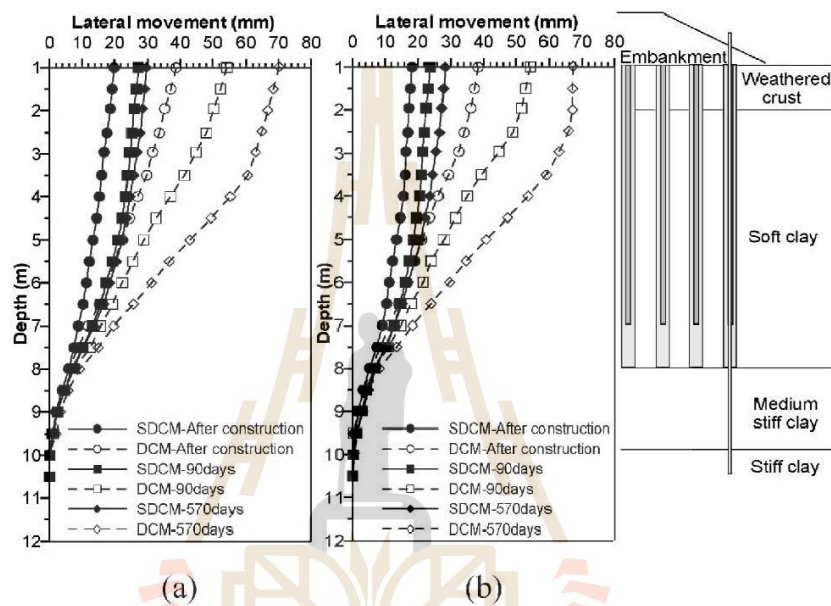


Figure 2.28 Lateral movement (a) DCM pile and SDCM pile; (b) adjacent soil of SDCM and adjacent soil of DCM.

Tanseng (2011) studied the SCC as a temporary retaining wall structure in soft Bangkok clay (Figure. 2.29). The different type of SCW is shown in Figure 2.30.

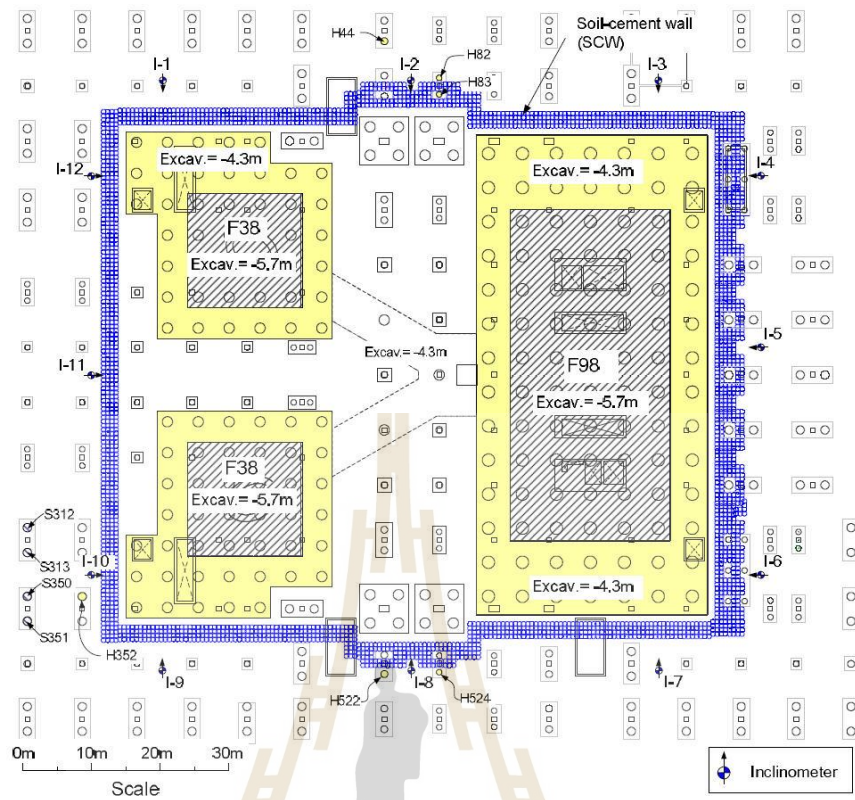


Figure 2.29 Layout of soil protection system and mat footing.

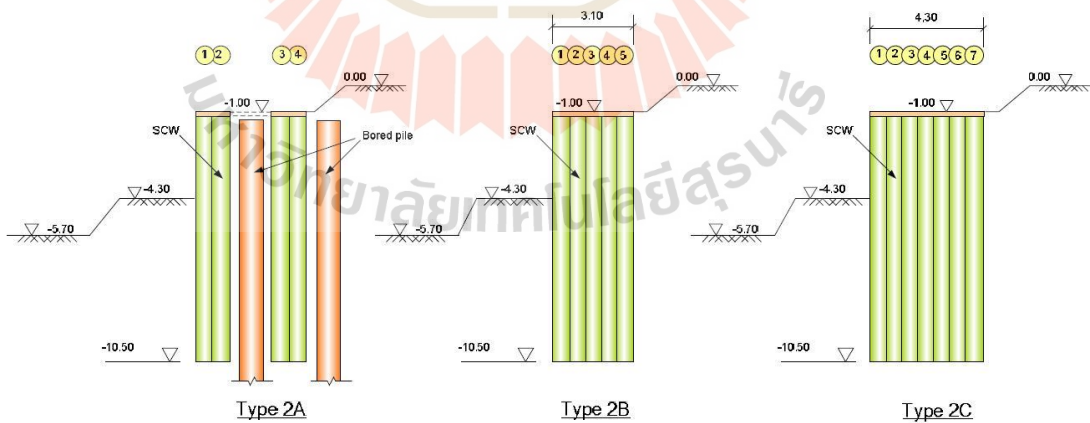


Figure 2.30 Typical cross section of SCW type 2.

Figure. 2.31 shows the monitored movements compared with the simulated movement from finite element simulation. All piles for mat footing are still in good

condition after final excavation, which indicated the excellent performance of SCW to resist ground movement.

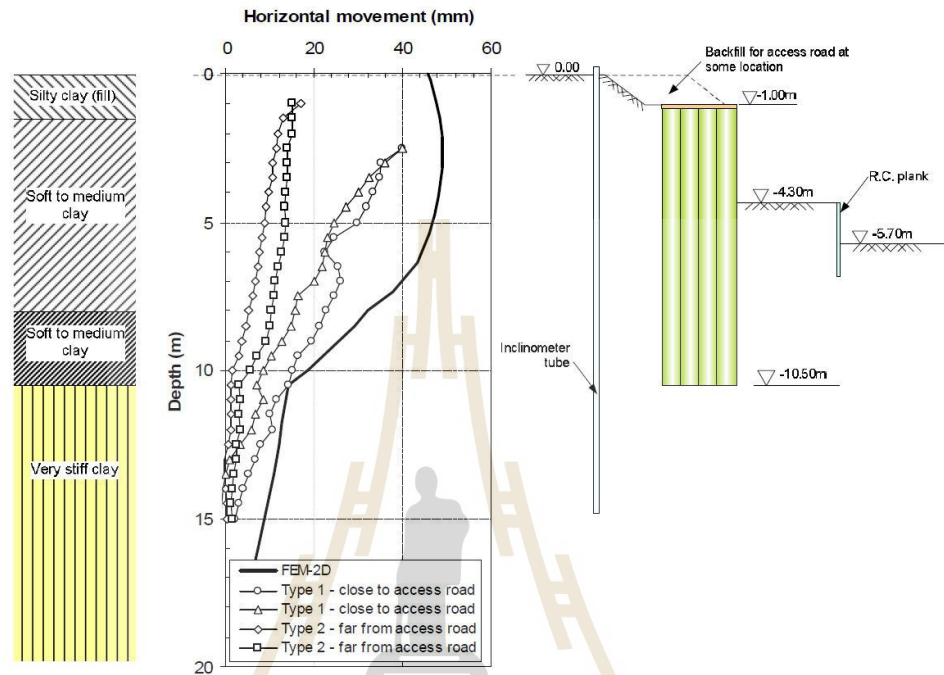


Figure 2.31 Performance of SCW after excavate to final depth.

The construction cost and time were also reduced as no internal bracings were required and no obstruction from bracing installations. The movement of the ground could be effectively limited with pre-boring technique and the ground movement caused by SCW construction did not cause any defect to the unrestraint pile. The movement of ground during excavation was not greater than the predicted value from finite element analysis. Shallow shrinkage cracks and deterioration of SCW surface due to exposure to the environment did not show any significant reduction of stability of SCW. Field observation showed that the crack did not penetrate to the inner zone of SCW.

Boathong et al. (2014) investigated the parameters affecting the lateral movement of an excavated slope at Suvarnabhumi Drainage Canal Project in soft Bangkok clay stabilized with DCM piles. The parameters considered included the spacing, depth, elastic modulus and volume of the row of DCM columns. A three-dimensional finite element model (3D-FEM) was used for the analyses, with the initial calibration based on the results of full-scale field tests conducted to determine the elastic modulus of the soil. Figure 2.32a shows a field test with the initial configuration of DCM columns, which indicated that the slope failure occurred when the excavation depth of the canal reached 3.0 m. Unfortunately, no instrumentation was installed during the excavation. However, excessive lateral movement was believed to be the major cause of the failure. To remedy the slope failure, additional DCM piles were added under the berm area between the DCM bearing piles and the DCM pile row, as well as in front of the DCM pile row (Figure 2.32b).

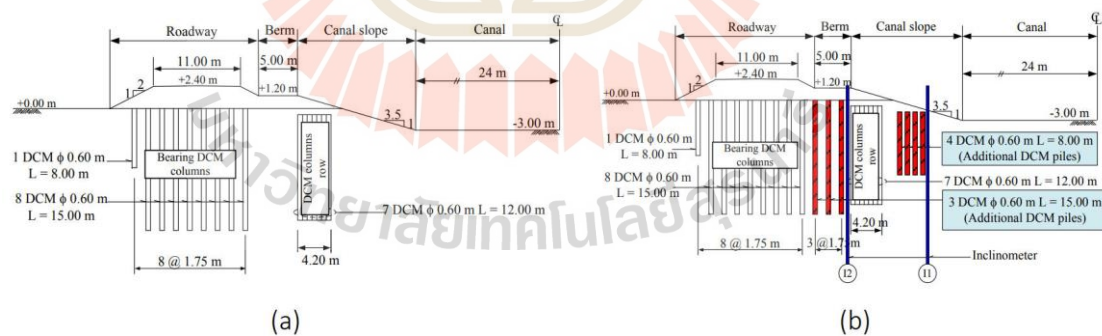


Figure 2.32 Canal and roadway cross-section with DCM column configuration. (a) Initial DCM column configuration, (b) Remedial DCM column configuration.

The lateral movement of the soil decreased as the DCM column row spacing (S_r) decreased. When the spacing was close ($S_r \leq 5D$), soil arching was more pronounced and the soil-pile system behaved as a strong composite material in resisting the sliding soil. When the spacing was large ($S_r=10D$), the piles behaved almost like an individual isolated pile, and the soil flows between pile. The optimum spacing (S_r) was judged to be in the range of $2.5D$ to $5D$. The DCM pile row depth (D_r) had a significant influence on the lateral movement of the soil and the failure mode of the pile. When the DCM pile row depth ($D_r \leq 11$ m) was not sufficient to provide fixity, the DCM pile row exhibited rigid-body rotation without substantial flexural resistance, and the lateral movement of the soil was large. Therefore, to utilize the full capacity of the DCM pile row to resist the sliding soil, the fixity condition was needed. The results showed that the optimum DCM piles row depth was in the range of 1.9 to 2.1 times the critical slip surface depth. The lateral soil movement decreased as the elastic modulus of the DCM column row (E_r) increased. The results showed that the influence of E_r was only significant when the DCM pile row had low stiffness. The optimum E_r was found to be in the range of 200 to 300 MPa. Increasing the volume of the DCM piles row was highly effective in limiting the lateral movement of the soil and improved the factor of safety of the slope because the DCM pile row was stiff enough to resist the sliding soil mass.

Meepon et al. (2016) studied a full scale test on DCM walls and SDCM walls of 60 cm in diameter and 8.0 m depth constructed in soft Bangkok clay in various forms. There were five types of wall (Figure 2.33) namely, type A: three rows of DCM pile, type B: two rows of DCM pile, type C: one row of SDCM with steel H-

beam in each column, type D: one row of SDCM alternately inserted with H-beam, and type E: one row of DCM without reinforcement.

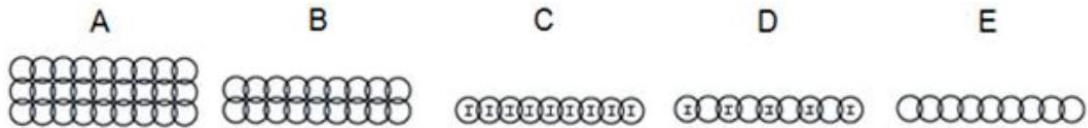


Figure 2.33 Five patterns of soil cement wall.

To reduce construction area, DCM walls with H-shaped steel reinforcement can replace DCM walls without reinforcement. The relationship between excavation depth, effective thickness ratio, and horizontal displacement is shown in Figure 2.34.

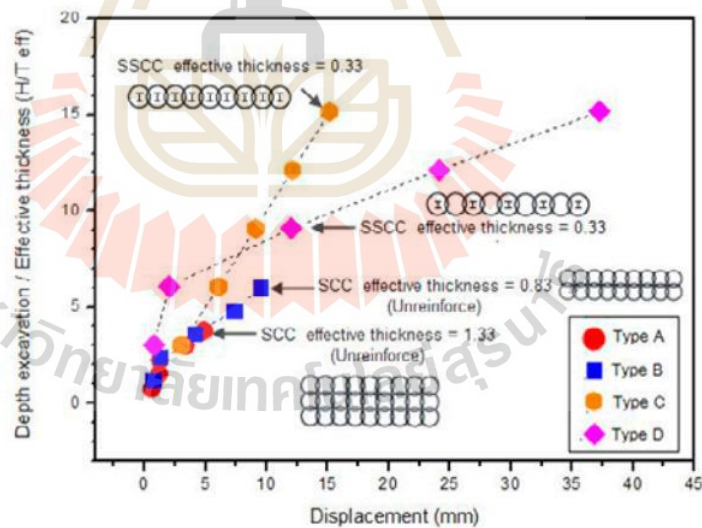


Figure 2.34 Relationship between excavation depth to effective thickness ratio and horizontal displacement.

The lateral movement of DCM wall at excavation depth of 5.0 m of five patterns of DCM wall are shown in Figure. 2.35.

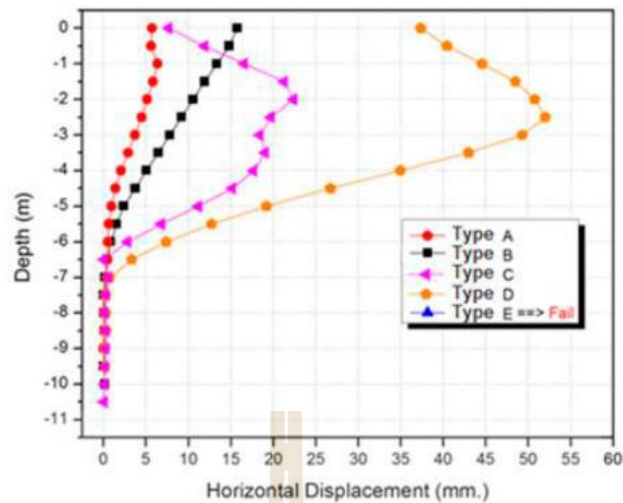


Figure. 2.35 Horizontal lateral movement of soil cement wall at excavation depth of 5.0 m.

The relationship between excavation depth to effective thickness ratio (H/T_{eff}) had an effect on horizontal displacement of DCM wall. The horizontal movement of the wall was less than 15 mm for Type C one row of DCM, which could be equivalent to Type A (three rows without reinforcement) and Type B (two rows without reinforcement). The alternate H-shaped steel reinforcement in type D wall resisted bending moment due to lateral earth pressure up to certain excavation depths. The SSCC wall resisted bending moment due to lateral earth pressure through the embedded H-shaped steel in the soil cement columns. The detected strain indicated that horizontal force was transferred to the embedded steel. The horizontal movement at the pile cap increased as horizontal force increased. The SSCC continuously resisted the horizontal force through the embedded H-shaped steel, and a linear relationship between the horizontal load and horizontal displacement was observed.

Thanasisathit et. al. (2018) studied parameters affecting the lateral movement of a compound deep cement mixing retaining wall (Figure 2.36) using the three-dimensional finite element method. The case history was of a reservoir construction project belonging to the Electricity Generating Authority of Thailand (EGAT) at Wang Noi Power Plant, Thailand.

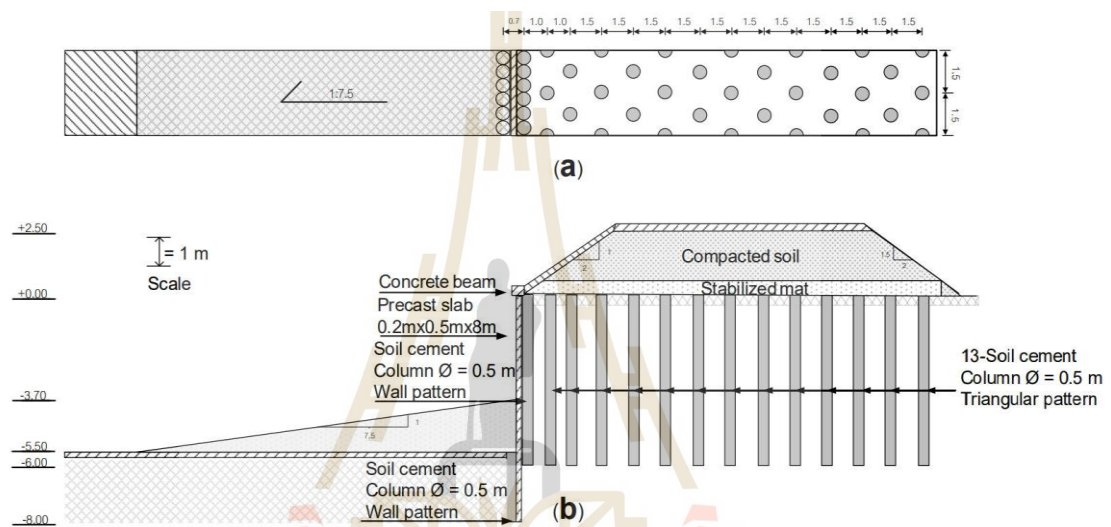


Figure 2.36 Layout of compound DCM wall: (a) plan view, (b) section view.

A numerical model is first calibrated with an instrumented case history. Then, a parametric study was performed. The influences of various parameters were compared and rated in terms of the degree of importance. The degree of influence of each influential factor on the maximum lateral movements was defined as the ratio of the variation in the maximum lateral movements to the mean of the maximum lateral movements (Huang and Han, 2010). The degrees of influence less than 30%, between 30 and 60% , between 60 and 100% , between 100 and 130% , and greater than 130 were considered to be low, medium, high, very high, and extreme, respectively. The

numerical results showed that the stabilized mat, the modulus of elasticity of the DCM column, and the thickness of the soft clay layer were the 3 most important design parameters for minimizing the lateral movements of the DCM wall as shown in Figures 2.37, 2.38 and 2.39 respectively. The thickness of the soft clay layer seemed to be the most important factor. Increasing the thickness of the soft clay layer resulted in larger lateral soil movement. However, the embedment of the DCM pile, the DCM pile pattern, the front DCM wall, and size of DCM pile were insignificant design parameters.

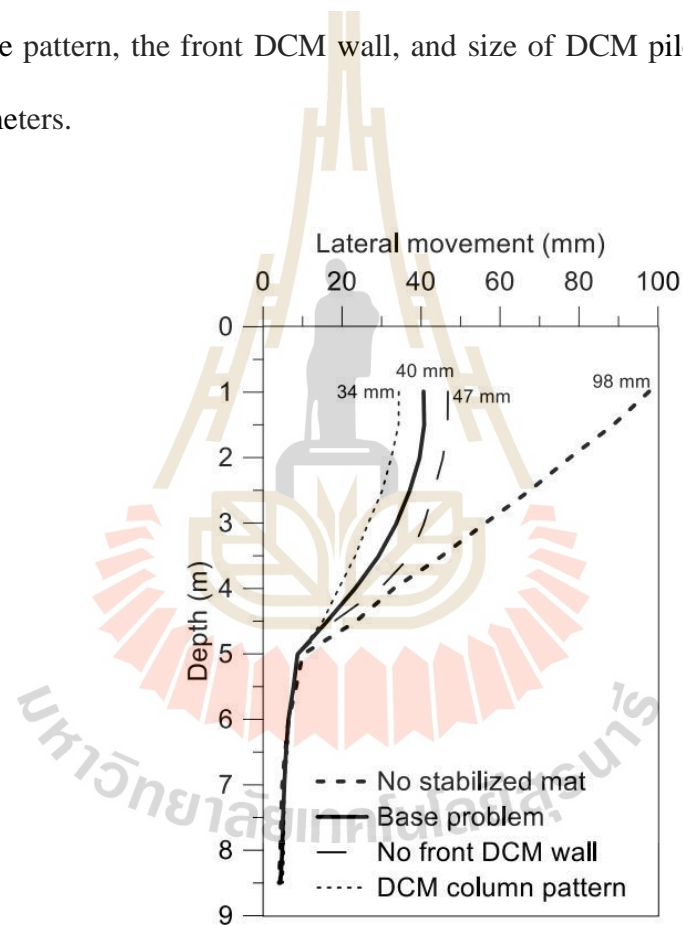


Figure 2.37 Effects of stabilized mat, nonexistence of front DCM wall, and DCM column pattern.

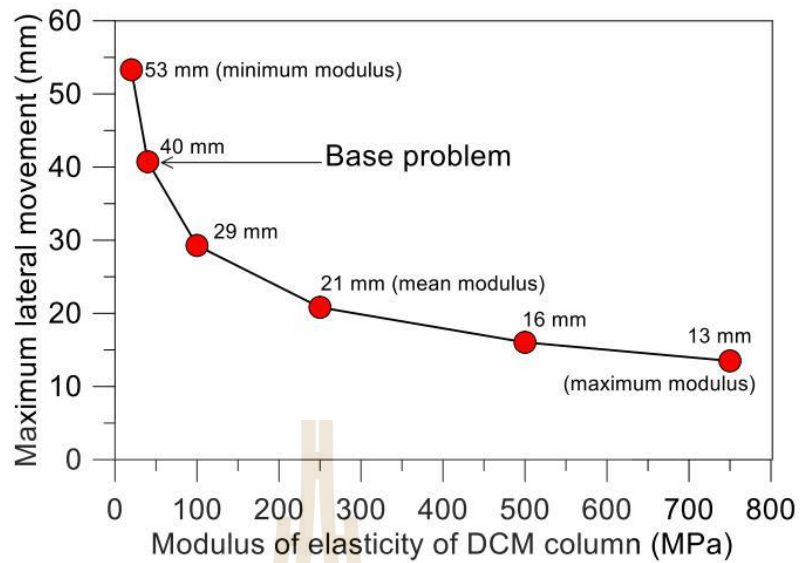


Figure 2.38 Effect of modulus of elasticity of DCM column.

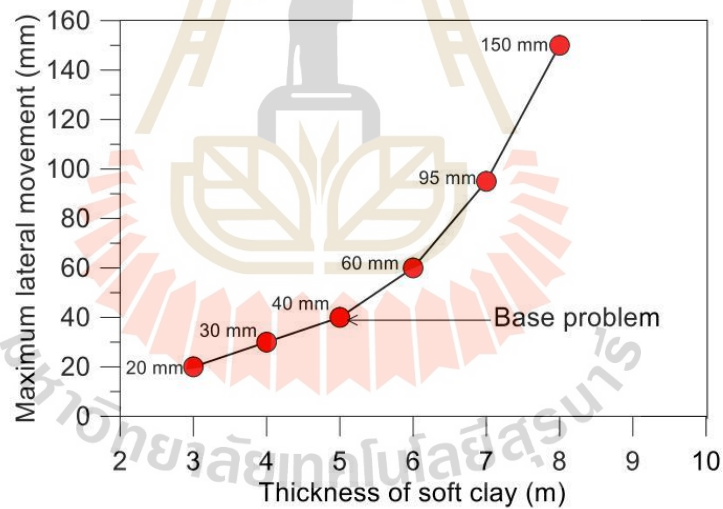


Figure 2.39 Effect of thickness of soft clay.

Table 2.5 show the summary of rank of degree of influence on maximum lateral movement.

Table 2.5 Rank of degree of influence on maximum lateral movement.

Rank	Factors	Degree of influence	
		(%)	Class
1	Thickness of soft clay layer	153	Extreme
2	Modulus of elasticity of DCM column	121	Very high
3	Nonexistence of stabilized mat	84	High
4	Modulus of elasticity of stabilized mat	54	Medium
5	Embedment of DCM column	16	Low
5	DCM column pattern	16	Low
5	Nonexistence of front DCM wall	16	Low
6	Size of DCM column	11	Low

2.7 References

- Bin, H.X., W, J.Y., Yi, Y., & Fan., Y. (2017). **Vertical bearing capacity numerical analysis of prestressed concrete piles based on piles and soil material constitutive model**. APETC 2017, 1171-1176.
- Butler, H. D, & Hoy, H.E (1977). **The Texas quick load method for foundation load testing-user's manual**. Federal Highway administration report, no. FHWA-IP-77-8.
- Chin, F. K. (1970). **Estimation of the ultimate load of pile not carry to fail**. Proceed of 2nd Southeast Asian Conference on Soil Engineering, 10p.
- Davission, M. T (1972). **High capacity piles**. Oroc. Lect. Series, **Innovations in Found**. Const ASCE, Illinois Section, 52.
- Debeer, E. E. (1970). **Experimental determination of shape factor and bearing capacity factors of sand**. Geotechnique, 20(4), 387-441.
- Horpibulsuk, S., Miura, N., Nagaraj, S., & Koga, H. (2002). **Improvement of soil marine clay by deep mixing technique**. Proceeding of the Twelfth International Offshore and Polar Engineering Conference, 584-591.

- Jamsawang, P., Bergado, D.T., & Voottipruex, P. (2010). **Field behaviour of stiffened deep cement mixing piles**. Proceedings of the Institution of Civil Engineers, 164, 33-49.
- Kamat, A. A., & Mahuli, R. R. (2010). **Cyclic pile load test on large diameter piles: A case study**. Indian Geotechnical Conference, 779-782.
- Lai, Y., Bergado, D., Lorenzo, G., & Duangchan, T. (2006). **Full-scale reinforced embankment on deep jet mixing improved ground**. *Proceedings of the Institution of Civil Engineers-Ground Improvement*, 10(4), 153-164.
- Lin, K. Q., & Wong, I. H. (1999). **Use of deep cement mixing to reduce settlements at bridge approaches**. *Journal of geotechnical and geoenvironmental engineering*, 125(4), 309-320.
- Livneh, B., & El Naggar, M. H. (2008). **Axial testing and numerical modeling of square shaft helical piles under compressive and tensile loading**. *Canadian Geotechnical Journal*, 45(8), 1142-1155.
- Mitsch, M. P., & Clemence, S. P. (1985). **UPLIFT CAPACITY OF HELIX ANCHORS IN SAND** (pp. 26-47): American Society of Civil Engineering (ASCE), New York.
- Monkaew, S., & Nawalerspunya, T. (2013). **Productivity of bored pile dry process**. *The research in funded by faculty of engineering Rajamangla University of Technology Phra Nakhon (In Thai)*.
- Mooney, J. S., Adamczak, S., & Clemence, S. P. (1985). **UPLIFT CAPACITY OF HELICAL ANCHORS IN CLAY AND SILT** (pp. 48-72): American Society of Civil Engineers (ASCE).

- Nasr, M. (2004, 20-22 December). **Large capacity screw piles**. Paper presented at the Proceedings of the International Conference: Future Vision and Challenges for Urban Development, Cairo, Egypt.
- Nasr, M. (2009). **Performance-based design for helical piles** *Contemporary Topics in Deep Foundations* (pp. 496-503).
- Poonlappanish, C., & Buasri, P. (2017). **Capacity of dry-process bored piles in Bangkok**. Paper presented at the The 22nd National Convention on Civil Engineering, Khao Yai Convention Center, Pak Chong, Nakhon Ratchasima, Thailand.
- Poulos, H. G., & Davis, E. H. (1980). **Pile foundation analysis and design**. New York: Wiley.
- Rao, S. N., & Prasad, Y. (1993). **Estimation of uplift capacity of helical anchors in clays**. *Journal of Geotechnical Engineering*, 119(2), 352-357.
- Ruberti, M. (2015). **Investigation of installation torque and torque-to-capacity relationship of screw-piles and helical anchors**.
- Sakr, M. (2009). **Performance of helical piles in oil sand**. *Canadian Geotechnical Journal*, 46(9), 1046-1061.
- Sakr, M. (2011). **Installation and performance characteristics of high capacity helical piles in cohesionless soils**. *DFI Journal-The Journal of the Deep Foundations Institute*, 5(1), 39-57.
- Schmidt, R., & Nasr, M. (2004). **Screw piles: uses and considerations**. *Structure magazine*, 29-31.

- Shen, S. L., Wang, Z. F., Sun, W. J., Wang, L. B., & Horpibulsuk, S. (2013a). **A field trial of horizontal jet grouting with composite-pipe method in soft deposit of Shanghai.** *Tunnelling and Underground Space Technology*, 35, 142-151.
- Shen, S.L., Wang, Z. F., Horpibulsuk, S, & Kim, Y. H. (2013b). **Jet-Grouting with a newly developed technology: The Twin-Jet Method.**” *Engineering Geology*, 152(1), 87-95. doi: 10.1016/j.enggeo.2012.
- Shen, S.L., Wang, Z.F., Cheng, W.C. (2017). **Estimation of lateral displacement induced by jet grouting in clayey soils.** *Géotechnique*, 67(7), 621-630.
- Skempton, A. (1966). **Summing up Large bored piles** (pp. 155-157): Thomas Telford Publishing.
- Srijaroen, C., Rachan, R., & Horpibulsuk, S. (2014). **Strength Development in Soil Cement Column and Soil Fly ash-Cement Column in Soft Bangkok Clay Deposit.** *KMUTT Research and Development Journal*, 37(2), 151-164.
- Tappenden, K., Segoo, D., & Robertson, P. (2009). **Load transfer behavior of full-scale instrumented screw anchors** *Contemporary Topics in Deep Foundations* (pp. 472-479).
- Tomlinson, M. J., & Boorman, R. (2001). **Foundation design and construction: Pearson education.**
- Voottipruex, P., Bergado, D. T., Suksawat, T., Jamsawang, P., & Cheang, W. (2011). **Behavior and simulation of deep cement mixing (DCM) and stiffened deep cement mixing (SDCM) piles under full scale loading,** *Soil and foundations*, 5(2), 307-320.
- Wang, S., & Sitar, N. (2004). **Numerical Analysis of piles in elasto-plastic soils under axial load.** *ASCE Engineerinf Mechanics Conference 17th*, 1-8.

Wonglert, A., Jongpradist, P., Jamsawang, P., & Petchgate, W. (2015). **Efficiency of using eucalyptus wood to reinforce deep cement mixing piles in field: Pile load and embankment tests.** KMUTT Research & Development Journal, 38(3), 225-242 (In Thai).



CHAPTER III

SOIL-CEMENT SCREW PILE: ALTERNATIVE PILE FOR LOW- AND MEDIUM-RISE BUILDINGS IN SOFT BANGKOK CLAY

3.1 INTRODUCTION

The foundation is a medium through which building loads are transferred from the superstructure to the ground (Poulos & Davis, 1980). The foundation can be classified into two predominant types, namely shallow foundation and deep foundations. The selection of the foundation system is mainly dependent upon several factors, which include: location, type of structure, ground condition, access for construction equipment, effect of installation on adjacent foundation, local construction practice, and availability of construction material and relative cost.

The shallow foundation system is used when the soil has high bearing capacity and can carry superstructure loads with small settlement such as Northeast region of Thailand. On the other hand, in some areas, the ground conditions are unsuitable for a shallow foundation system to support heavy-load buildings where the vertical and lateral loadings imposed on the foundation are significant. In these circumstances, the deep foundation system, particularly with the usage of piled foundations, are more applicable. The use of piled foundations is also a method of overcoming the difficulties of foundation on soft soil, which has low shear strength and high compressibility such as soft Bangkok clay.

Based on the construction method, piled foundations can be classified into two predominant types, being driven piles and cast in-situ piles. Driven pile foundations can be made from concrete, steel or timber. For reinforced concrete driven pile, it is prefabricated before placing at the construction site and it is driven to the ground using a pile hammer. The driven pile is easy to install; hence it becomes a common foundation construction in many projects. In addition, the transportation of the driven piles from the manufacturer to the construction site is more convenient and cost-effective when compared with the cast-in-situ pile method. However, the construction method of driven pile produces the noise, vibration, and soil movement, which might cause damage to the neighboring buildings.

The cast-in-situ or bored pile comprises of a reinforced concrete pile, which is constructed at the construction site by drilling a hole into the ground to the required depth, placing the reinforcement and then filling the steel tube with concrete. The installation of a cast-in-situ pile has two methods, namely the dry or wet process. The suitable installation process used at the construction site depends on the nature of the soil and the superstructure loads. For soft Bangkok clay, the dry-process bored piles are commonly used for low- to medium-rise buildings. However, the dry-process bored piles have two main disadvantages: low productivity and low load capacity, when compared with driven piles of the same diameter and length. The ultimate bearing capacity of dry-process bored piles at the construction site in central Bangkok area was recently investigated by Poonlappanish and Buasri (2017). The static pile load tests were conducted on 42 bored piles, which have diameters of 0.5 – 0.60 m and 19 – 21 m in length. Using the Mazurkiewicz's method, the average factor of safety was found to be over 2.0. The study on the installation productivity of 172

bored piles (0.50 m in diameter and 24 m in length) at a construction site in Bangkok was investigated by Monkaew and Nawalerspunya (2013). The approximate rate of productivity was 275.31 minutes/pile.

Soft Bangkok clay has a thickness of about 15-30 m with high water content and low shear strength (Horpibulsuk et al., 2007), consequently the installation of bored piles requires steel casing. The driving and extraction of the steel casing is time-consuming and requires a lot of labors. The low load capacity of dry-process bored pile is caused by the soil disturbance by driving and removal of the steel casing, which reduce soil friction around the pile (Skempton, 1966). Furthermore, the installation of cast-in-situ piles requires skillful supervision and quality control of all piling construction materials. This method also needs sufficient space for storage of materials used in the construction, which is not suitable for the limited space of the construction site.

To overcome these problems of using bored piles in Bangkok area, an alternative piling solution, designated as soil-cement screw piles (SCSP) has been introduced in Thailand. The SCSP is the combination of a screw pile (SP) with a soil-cement column (SCC), in which the SP is inserted in a previously installed SCC. The SCC can be rapidly installed in soft Bangkok clay as a friction pile without the requirement of a steel casing. Since the strength of SCC is relatively low, the inserted SP is used to stiffen and strengthen the SCC to prevent pile failure. Previous researchers have demonstrated the successful usage of SCC to support low-rise buildings and road embankments (Shen et al., 2013a and b, 2017; Wang et al., 2018, 2019).

The SCSP construction method provides many advantages including easy and quick installation, minimal dewatering, and minimal equipment. It also provides high tensile and acceptable compressive capacities and produces minimal noise and vibration during installation (Zhang et al., Livneh & El Naggar, 2008; Sakr, 2009, 2011; Schmidt & Nasr, 2004; 1998). This SCSP by the Thai Piling Rig Co., Ltd has successfully used in piled foundation in the two important projects: The Royal Chitralada Pasteurized Milk Factory and The Royal Chitralada Rice Mill of Chitralada Palace, Bangkok Thailand, which required significantly low noise, clean and rapid construction.

SCSP entered the Thailand market by Thai Piling Rig Co., Ltd in the early of 2018 and this piling system is expected to be very popular due to its many advantages over conventional driven and bored piles. The success of construction project of SCSP depends mainly on three indicators of performance including construction schedule, cost, and quality (Kim et al., 2020; McKim et al., 2000; Moon et al., 2020), which is the focus of this research. A quality performance is the precise determination of ultimate load capacity of SCSP at a construction site using a simple and rational closed-form calculation and/or pile load test. This precise determination leads to the best selection of the SCSP section properties and length suitable for cost and time conditions.

To the best authors' knowledge, a complete research study on the determination of load capacity and the analysis of economic decision of SCSP in term of construction cost and time, which is the key success of construction management, has not been previously undertaken. Therefore, this research forms an innovative study on construction engineering and management on SCSP system. The outcomes

of this research will result in the development of guideline for the effective design of SCSP, in term of their load capacity calculation construction time and installation cost in soft clays, such as Bangkok clay.

3.2 METHODOLOGY

In order to investigate the effectiveness of the SCSP, the ultimate load capacity and execution cost and time of the SCSP were compared with those of soil cement column (SCC) and SP. The ultimate load capacity of SP and SCSP were measured by static load tests. The results of load tests on SCSP were then compared with the available load predictive methods including the cylindrical method proposed by Rao and Prasad (1993), the individual bearing method by Sakr (2009) and the soil cement column method by Bergado et al. (1996). The undrained shear strength (c_u) of SCC, which is one of the most important parameters in the estimation of the ultimate load capacity of SCSP, is determined from the unconfined compressive strength of the field cored samples.

3.2.1 Detail of studied piles

Figure 3.1 shows a schematic of studied SP. The SP was made of circular hollow steel pipe with helices at every 1.5 m and the filled concrete in the pipe. The hollow steel pipe (JIS G 3444-2010) had a diameter of 0.20 m, thickness of 4.5 mm, cross-sectional area (A_s) of 29.94 cm², and tensile strength (f_s) of 240 MPa. The helix was a hot rolled steel plate with a diameter of 0.40 m and 5 mm thickness. The filled concrete had a cross-sectional area (A_c) of 337.51 cm² and compressive strength (f_c) of 18 MPa. The SPs were galvanized to prevent the rust and corrosion in accordance with ASTM-A123 (2017).

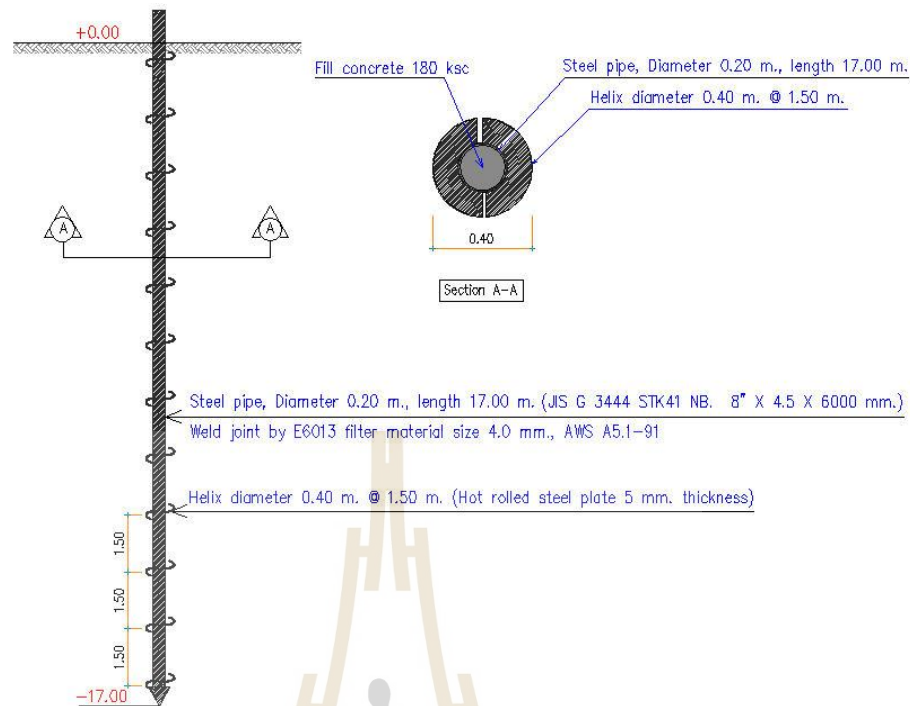


Figure 3.1. A schematic of screw piles.

Four different types of studied piles are shown in **Figure 3.2**. All piles were installed at a fixed depth of 17.0 m. Pile no 1 (**Figure 3.2a**) was a SCC with a diameter of 0.6 m (without screw pile) and Pile no 2 (**Figure 3.2b**) was SP. Pile no 3 and 4 (**Figure 3.2c and 3.2d**) were partial SCSP and full SCSP, respectively where the SP was installed in the SCC. A partial SCSP is a combination of SP (17.0 m length) and SCC with a diameter of 0.6 m and a length of 13 m from the ground surface. A full SCSP comprises SP (17.0 m length) and the SCC with a diameter of 0.6 m and a length of 17.0 m.

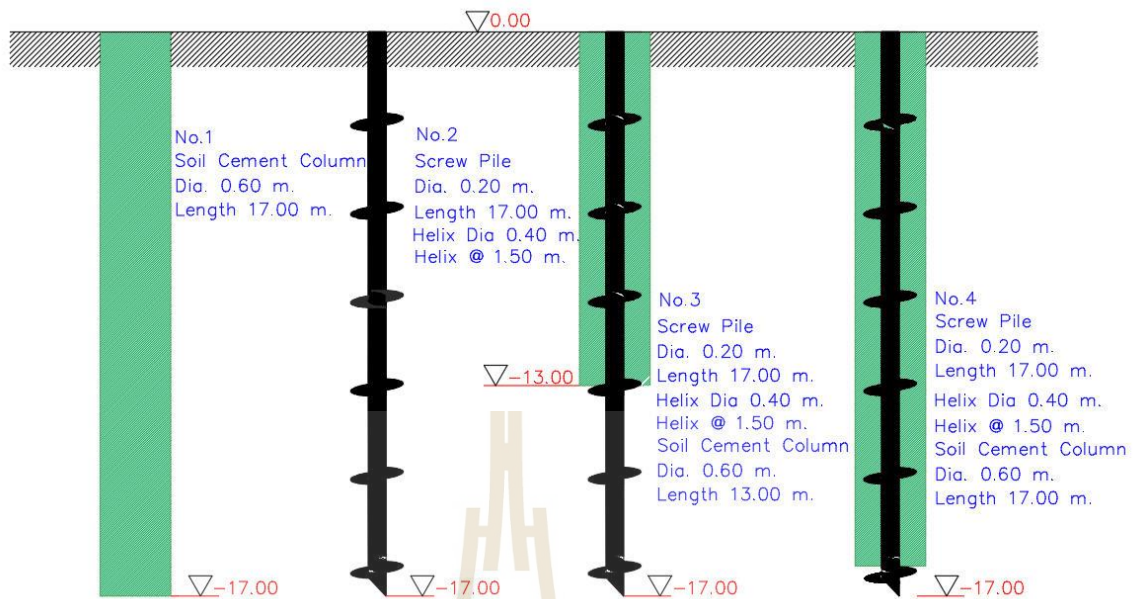


Figure 3.2. Types of studied piles: a) SCC, b) SP, c) Partial SCSP and d) Full SCSP.

The construction site was located at Nongchok District, Bangkok, Thailand. The soil profile varied from a very soft to a stiff clay as shown in **Figure 3.3**. The SCC (Pile no 1) was installed by the wet mixing method. The cement content of 200 kg/m³ of soil and the water to cement (w/c) ratio of 1.0 were used for SCC execution. The installation (both for penetration and withdrawal) rate was 1.0 m/min, which was recommended by Horpibulsk et al. (2011) and Srijaroen et al. (2014) for soft Bangkok clay. The SP (Pile no 2) was installed to the depth of 17.0 m by the installation machine as shown in **Figure 3.4**. The execution process of the partial SCSP (Pile no 3) and full SCSP (Pile no 4) was similar. The SCC with 0.6 m diameter was firstly installed by the wet mixing method of deep mixing machine to the designed depths of 13.0 m and 17.0 m for pile no 3 and pile no 4, respectively. The 17.0 m length of SP was then immediately installed at the center of the SCC for both partial and full SCSP. The hollow steel pile was next filled with concrete.

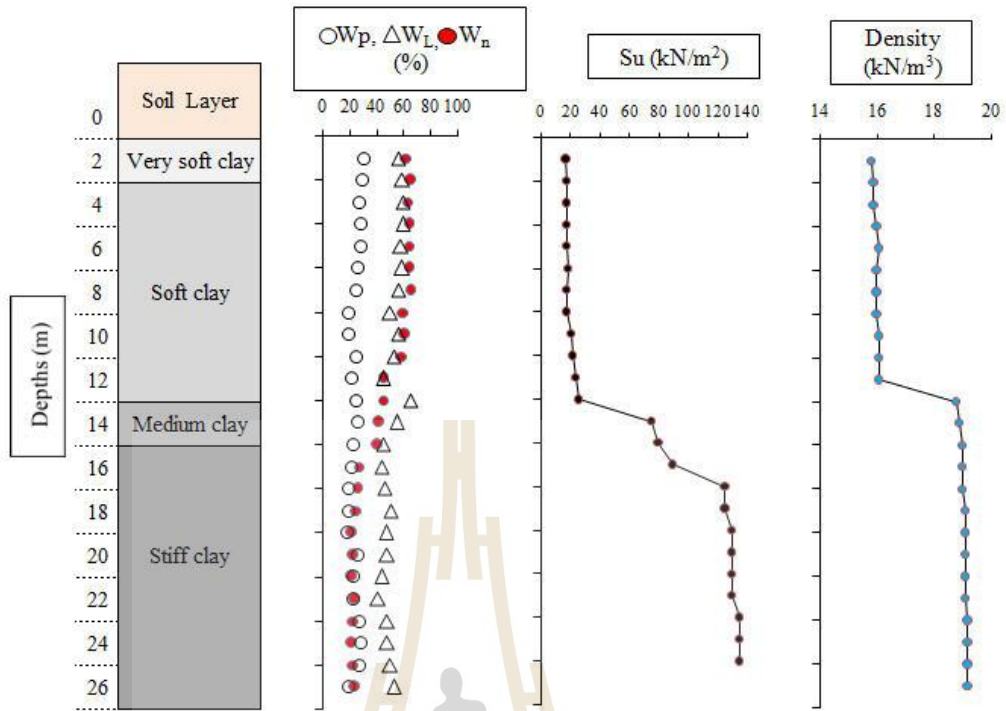


Figure 3.3. The soil profile at the construction site, Nongchok District, Thailand.



Figure 3.4. The installation process of SP and SCSP.

3.2.2 Determination of ultimate bearing capacity

3.2.2.1 Static load test

The static load test was performed in accordance with ASTM-D1143 (2013); the loading was incrementally applied on the piles, and the corresponding settlement was measured to produce the load-settlement curves. For the partial and full SCSP, the loading was applied on SP via a concrete pile cap. The ultimate load capacity of the test piles was calculated using Butler and Hoy (1976) method that defines the ultimate load as the load at the intersection of the tangent slope (0.05 in/ton) and the tangent to the initial straight portion of the curve, or to a

line that is parallel to the rebound portion of the curve. The target design safe load for SP, partial and full SCSP (Piles no 2, 3 and 4) was 400 kN for this study. Whereas for SCC (Pile no 1), the design safe load at 68 kN.

The static load testing apparatus (**Figure 3.5**) consists of:

- The reaction beams (steel girders) were laid across the test pile.
- The two reference beams (channel 125 x 65 x 5 mm) were cross connected and laid on the support, which was firmly embedded in ground with one fix and the other end free.
- The hydraulic jack with a capacity of 3000 kN was used to apply load on the pile head.
- The ball bearing was inserted between the reaction beam and the hydraulic jack to provide a non-eccentric load to pile head.
- The four dial gauge micrometers 0 – 50 mm with an accuracy of 0.01 mm were used to monitor the pile movements by mounting between the pile head and reference beam.
- The leveling instrument with an accuracy of 0.01 mm was used to check the relative movements of the test pile head and reference beam. Reading was made on fixed ruler scale on the reading point (1 point at pile head and 2 points at reference beam).

For Pile no 2, 3 and 4, the static load test was carried out according to ASTM-D1143 (2013) by standard loading procedure with load sequence in percentage of design load at 400 kN. In this study, two cycles of test were performed by the following procedures:

Cycle 1 (maximum to 200% of the design load)

- a. The applied loads were gradually increased from initial 0 to 25%, 50%, 75%, 100%, 125%, 175%, and 200% of the design load.
- b. The load increment was added only when the settlement was less than 0.25 mm per hour or after two hours of the previous achieved load increment.
- c. At each load increment, load, settlement and time were recorded at 1, 2, 4, 8, 15, 30, 60, 90, 120, 240 minutes and every 2 hour with an accuracy of at least 0.01 mm.
- d. The maximum load was kept constant for at least 24 hours and then reduced to 150%, 100%, 50% and 0% of the design load, respectively. Each load was maintained until the rate of settlement greater than 0.25 mm per hour or after two hours.
- e. At initial load, the rebound movements were recorded at 1, 2, 4, 8, 15, 30, 40, 60 minutes and every hour thereafter until a constant settlement was reached.

Cycle 2 (Loading in excess of standard test load)

- a. The applied loads were gradually increased from initial 0 to 25%, 50%, 75%, 100%, 125%, 175%, and 200% of the design load.
- b. When each load increment was achieved, the next load increment was added every after 20 minute.
- c. The load was added gradually by increasing 10% of the design load until pile failure.
- d. At each load increment, load, settlement and time were recorded at 1, 2, 4, 8, 15 and 20 minutes with an accuracy of at least 0.01 mm.

For SCC (Pile no 1), the static load test was carried out in accordance with ASTM-D1143 (2013) by quick load test method with load sequence in percentage of design load at 68 kN. The cycle of test was performed by the following procedures:

- a. The load was added gradually by increasing 15% of the design load until pile failure.
- b. At each load increment, load, settlement and time were recorded at 5 minutes with an accuracy of at least 0.01 mm.



Figure 3.5. Static load test apparatus.

3.2.2.2 Conventional calculation methods

The cylindrical shear method (Rao & Prasad, 1993) and individual bearing method (Sakr, 2009) were used to estimate the ultimate load capacities of the SP, while the soil cement column method (Bergado et al., 1996) was

used for the SCC and full SCSP, whereby the undrained shear strength of SCC at 28 days of curing was used for calculation.

3.2.2.2.1 Cylindrical shear method

The cylindrical shear method was pioneered by Mitsch and Clemence (1985) and Mooney et al. (1985) to estimate the axial capacity of SP in sand and clay/silt, respectively. **Figure 3.6** shows the cylindrical shear model assuming that the cylindrical shear failure is formed in the connection between the top and bottom helices. Nasr (2004, 2009) concluded that the ultimate load capacity is influenced by the number of helices, the pile geometry, the soil condition and the helical spacing. The ultimate load capacity is the sum of the end bearing resistance below the bottom helix, the sum of shear resistance along the cylindrical shear surface and the shaft friction above the top helix as shown in Eq. (1) (Hawkins & Thorsten, 2009; Livneh & El Naggar, 2008; Sakr, 2009, 2011; Tappenden et al., 2009; Zhang et al., 1998):

$$Q_{ult} = Q_{helix} + Q_{bearing} + Q_{shaft} \quad (3.1)$$

where Q_{ult} = ultimate load capacity; Q_{helix} = shearing resistance mobilized along the cylindrical failure surface; $Q_{bearing}$ = end bearing capacity; and Q_{shaft} = resistance developed along the steel shaft.

The ultimate load capacity of SP in cohesive soil is therefore derived from Eq. (1) as follows (Mooney et al. 1985):

$$Q_{ult} = S_f(\pi DL_c)c_u + A_H c_u N_c + \pi d H_{eff} \alpha c_u \quad (3.2)$$

where S_f = spacing ratio factor; D = diameter of pile helix; L_c = distance between top and bottom helical plates; A_H = area of the helix; c_u = undrained shear strength of soil; N_c = bearing capacity factor for cohesive soils; d = diameter of pile shaft; H_{eff} = effective length of pile above top helix; and α = adhesion factor. Rao and Prasad (1993) reported that the spacing to diameter (S/D) ratio of pile helix significantly affects the ultimate load capacity. Increasing S/D ratio results in reduction of the ultimate load capacity. Rao and Prasad (1993) proposed equations to determine the spacing ratio factor (S_f) as follows:

$$\text{For } S/D < 1.5 \quad S_f = 1.00 \quad (3.3)$$

$$\text{For } 1.5 \leq S/D \leq 3.5 \quad S_f = 0.683 + 0.069(3.5 - S/D) \quad (3.4)$$

$$\text{For } 3.5 \leq S/D \leq 4.6 \quad S_f = 0.700 + 0.148(4.6 - S/D) \quad (3.5)$$

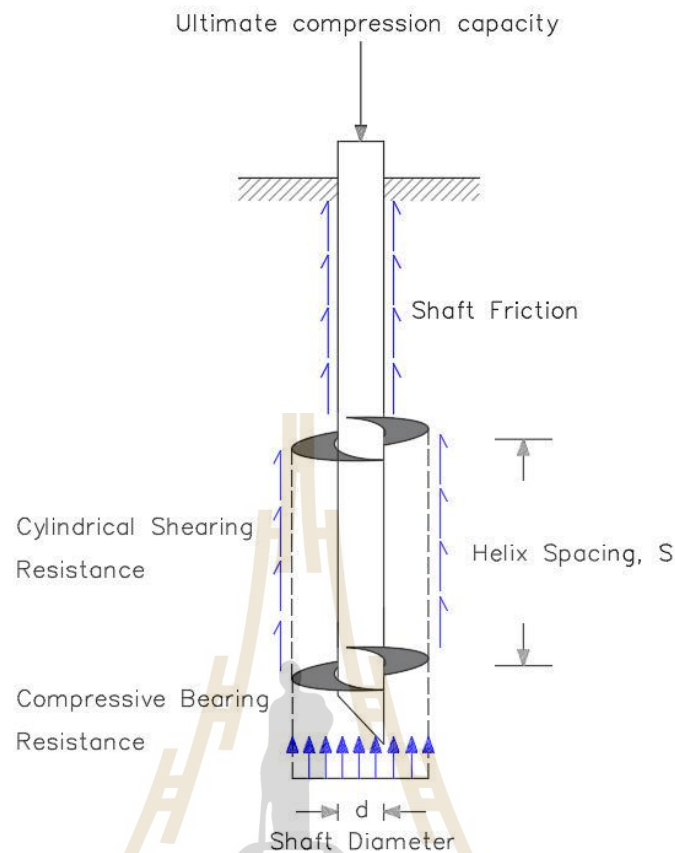


Figure 3.6. Cylindrical shear model for screw pile under compression load.

3.2.2.2.2 Individual bearing method

Adams and Klym (1972) reported that the load capacity of SP can be estimated individually, where the spacing distance between each plate is large enough. **Figure 3.7** shows the individual bearing method. The parameters affecting the load capacity are screw plate bearing area and the undisturbed surrounding soil. Furthermore, the equations for individual bearing method involves both the resistance from each individual helix and the shaft resistance. Therefore, the overall ultimate load capacity of the SP can be calculated by the sum of all the individual helical capacities along with the shaft resistance as

presented in Eq. (6) (Hawkins & Thorsten, 2009; Livneh & El Naggar, 2008; Sakr, 2009, 2011; Zhang et al., 1998).

$$Q_{ult} = \sum A_H c_u N_c \quad (3.6)$$

where A_H is the area of helix, c_u = undrained shear strength of soil, and N_c = bearing capacity factor for cohesive soils.

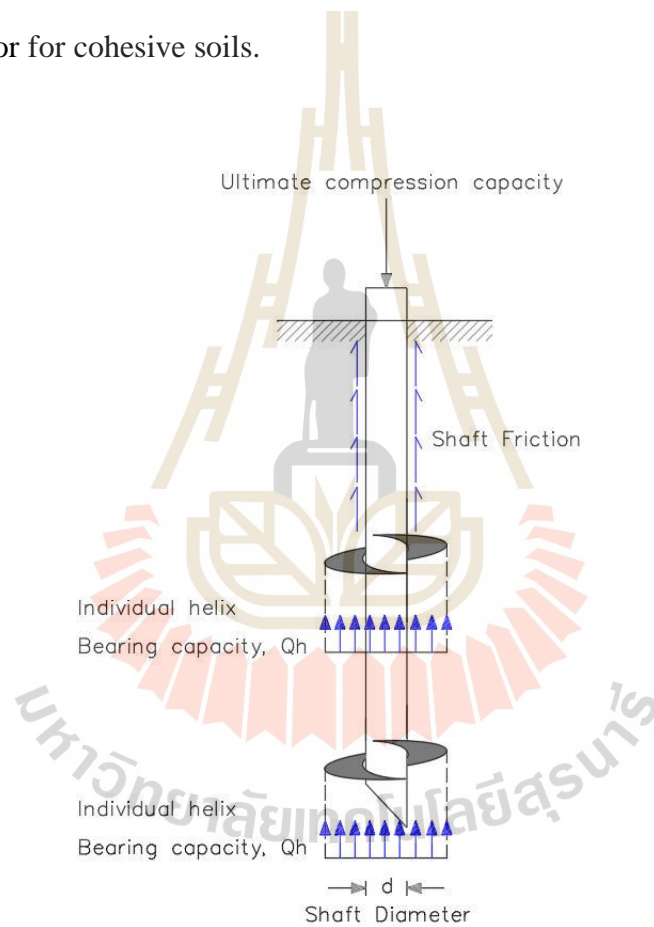


Figure 3.7. Individual bearing model for screw pile under compressive load.

3.2.2.2.3 Load capacity of SCC

The load capacity of a single SCC can be estimated based on the mode of failure by either soil failure or column failure. The ultimate load capacity of SCC in soft clay for soil failure mode can be calculated from Eq. (7) (Bergado et al., 1996):

$$Q_{ult,soil} = (\pi dH + 2.25\pi d^2)c_u \quad (3.7)$$

where $Q_{ult,soil}$ is the load capacity of single column due to soil failure; d is the diameter of the column; and H is the column length. It has been assumed that the skin resistance is equal to the undrained shear strength of the surrounding clay and that the end resistance corresponds to $9c_u$.

Since the shear strength of the SCC is insignificantly influenced with the increase in column length (Horpibulsuk & Miura, 2001 and Horpibulsuk et al. 2011), the ultimate load capacity due to column failure is estimated by the following expression:

$$Q_{ult,col} = A_{col}q_{uf} \quad (3.8)$$

where $Q_{ult,col}$ is the load capacity due to column failure; A_{col} is the cross-sectional area of the column and q_{uf} is the field strength of the column.

3.3 RESULTS

After 28 days of curing, the cored samples were collected by a coring machine from the middle of SCC (Pile no 1) at every 1-meter depth for determination of

unconfined compressive strength (q_u). The cored samples were trimmed to the required nominal dimension of 50 mm in diameter and 100 mm in height. **Figure 3.8** shows the relationship between the SCC length and q_u , indicating the average $q_u = 730$ kPa. Comparing the ultimate load capacity calculated from Eqs. (7) and (8), the SCC fails in the mode of pile failure with $Q_{ult,col} = 207$ kN. **Figure 3.9** shows the load-settlement curve of SCC (Pile no 1) obtained from the field static load test. The measured ultimate load capacity (200 kN) was found to be in agreement with the predicted value (207 kN).

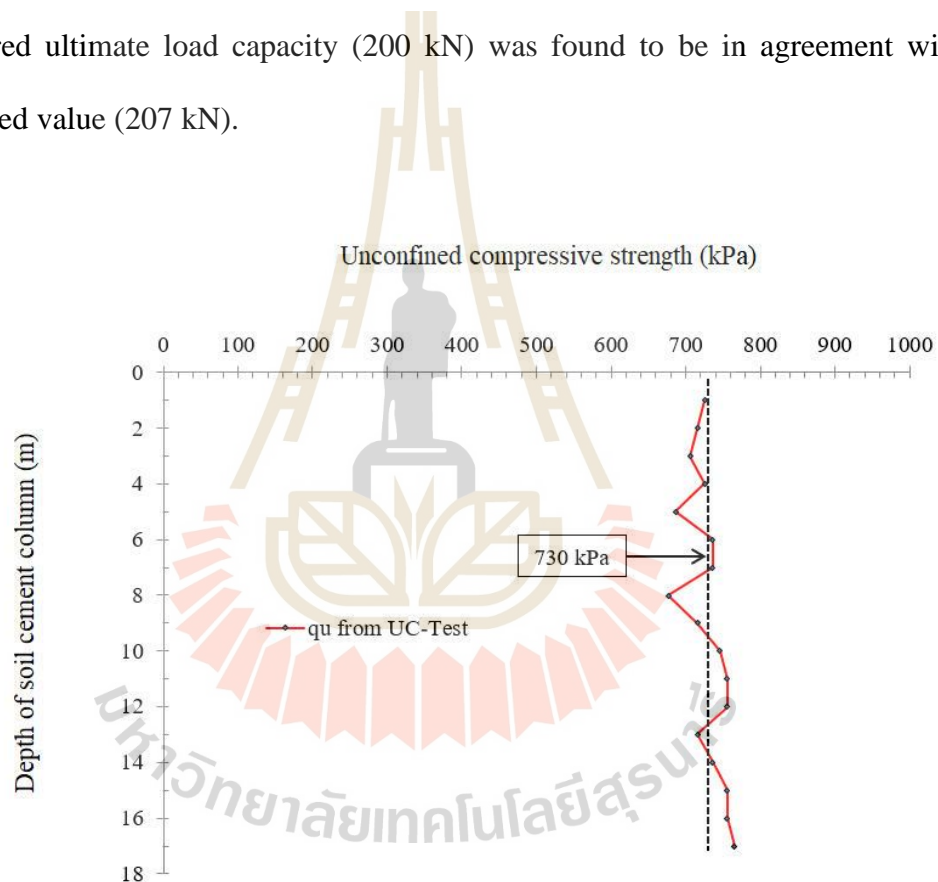


Figure 3.8. A relationship between the depth of SCC and its unconfined compressive strength.

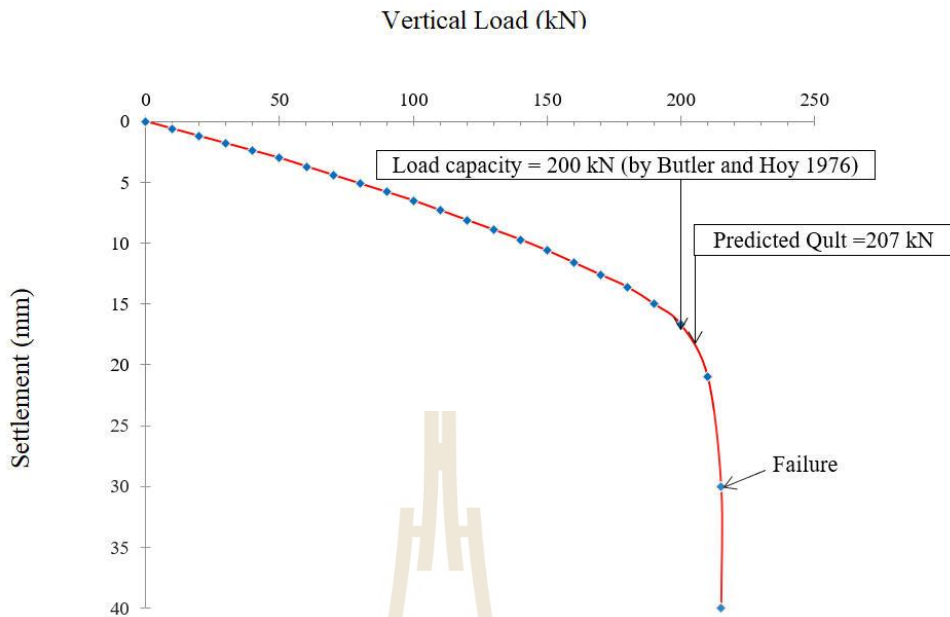


Figure 3.9. Load-settlement curve of SCC (Pile no 1).

The ultimate load capacity of SP (Pile no 2) obtained from the static load test is 565 kN as shown in **Figure 3.10**. It clearly demonstrates that the ultimate load capacity of SP is notably higher than that of SCC for the same length and soil condition. This indicates that the shear strength of SCC controls the load capacity of the piles studied. The ultimate load capacity of SP estimated by cylindrical shear method and individual bearing method is 781 kN and 553 kN, respectively. It is evident that the ultimate load capacity estimated by individual bearing method has a good agreement with static load test rather than cylindrical shear method for SP (Pile no. 2).

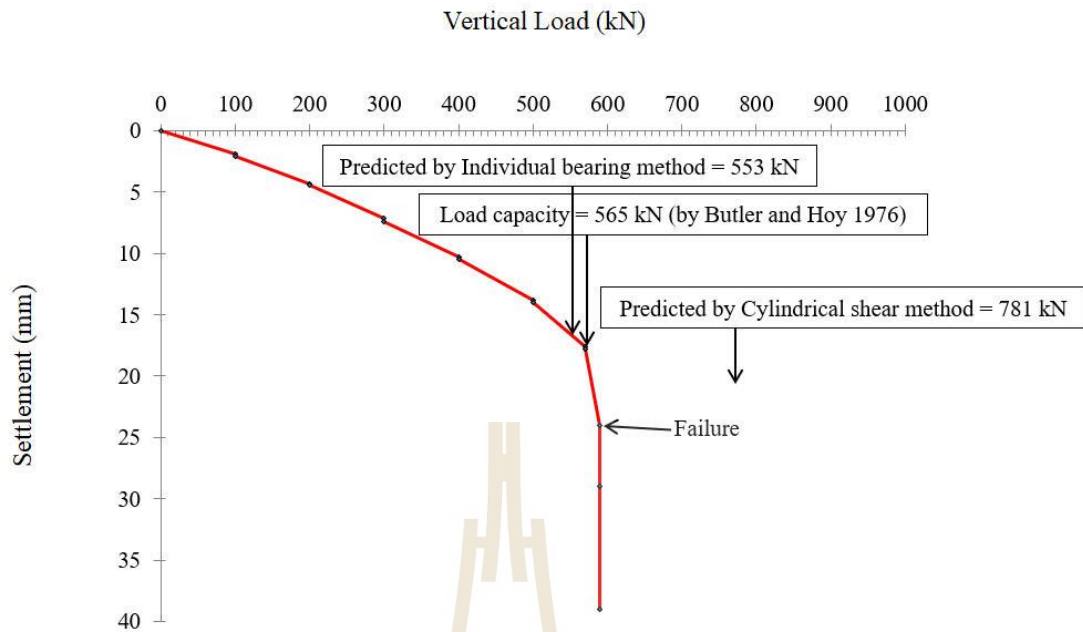


Figure 3.10. Load-settlement curve of SP (Pile no 2).

The ultimate load capacity of a partial SCSP (Pile no. 3) can be obtained from the static load test results as shown in **Figure 3.11**. The failure occurred in the cycle 2 of loading test (factor of safety = 2), whereby the load was maintaining around 900 kN while the pile continued to move downward. The ultimate load capacity of a partially SCSP (Pile no 3) was estimated to be 860 kN by Butler and Hoy (1976) method. It is interesting to note that the ultimate load capacity of the partial SCSP (Pile no 3) is higher than that of the SCC (Pile no 1) and SP (Pile no 2), respectively. In other words, the ultimate load capacity of SP can be improved significantly by the SCC. The ultimate load capacity is contributed from the individual bearing of SP and the load capacity of SCC (due to either soil failure or pile failure). Assuming that the pile material is strong enough against pile failure, the predicted ultimate load capacity is 870 kN, which is close to the measured value. It is thus evident that the partial

SCSP behaves as a rigid composite pile so that the load capacity is contributed from the soil failure mode.

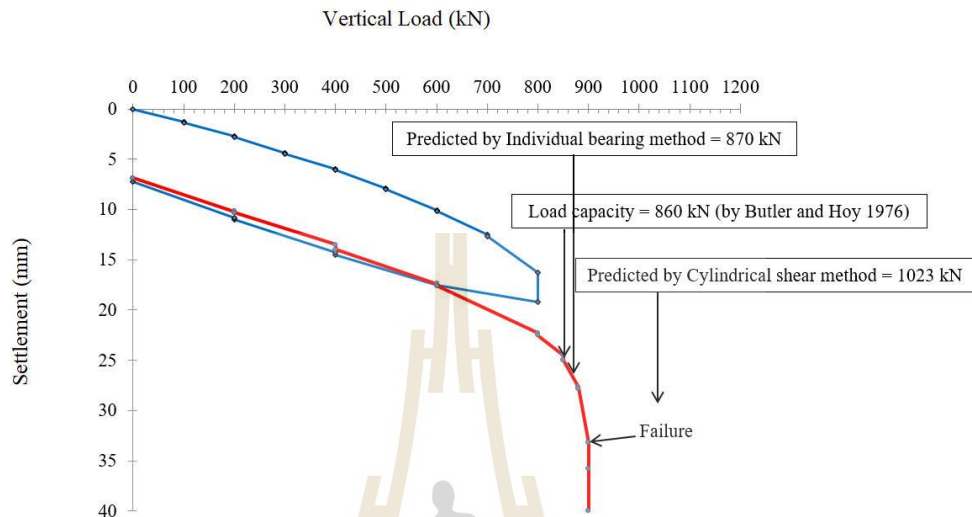


Figure 3.11. Load-settlement curve of a partially SCSP (Pile no 3).

The measured ultimate load capacity of the full SCSP (Pile no 4) is 1030 kN as depicted in **Figure 3.12**. It is evident that the full SCC can enhance the ultimate load capacity of the SP significantly as seen by the highest ultimate load capacity compared to the other studied piles. Similar to Pile no 3, assuming that the pile material is strong enough against the pile failure, the ultimate load capacity can be estimated from Eq. (7), which is controlled by the shear strength of surrounding clay. The predicted ultimate load capacity is therefore equal to 1089 kN, which is in good agreement with the measured value from the field test result. Assuming high interface shear strength between SP and SCC, the calculated ultimate load capacity of the test SCSP (Pile no 4) using the individual bearing method and shear strength of SCC (Eq.(6)), is equal to 3406 kN. This confirms that the failure of SCSP is governed by

the strength of surrounding clay without the failure at interface; both SCC and SP act as a rigid composite SCSP. **Table 3.1** summaries the predicted and measured ultimate load capacity of all studied piles. It is noted that the ultimate load capacity of all studied piles can be predicted satisfactorily by the proposed methods.

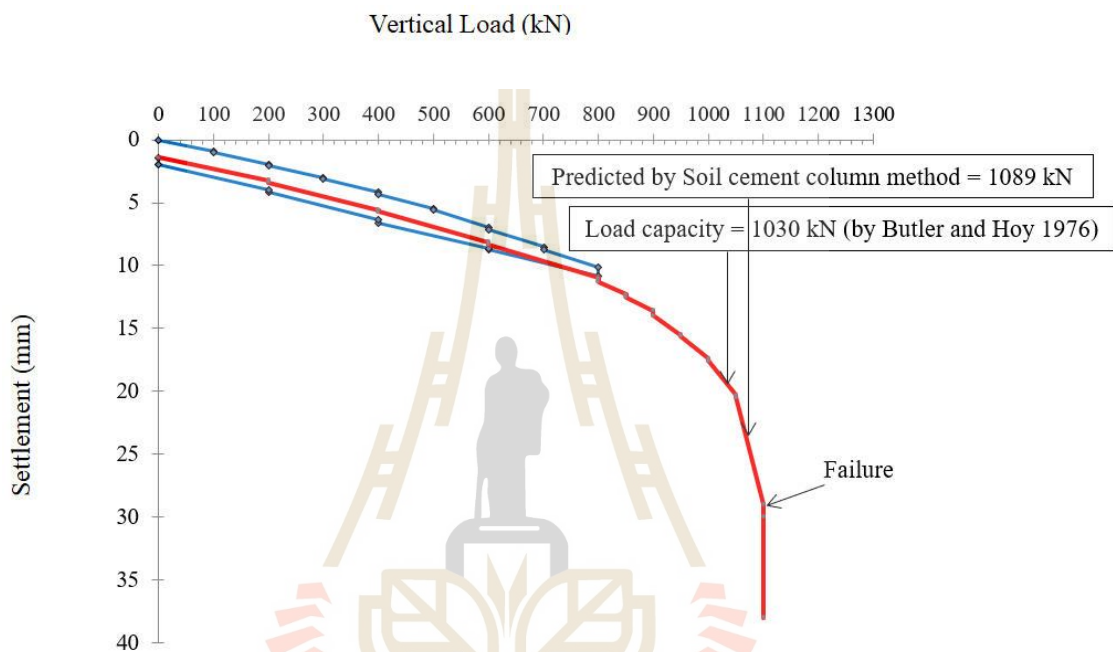


Figure 3.12 Load-settlement curve of a fully SCSP (Pile no 4).

Table 3.1 Summary of ultimate bearing capacity of all types of studied piles.

Type of piles	SCC (Dia. 0.6 m) Length	SP (Dia. 0.2 m) Length	Ultimate Bearing Capacity (kN)					
			Cylindrical	Individual	Soil	Cylindrical	Individual	Static
			Shear	Bearing	Cement	Shear and	Bearing and	Load
			Method	Method	Column	Soil Cement	Soil Cement	Test
				Method	Column	Column		
					Method	Method		
Pile no 1	17.0	-	-	-	207	-	-	200
Pile no 2	-	17.0	781	553	-	-	-	565
Pile no 3	13.0	17.0	4584	3190	-	1023	870	860
Pile no 4	17.0	17.0	5248	3406	1089	-	-	1030

3.4 ULTIMATE LOAD, TIME AND COST ANALYSIS

It is evident from the previous section that the ultimate load capacity of all studied piles was estimated based on soil failure mode. Ideally, the cost-effective design exists when the ultimate load capacity is mobilized from the full capacity of both pile material and surrounding soil equally. The ultimate load capacity of SP due to the material failure is determined by the following expression:

$$Q_{ult} = f_c(A_c) + f_s(A_s) \quad (3.9)$$

Thus, the ultimate load capacity of SP (**Figure 3.1**) due to material failure (Eq. 9) is equal to 1300 kN ($f_c A_c = 595$ kN and $f_s A_s = 705$ kN), which is higher than that of all studied piles (due to soil failure) as shown in **Table 3.1**. This demonstrates uneconomical usage of the SP and SCSP. Therefore, it is important, in term of cost effectiveness, to analyze the ultimate load capacity of SP and SCSP, taking the value of 1300 kN (material failure) as a benchmark.

3.4.1 Screw Pile

For a particular diameter, the ultimate load capacity of SP is dependent on the length of the SP. The studied diameter of SP was fixed at 0.20 m as it is commonly available in the market. Based on the soil profile as shown in **Figure 3.3**, the relationship between the ultimate load and length of SP is shown in **Figure 3.13**. Using the individual bearing method, the calculated ultimate load of SP increases linearly with increasing the length and the ultimate load capacity of 1300 kN is reached at 27.5 m length (10 m longer than the test pile). In order to maximize the soil cement screw pile application, the optimum ultimate load capacity of SP and SCC combination must be appropriately estimated. The empirical methods are proposed to predict the ultimate load of SCSP in soft clay material. The cost analysis in terms of construction materials, labor, and time were studied to verify the SCSP performance.

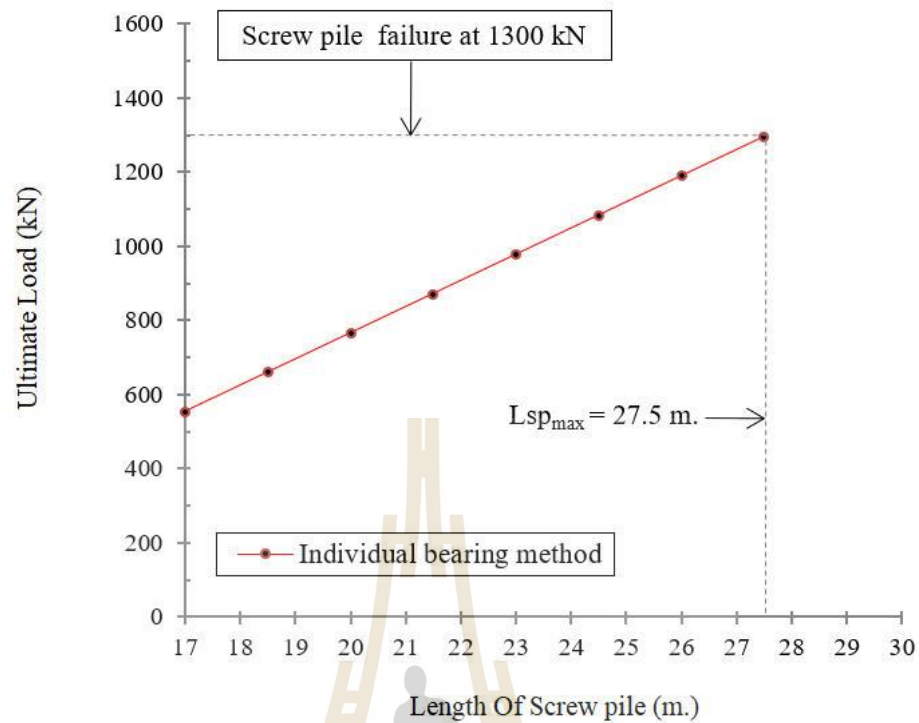


Figure 3.13. A relationship between ultimate load and length of screw pile.

3.4.2 Soil-Cement Screw Pile

To investigate the influence of SCC and SP on the ultimate load capacity of SCSP, the length of SCC was varied at 3 m, 5 m, 7 m, 9 m, 11 m, 13 m, 15 m, and 17 m whereas the length of SP was varied from 17 m to reach the ultimate load capacity of 1300 kN. The diameter of SCC was fixed at 0.6 m. The proposed equations to estimate the ultimate load capacity of the SCSP are shown in Eqs (3.10) and (3.11) for partial and full SCSP, respectively. The ultimate load capacity of the partial SCSP is the sum of ultimate load capacity of SCC, and individual helical capacities along with the shaft resistance and at pile base of SP below SCC. When calculate the ultimate load of the full SCSP, Eq. (10) will become Eq. (11) whereby the individual helical capacity is not considered $nA_H c_{u_j}$

$$Q_{ult} = \pi d(\alpha_i L_{scc_i} c_{u_i}) + 9nA_H c_{u_j} + 9A_{pb} c_{u_{pb}} \quad (3.10)$$

$$Q_{ult} = \pi d(\alpha_i L_{scc_i} c_{u_i}) + 9A_{ph} c_{u_{pb}} \quad (3.11)$$

where d = diameter of SCC; α = adhesion factor; L_{scc_i} = length of SCC; c_{u_i} = undrained shear strength of soil surrounding SCC; c_{u_j} = undrained shear strength of soil below SCC; $c_{u_{pb}}$ = undrained shear strength of soil layer at pile base; n = number of the helix below SCC; A_H = area of the helix (without filled concrete); and A_{pb} = combined area of the helix and shaft at pile base.

The estimation of ultimate load capacity was made based on the soil profile in **Figure 3.3**. **Figure 3.14** show relationship between the SP length versus ultimate load capacity of SCSP with various SCC lengths. The ultimate load capacity of SCSP increases with increasing SP length. At a particular length of SP, for example, length of SP = 18.80 m, the ultimate load capacity of partial SCSP slightly increases with increasing SCC length (from 3.0 m to 15.0 m). At a particular ultimate load of partial SCSP, the length of SP can be reduced by increasing the length of SCC and the SCSP has always higher ultimate load capacity than SP at the same pile length. For instance, to reach the benchmark ultimate load capacity of 1300 kN, the SP lengths for the partial SCSP with SCC = 3.0 m and 15.0 m are 26.5 m and 21.5 m, respectively. Whereas, the length of SP for the full SCSP is only 18.8 m. In other words, for the partial SCSP with SCC = 3.00 m and SP = 26.50 m (SP equal to about 9 times of SCC), the SP length have to increase about 55.9% to reach the benchmark ultimate load capacity. For the partial SCSP with SCC = 15.00 m and SP = 21.50 m (SP equal to about 1.5 times of SCC), the SP length have to increase about 26.5%, while for the

full SCSP, the SP length have to increase only about 10.6% to reach the benchmark ultimate load capacity. This indicates the economic advantage of the full SCSP application in term of raw material cost, because the SCC material is cheaper than the SP material for the same length.

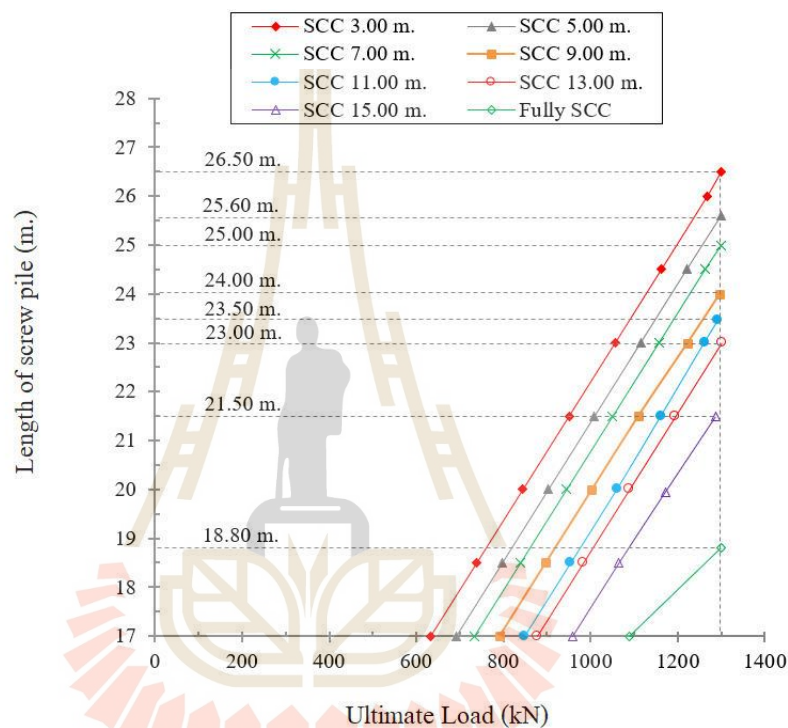


Figure 3.14 Relationships between length of screw pile versus ultimate load of SCSP at various lengths of SCC.

The undrained shear strength of soil mobilized by the helical anchor affects the load capacity of SP (Ruberti, 2015). Hence, the undrained shear strength of SCC must be studied to confirm the stability of the SCSP. There are 2 conditions in the calculation of ultimate load capacity for SCSP: failure at the interface of SCC and SP and the failure in surrounding soil. To confirm that no failure at the interface of SCC

and SP occurs, the Q_{ult} was first calculated using Eqs. (10) and (11) for partial and full SCP and with undrained shear strengths (c_u) of surrounding clay. The Q_{ult} results were used as controlled values and then the back-calculation method was performed to determine the required minimum c_u value of the SCC, which cause the interface failure between SCC and SP. A relationship between the SCC friction and its undrained shear strength of SCC is shown in **Figure 3.15**. The SCC friction is defined as the maximum force that results in the interface failure between SCC and SP. The q_u of SCC for a given SCC friction is back-calculated from Eq. (3.6) by taking SCC friction as Q_{ult} . The q_u for various SCC frictions is calculated to be in a range of 120 to 170 kPa for the partial SCSP, while it is 186 kPa for the full SCSP. This means that the partial SCSP and the full SCSP require a minimum q_u of about 120 to 170 kPa and about 186 kPa within the SCC to ensure no failure at the SCC and SP interface. However, the typical q_u value of about 600 kPa at 28 days of curing was used for SCC in soft Bangkok clay. It indicates that the design q_u value is significantly higher than the required q_u values, which confirms the excellent bonding between SP and SCC (no interface failure between SCC and SP).

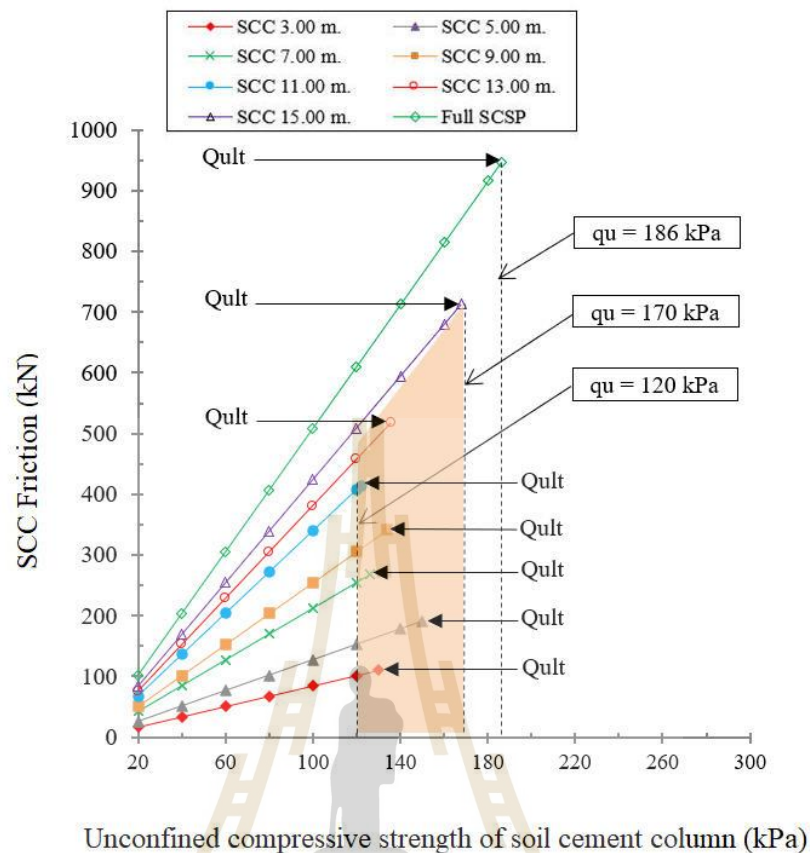


Figure 3.15 Relationships between SCC friction versus unconfined compressive strength of SCC.

The cost of SCSP execution was also studied to illustrate the economic advantage of its application in soft Bangkok clay. The execution costs included those of raw materials for the SCC and SP, as well as labor costs based on the local construction rates in Thailand for 2018. The calculated cost versus ultimate load relationship of SP, partial SCSP and full SCSP is plotted in **Figure 3.16** and the corresponding execution time and unit cost are shown **Table 3.2**. The execution cost including material and labor expenses is 37.5 US dollars per 1 m length for SP and 8.85 US dollars per 1 m length for SCC. It is evident that the execution cost of SP is 4.2 times higher than that of SCC for the same pile length. **Figure 3.16** shows that for

a particular ultimate load, the execution cost of SP is the highest while the execution cost of SCSP is the lowest. The longer SCC length in partial and full SCSP can reduce the SP length for the same target ultimate load capacity. In other words, the execution cost of partial and full SCSP is governed by the SCC length; the longer SCC length results in the cheaper execution cost. For example, at the benchmark ultimate load at 1300 kN, the execution cost is only 871 US dollars for the full SCSP with 18.8 m pile length while it is 1030 US dollars for the SP with 26.50 m pile length (see **Figures 3.14** and **3.16**). Overall, the execution cost of full SCSP is approximately 15% lower than that of SP.

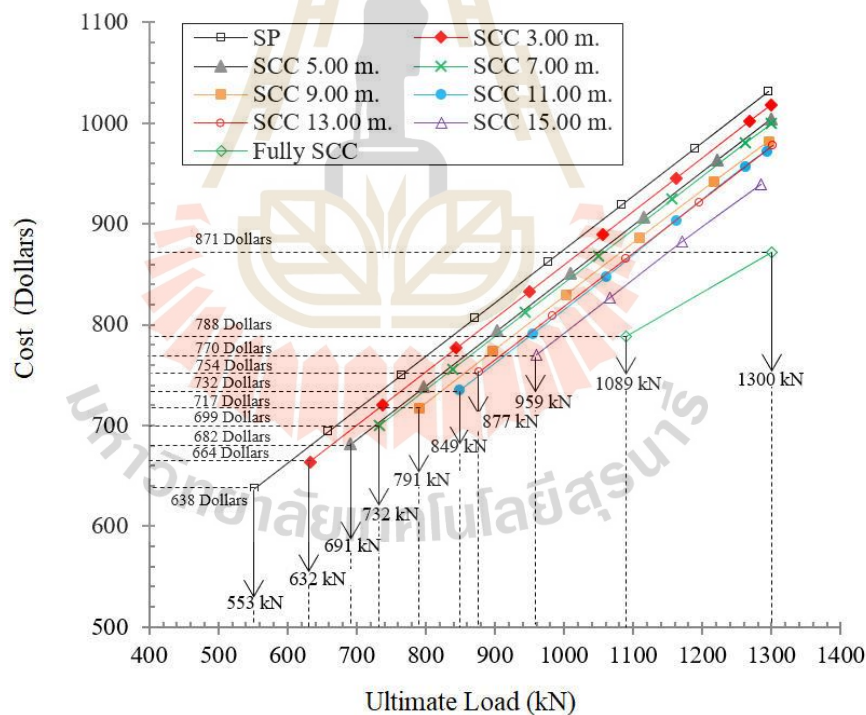


Figure 3.16 Relationships between cost versus ultimate load of SP and SCSP.

Table 3.2 Cost and time analysis of SP and SCSP execution.

Pile Type	Pattern	SCC (m)	SP (m)	Q_{ult} (kN)	Q_a (kN) (FS. = 2.50)	Time of installation (hr./no.)	Total Cost (US dollars)	Unit Cost (dollars /kN)
SP	1	-	17.00	553	221	0.50	637.50	2.88
Partially SCSP	2	3.00	17.00	632	253	0.60	664.05	2.62
	3	5.00	17.00	691	273	0.70	681.75	2.50
	4	7.00	17.00	732	293	0.80	699.45	2.39
	5	9.00	17.00	791	317	0.90	717.15	2.26
	6	11.00	17.00	851	340	1.00	734.85	2.16
	7	13.00	17.00	877	351	1.10	752.55	2.14
	8	15.00	17.00	959	384	1.20	770.25	2.00
Fully SCSP	9	17.00	17.00	1089	436	1.30	787.95	1.80
	10	18.80	18.80	1300	520	1.40	871.38	1.68
Bore Pile (Dia.0.60)	11	-	-	1300	520	3.50	843.75	1.62

Remark

Execution cost of SCC with 0.6 m diameter = 8.85 dollars/m (material cost = 3.40 dollars/m, and labor cost = 5.45 dollars/m)

Execution cost of SP = 37.5 dollars/m (material cost = 18 dollars/m, and labor cost = 19.5 dollars/m)

Execution cost of dry-process bored pile = 40.18 dollars /m (material cost = 24.60 dollars/m, labor cost = 15.58 dollars/m)

1 US dollar = 32 baht

When compared to the dry-process bored pile commonly used in Thailand, it is evident that the execution cost of both the full SCSP and the bored pile is essentially similar for the same target ultimate load as seen **Table 3.2**. The required pile length of bored pile is slightly longer than that of full SCSP because of the friction between pile and surrounding soil being lower due to the soil removal for installation of reinforcement and filling of concrete.

Table 3.2 shows that the execution time for SP is the lowest of 0.5 hour/pile while the execution time for the full SCSP is the highest of 1.3 hour/pile (the execution time for the SCC is approximately 0.8 hour/pile) at the same pile length of 17 m. In other words, the execution time is 0.03, 0.05 and 0.08 hour/m length for SP, SCC and full SCSP; the execution time of the full SCSP is approximately 2.5 times longer than that of the SP. It is evident that the execution time of SCC governs the execution time of partial and full SCSP. The execution time of SCSP increases with the increase in the SCC length. It is also noted that the execution time of dry-process bored pile is 2.5 times longer than that of full SCSP.

The unit cost of SP, partial and full SCSP and dry-process bored pile at various pile lengths is also presented in **Table 3.2**. The unit cost of SP is found to be highest of 2.88 dollars/kN while the unit cost of full SCSP and bored pile is more or less than same and is found to be lowest of approximately 1.62 to 1.80 dollars/kN. As a result, the application of the full SCSP and bored pile has more economical benefits than both partial SCSP and SP under the same ultimate load design. But the partial SCSP and SP have more advantage in term of construction time and is suitable for a time-constrained project. When comparing the full SCSP with the traditional dry-process bored pile at the same target ultimate load capacity, the full SCSP has higher

efficiency and productivity than the bored pile. A stepwise procedure for designing the ultimate bearing capacity of SCSP at optimal time and cost based on the critical analysis of the test results is suggested as follows:

1. Conduct the in-situ soil investigation at the construction site and laboratory test on soil samples to obtain soil profiles and undrained shear strength (c_u).
2. Determine the relationship between ultimate load capacity of SCSP versus SCC and SP lengths (*see Figure 3.14*). From the target ultimate load, determine SP and SCC lengths from the developed relationship.
3. Determine required c_u of SCC to have sufficient SCC friction for each set of calculated SP and SCC (*see Figure 3.15*).
4. Plot the relationship between execution cost and ultimate load capacity (*see Figure 3.16*) and determine the corresponding execution time.
5. Select the SCC and SP lengths to meet the time and cost criteria of the construction project.

3.5 CONCLUSIONS

This research paper presented the ultimate load, time and cost analysis and suggested effective design method for soft Bangkok clay. The cost and time of executing SCSP were also compared with those of traditional dry-process bored pile to illustrate the advantage of SCSP. The ultimate load capacity of the piles studied was examined by the field static load test and compared with the conventional design methods. The ultimate load capacity of SP was significantly enhanced by the SCC. The full SCSP provided the highest ultimate load capacity comparing to SCC, SP, and partial SCSP at the same pile length. The conventional individual bearing method

could be used to estimate the ultimate load capacity of SP. The load capacity predictive equations for both partial and full SCSP due to soil failure were proposed and validated based on the field static pile load test results. The equations are applicable for soft Bangkok clay and were successfully used for some construction projects in Thailand.

In Thailand, the application of the full SCSP can save on the installation cost when compared to SP and partial SCSP at the same required ultimate load. The execution (raw material and labor) cost of SP is 4.2 times higher than that of SCC for the same pile length. In other words, the execution cost of partial and full SCSP is governed by the SCC length; the longer the SCC length results in the cheaper execution cost. The execution time was 0.03, 0.05 and 0.08 hour/m length for SP, SCC and full SCSP; the execution time of the full SCSP was approximately 2.5 times longer than that of the SP. The execution time of SCSP increased with the increase in the SCC length. The unit cost of SP was found to be the highest while the unit cost of SCSP was found to be the lowest for the same target ultimate load. As a result, the application of the full SCSP has more economical benefits than both partial SCSP and SP. But the partial SCSP and SP have more advantage in term of construction time and is suitable for a time-constrained project. When comparing SCSP with the traditional dry-process bored pile at the same target ultimate load capacity, the SCSP had higher efficiency and productivity than the bored pile.

It should be kept in mind that the construction process and construction cost are strongly dependent on the current cost of construction materials, which varies from country to country. The outcome of this research will lead to the development of a guideline and code of practice of SCSP in soft Bangkok clay and other similar soil

conditions. It can also be used as a fundamental knowledge for the usage of SCSP in other countries, which have different soil profiles and construction costs. This practice research highlights the critical elements for the design and construction management (cost and time), installation process and load test results of SCSP, which are useful for construction industry particularly pertaining to the scheduling and cost performance of SCSP in construction projects. It provides recommendations for good practice in Thailand, which can be used as a reference for project engineers, developers, contractors, local authorities and other relevant end-users. Outcomes of this research are also applicable to other developed and developing countries.

3.6 REFERENCES

- Adams, J., & Klym, T. (1972). **A study of anchorages for transmission tower foundations.** Canadian Geotechnical Journal, 9(1), 89-104.
- ASTM-A123. (2017). **Standard Specification for Zinc (Hot-Dip Galvanized) Coatings on Iron and Steel Products:** West Conshohocken, PA; ASTM International, 2017.
- ASTM-D1143. (2013). **Standard Test Methods for Deep Foundations Under Static Axial Compressive Load:** West Conshohocken, PA; ASTM International, 2013.
- Bergado, D., Anderson, L., Miura, N., & Balasubramaniam, A. (1996). **Soft ground improvement in lowland and other environments.**
- Butler, H., & Hoy, H. E. (1976). **The Texas quick-load method for foundation load testing, user's manual.** Nasa Sti/recon Technical Report N, 77.

- Hawkins, K., & Thorsten, R. (2009). **Load test results—large diameter helical pipe piles** *Contemporary Topics in Deep Foundations* (pp. 488-495).
- Horpibulsk, S., Rachan, R., Suddepong, A., & Chinkulkijniwat, A. (2011). **Strength development in cement admixed Bangkok clay: laboratory and field investigations.** *Soils and Foundations*, 51(2), 239-251.
- Horpibulsuk, S., & Miura, N. (2001). **A new approach for studying behavior of cement stabilized clays.** Paper presented at the International Conference on soil mechanics and geotechnical engineering.
- Horpibulsuk, S., Shibuya, S., Fuenkajorn, K., & Katkan, W. (2007). **Assessment of engineering properties of Bangkok clay.** *Canadian Geotechnical Journal*, 44(2), 173-187.
- Kim, J. J., Miller, J. A., & Kim, S. (2020). **Cost Impacts of Change Orders due to Unforeseen Existing Conditions in Building Renovation Projects.** *Journal of Construction Engineering and Management*, 146(8), 04020094. doi:doi:10.1061/(ASCE)CO.1943-7862.0001888
- Livneh, B., & El Naggar, M. H. (2008). **Axial testing and numerical modeling of square shaft helical piles under compressive and tensile loading.** *Canadian Geotechnical Journal*, 45(8), 1142-1155.
- McKim, R., Hegazy, T., & Attalla, M. (2000). **Project Performance Control in Reconstruction Projects.** *Journal of Construction Engineering and Management*, 126(2), 137-141. doi:doi:10.1061/(ASCE)0733-9364(2000)126:2(137)

- Mitsch, M. P., & Clemence, S. P. (1985). **UPLIFT CAPACITY OF HELIX ANCHORS IN SAND (pp. 26-47)**: American Society of Civil Engineering (ASCE), New York.
- Monkaew, S., & Nawalerspunya, T. (2013). **Productivity of bored pile dry process**. The research in funded by faculty of engineering Rajamangla University of Technology Phra Nakhon (In Thai).
- Moon, H., Kim, K., Lee, H.-S., Park, M., Williams, T. P., Son, B., & Chun, J.-Y. (2020). **Cost Performance Comparison of Design-Build and Design-Bid-Build for Building and Civil Projects Using Mediation Analysis**. *Journal of Construction Engineering and Management*, 146(9), 04020113. doi:doi:10.1061/(ASCE)CO.1943-7862.0001873
- Mooney, J. S., Adamczak, S., & Clemence, S. P. (1985). **UPLIFT CAPACITY OF HELICAL ANCHORS IN CLAY AND SILT (pp. 48-72)**: American Society of Civil Engineers (ASCE).
- Nasr, M. (2004, 20-22 December). **Large capacity screw piles**. Paper presented at the Proceedings of the International Conference: Future Vision and Challenges for Urban Development, Cairo, Egypt.
- Nasr, M. (2009). **Performance-based design for helical piles Contemporary Topics in Deep Foundations (pp. 496-503)**.
- Poonlappanish, C., & Buasri, P. (2017). **Capacity of dry-process bored piles in Bangkok**. Paper presented at the The 22nd National Convention on Civil Engineering, Khao Yai Convention Center, Pak Chong, Nakhon Ratchasima, Thailand.

- Poulos, H. G., & Davis, E. H. (1980). **Pile foundation analysis and design**. New York: Wiley.
- Rao, S. N., & Prasad, Y. (1993). **Estimation of uplift capacity of helical anchors in clays**. *Journal of Geotechnical Engineering*, 119(2), 352-357.
- Ruberti, M. (2015). **Investigation of installation torque and torque-to-capacity relationship of screw-piles and helical anchors**.
- Sakr, M. (2009). **Performance of helical piles in oil sand**. *Canadian Geotechnical Journal*, 46(9), 1046-1061.
- Sakr, M. (2011). **Installation and performance characteristics of high capacity helical piles in cohesionless soils**. *DFI Journal-The Journal of the Deep Foundations Institute*, 5(1), 39-57.
- Schmidt, R., & Nasr, M. (2004). **Screw piles: uses and considerations**. *Structure magazine*, 29-31.
- Skempton, A. (1966). **Summing up Large bored piles (pp. 155-157)**: Thomas Telford Publishing.
- Srijaroen, C., Rachan, R., & Horpibulsuk, S. (2014). **Strength Development in Soil Cement Column and Soil Fly ash-Cement Column in Soft Bangkok Clay Deposit**. *KMUTT Research and Development Journal*, 37(2), 151-164.
- Tappenden, K., Sego, D., & Robertson, P. (2009). **Load transfer behavior of full-scale instrumented screw anchors** *Contemporary Topics in Deep Foundations (pp.472-479)*.

Zhang, D., Chalaturnyk, R., Robertson, P., Segoo, D., & Cyre, G. (1998). **Screw Anchor Test Program (Part I): Instrumentation, Site Characterization and Installation.** Paper presented at the Proc. 51st Canadian Geotech. Conf., Edmonton.



CHAPTER IV

APPLICATION OF SOIL CEMENT COLUMNS AS A TEMPORARY RETAINING WALL FOR NARROW DEEP EXCAVATION IN SOFT BANGKOK CLAY

4.1 Introduction

Soil excavation is practically constructed to maximize the underground construction project including office and parking space, storage, mechanical and electrical rooms, and living units. The excavation work is typically conducted with a stable slope to prevent the soil collapse in available area adjacent to the excavation site. In many cases, the construction site's property lines and surrounding conditions are the constraint of the soil excavation within the property lines especially in urban areas. Temporary earth retaining structure with or without support system to protect the soil collapse is therefore practically adapted. The design of excavation work depends on many factors including depth of excavation, geotechnical properties, groundwater table, superimposed vertical and lateral loads from surrounding buildings, and construction equipment and material storage. In other words, different types of retaining walls can be adapted depending upon construction procedures and methods.

In recent years, shallow (3 to 5 m depth) and narrow excavation projects in Bangkok area for the installation of water treatment tanks are remarkably increasing due to the rapid growth of urbanization in limited space of land. The temporary

retaining wall structure is vital for the underground excavation due to large compressibility and low shear strength of soft Bangkok clay. Steel sheet pile wall is commonly used as a temporary retaining wall in many excavation projects in Bangkok. However, the mobility of steel sheet pile and heavy rig into the confined site is the main barrier of using sheet pile wall for some construction projects. In addition, the vibration of sheet pile and soil movement during the installation process might cause a damage to neighboring buildings. The soil-cement column (SCC) wall using the deep cement-soil mixing (DCM) technique is therefore an alternative construction of a temporary retaining wall.

DCM is one of the effective ground improvement techniques that the cementing agents including lime, cement slurry, and cement mortar are injected into the ground for soil stabilization (Wang et al., 2020, Shen et al., 2003, Shen et al., 2008, Horpibulsuk et al., 2012). DCM technique has been successfully employed in various projects such as building, road, railway, embankment, highway, and airport (Horpibulsuk et al., 2011, Shen et al., 2013, Shen et al., 2008, Shen et al., 2009, Srijaroen, et al., 2021). DCM method was successfully used to improve the bearing capacity and embankment settlement of the Bangna-Bangpakong highway in Thailand (Bergado et al., 1999). Jamsawang et al. (2015) used two types of pile for the construction of Rama Hospital at Bangplee, Samutprakarn Province, near the Bangkok area. Type 1 was SCC of 0.5 m in diameter and 10.0 m length, while type 2 was stiffened SCC (SSCC) that eucalyptus wood (0.15 m in diameter and 6.0 m length) was installed in the middle of SCC. It was reported that the ultimate load capacity of SSCC was 250 kN, which was about 30% higher than that of SCC. Similarly, the performance of the SCC and the SSCC was compared via a full-scale

pile load tests in soft Bangkok clay (Jamsawang et al., 2010). The SCC had a diameter of 0.60 m and 7.0 m length. The SSCC consisted of SCC with a precast reinforced concrete cored pile (0.22 x 0.22 m) installed in the middle. The average ultimate vertical and lateral load capacities of SSCC were about 2.2 and 15 times higher than those of SCC, respectively.

The behavior of the test embankment constructed on SCC in soft Bangkok clay has been investigated by many researchers (Chen, 1990; Lin and Wong, 1999; and Lai et al., 2006). Vootipruex et al. (2011a) also performed the comparison study between SSCC (precast reinforced concrete core pile inserted in its center) and SCC constructed in the soft ground via a full-scale embankment load test and finite element simulation. It was indicated that the SSCC can reduce the vertical settlement and lateral movement about 40% and 60%, respectively when compared with SCC.

SCC was also used for excavation works to build foundation and basement of high-rise buildings (Wang et al., 2010). Jamsawang et al. (2017) investigated the behavior of SCC wall using a top-down support system for unbalanced deep excavation in soft Bangkok clay. It was found that the SCC wall significantly reduced the effect of unbalanced pressure. The ground movement during excavation was within an acceptable range and did not cause any defect to the unrestraint pile. Tanseng (2012) also indicated that the SCC wall with wall-strut system could be used to minimize the ground movement of tunnel construction in soft Bangkok clay. The amount of observed lateral movement was relatively low compared with the conventional sheet pile and diaphragm wall.

Many researchers have mainly studied on the stability of the SCC and SSCC walls in soft Bangkok clay via finite element method (FEM) and full-scale tests.

However, no studies have completely reported on the relationship among execution time and cost and stability of SCC and SSCC. The comparison of SCC and SSCC walls with the conventional sheet pile wall system in terms of execution time and cost and stability (factor of safety and lateral movement) is useful in selection of the suitable retaining structures for different constraints such as site accessibility to attain the target stability with reasonable construction cost and time. In this research, the calibration of FEM model was first carried by comparing the simulated results of constructed SCC and SSCC walls at a studied construction site in Bangkok with the corresponding field measurement. Then, a parametric study was performed to investigate the influence of various factors on wall movement, stability and construction cost and time. The influential studied parameters included types, patterns, and length of SCC and SSCC walls. The outcome of this research will facilitate an effective design and selection of SCC and SSCC walls and sheet pile wall as a temporary support system for excavation work in soft Bangkok clay to have an adequate factor of safety and minimal lateral movement at reasonable cost and time.

4.2 Field Case Study

4.2.1 Project description

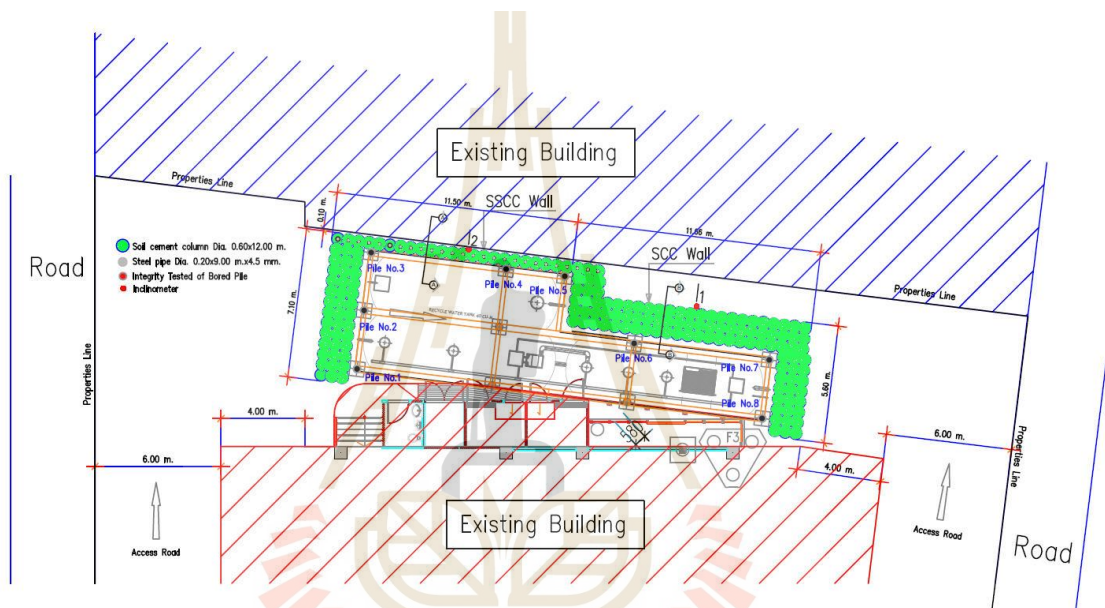
The construction site was located at Bangkok-Noi District, Bangkok, Thailand, and the site geometry is shown in **Figure 4.1a**. The excavation of up to 4.5-meter depth was required to install three huge recycled water tanks. This excavation is considered as shallow and narrow excavation and the 4.5 m deep excavation is common for the recycled water tank projects. The sheet pile wall with bracing typically used in soft Bangkok clay was not suitable at this site because the existing

buildings obstructed the entrance of the installation machine (**Figure 4.1a**). Due to the limitation of the property line of the construction site, two types of soil cement column wall, namely soil cement column (SCC) Wall and stiffened soil cement column (SSCC) Wall were designed as temporary walls in this project. The SCC was 0.6 m in diameter and 12.0 m length and was installed in 3 rows, designated as SCC-3Row Wall. While the SSCC consisted of the steel pipe (0.2 m in diameter and 9.0 m length) embedded in the middle of SCC (SSCC-1Row Wall) was installed in the confined area. **Figures 4.1b** and **4.1c** show the layouts and sections of SCC-3Row Wall and SSCC-1Row Wall.

Figure 4.2 demonstrates the construction sequence of this project. The construction of retaining wall and installation of recycled tanks took about 56 days. The construction process was started by the installation bored piles for about 7 days. The mobilization of equipment and the setup of plan mixing were prepared for 5 days. The SCC-3Row Wall was first installed for 8.5 days and followed by SSCC-1Row Wall installation for 2.5 days. Subsequently, the inclinometers were installed to measure the lateral movements behind the SCC-3Row Wall and SSCC-1Row Wall during the excavation and after the installation of recycled water tanks (**Figure 4.1a**). After 10 days of inclinometers installation, the excavation was commenced.

The soil excavation was carried out in two stages: (1) soil excavation to a depth of 2.0 m (for 2 days) and (2) soil excavation to a final depth of 4.5 m (for other 3 days). The first lateral movements were measured (28 days and 20 days after installation of SCC-3Row Wall and SSCC-1Row Wall, respectively). The duration for cutting pile head, and construction of lean concrete and basement was about 5 days. The installation of columns to support the recycled water tanks took about 4 days and

the installation of three recycled water tanks took other 4 days. The second lateral movement was then measured after the leaking test of recycled water tanks (41 days and 33 days after installation of SCC-3Row Wall and SSCC-1Row Wall, respectively). Finally, the filling sand was backfilled for constructing the concrete pavement on the top of water tanks (3 days).



(a) Site geometry.

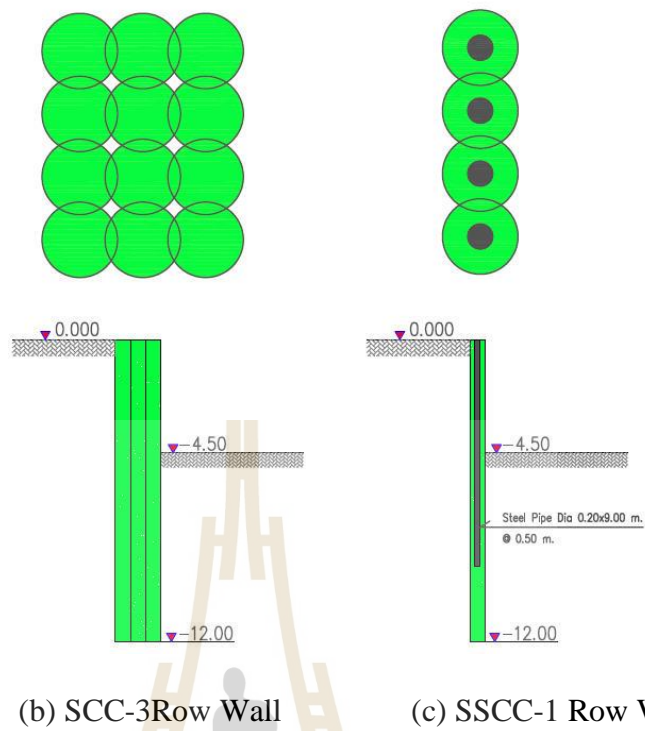


Figure 4.1. (a) Site geometry, and types of retaining wall that construction: (b) SCC-3Row Wall and (c) SSCC-1Row Wall.

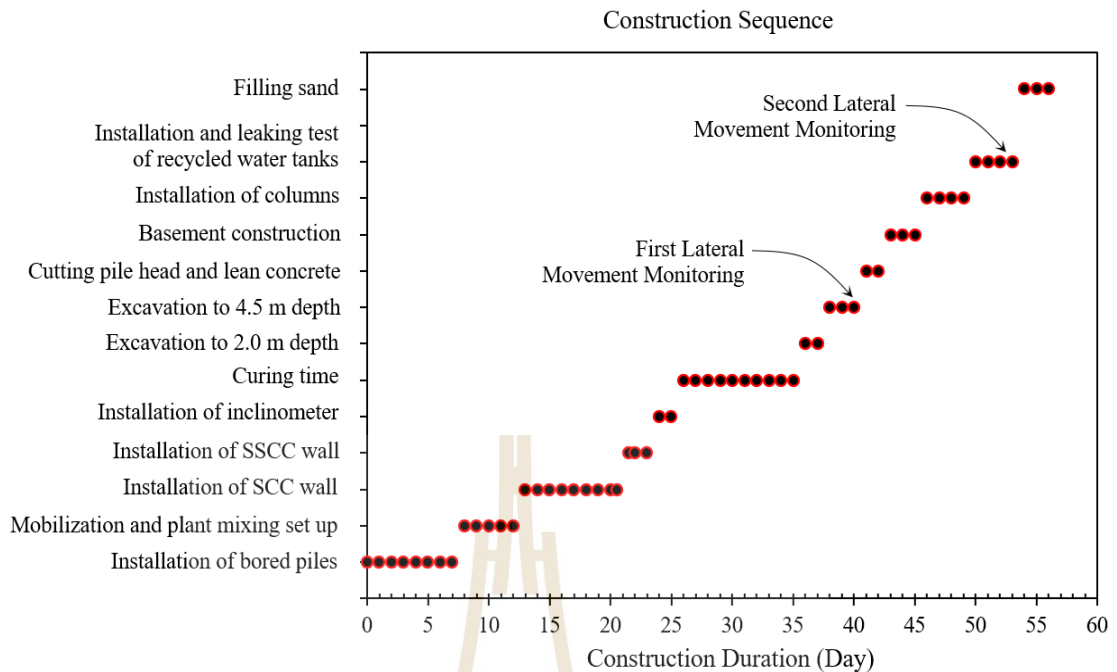


Figure 4.2. Construction sequence.

4.2.2 Soil and SCC properties

The soil profile at the construction site varied from soft to stiff clay where about 10 meters of soft clay had very low undrained shear strength (S_u) of approximately 20 kPa with a high water content (Figure 4.3). This soil profile is typical in central Bangkok (Horpibulsuk et al., 2007). The natural water content of the soft clay was approximately 80%, liquid limit = 60 – 80%, plastic limit = 20 – 30%, coefficient of compression = 0.35, and friction angle = 23°.

After 28 days of construction of SCC Wall, the core samples obtained from the middle of SCC at various depths by a coring machine were prepared for the unconfined compressive strength (q_u) tests. The q_u samples were trimmed to have a diameter to length ratio of 1:2 (50 mm in diameter and 100 mm length). The undrained shear strength of SCC ($S_{u_{SCC}}$) was approximated from q_u value as $S_{u_{SCC}} = 1/2q_u$.

Figure 4.4 indicates the $S_{u_{SCC}}$ values at various depths whereby the average $S_{u_{SCC}}$ value was about 535 kPa.

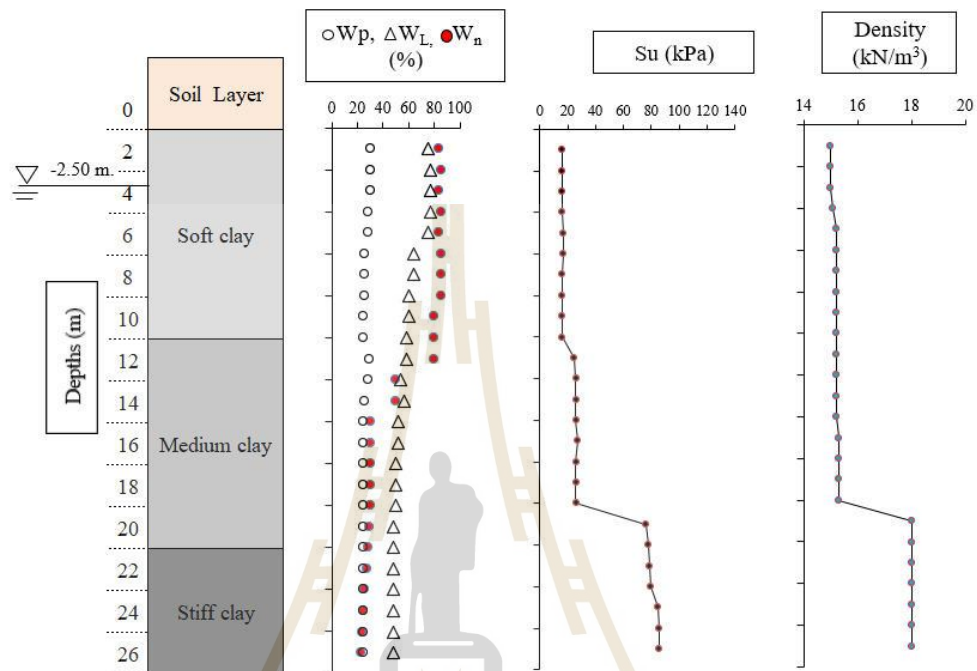


Figure 4.3. The soil profile at the construction site, Bangkok-Noi District, Thailand.

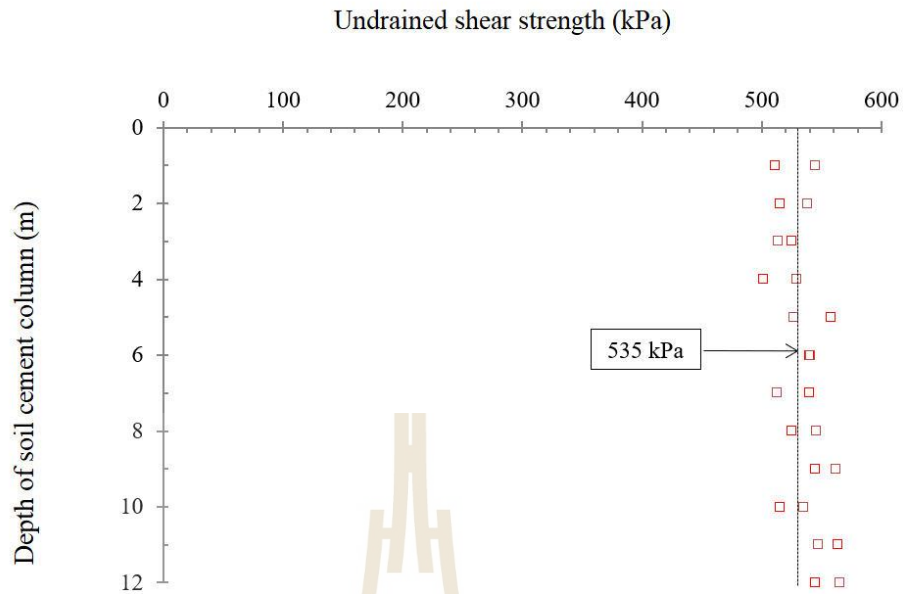


Figure. 4.4. A relationship between depth and undrained shear strength of SCC.

4.2.3 Finite element analysis

Finite element (FE) method using PLAXIS 2D program was used to investigate the behavior of constructed SCC Wall and SSCC Wall. The soil, SCC Wall and SSCC Wall were 15-node wedge elements. The Mohr-Coulomb failure criterion was used for SCC Wall and SSCC Wall, which were modeled as linearly elastic to perfectly plastic materials as suggested by previous researchers (Han et al., 2007; Abusharar et al., 2009; Voottipruex et al., 2011, Huang & Han, 2009; Mun et al., 2012, Wonglert et al., 2018).

The Mohr-Coulomb model was suggested to simulate the soft clay in some previous studies due to its simplicity (Hossain et al., 2006; Huang et al., 2006; Madhyannapu et al., 2006; Han et al., 2005; Chen et al., 2006). However, the Soft Soil model was employed to simulate the behavior of soft clay in this study. The Soft Soil model is suitable for materials that exhibit degree of compressibility such as

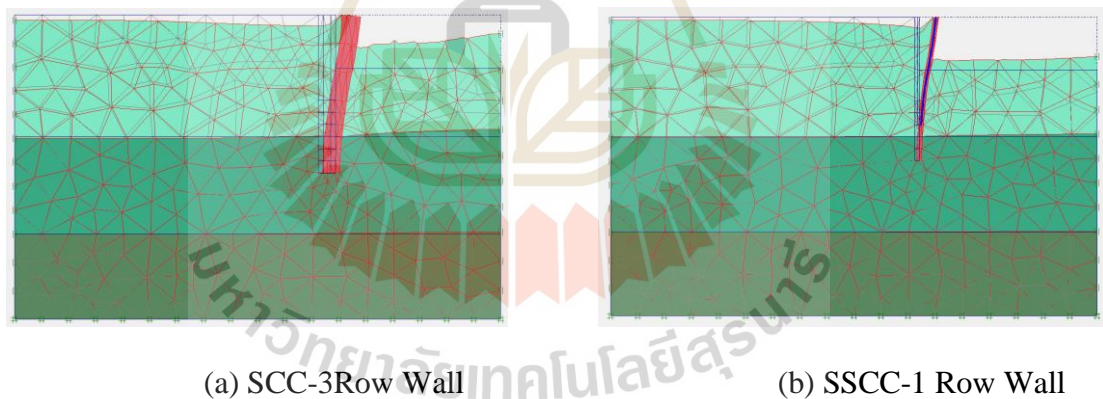
normally consolidated clays (Neher et al., 2000). The Soft Soil constitutive model was successfully used to model the behavior of soft Bangkok clay (Rukdeechai et al., 2009, Surarak et al., 2012). The model parameters for SCC and soft clay are shown in **Table 4.1**. **Table 4.2** summarizes the parameters of steel pipe. **Figure 4.5** demonstrates the FE mesh used for the simulation of SCC Wall and SSCC Wall. The construction stages of SCC Wall were performed as follows: Stage (1) the generation of initial stresses, Stage (2) the installation of the 12-m depth SCCs, Stage (3) the excavation of 2.0 m depth, Stage (4) the excavation of 4.5 m depth, and Stage (5) the determination of factor of safety (FS). Similarly, the construction stages of SSCC Wall were carried out by Stage (1) the generation of initial stresses, Stage (2) the installation of the 12-m depth SCCs, Stage (3) the installation of the steel pipes in the center of SCCs, Stage (4) and Stage (5) the excavation of 2.0 m depth and 4.5 m depth, respectively, and finally the determination of FS was performed in Stage (6).

Table 4.1 Soil parameters for finite element analysis.

Material Depth (m)	Model	Material Behavior	C' (kN/m ²)	Φ'	Poisson's Ratio, ν	λ^*	K^*	Young Modulus, E (kN/m ²)	k (m/day)	γ_{dry} (kN/m ³)	γ_{wet} (kN/m ³)
Soft Clay (0-10 m)	Soft Soil	Undrained	2	23	0.33	0.10	0.02	-	5×10^{-4}	9	15
Medium Clay (10-18 m)	Soft Soil	Undrained	3	25	0.30	0.03	0.008	-	2.5×10^{-4}	10	15
Stiff Clay (18-25 m)	Soft Soil	Undrained	5	26	0.30	0.02	0.006	-	2.5×10^{-4}	14	18
SCC (0-12 m)	Mohr-Coulomb	Undrained	500	1	0.33	-	-	$1.0E5$	2.5×10^{-4}	15	18

Table 4.2 Parameter of steel pipe and sheet pile (Plate) for finite element analysis.

Type of wall	Type of behavior	Normal Stiffness EA (kN/m)	Flexural Rigidity EI (kNm ² /m)	Equivalent thickness d (m)	Weight w (kN/m/m)	Poisson's Ratio, ν
SSCC	Elastic	1.22E6	6850	0.262	0.470	0.15
SSCC with bracing system	Elastic	6.10E5	3425	0.262	0.235	0.15
Sheet Pile	Elastic	1.5E6	3360	0.164	1.500	0.15

**Figure 4.5** FE mesh used for the back-analysis soil stiffness: a) SCC-3Row Wall and b) SSCC-1Row Wall.

The approximation of FS was performed by the shear strength reduction (ϕ -c reduction) method in PLAXIS 2D program, whereby the strength parameters $\tan\phi$ and

c of the soil were reduced until the structure failure occurred. The calculation of FS can be obtained from the following equations:

$$FS = \text{value of } \sum Msf \text{ at failure} = \frac{\text{available strength}}{\text{strength at failure}} \quad (4.1)$$

$$\sum Msf = \frac{\tan \phi_{input}}{\tan \phi_{reduced}} = \frac{c_{input}}{c_{reduced}} \quad (4.2)$$

where $\tan \phi_{input}$ and c_{input} are the strength parameters of the material sets input during modeling and $\tan \phi_{reduced}$ and $c_{reduced}$ were the reduced values obtained from the FE program. $\sum Msf$ was first set as 1.0 at the start of calculation and the incremental Msf was used to specify the increment of the strength from the first calculation step until its unreduced values (strength at failure).

4.3 Parametric study

After the finite element modeling has been validated, it was used for the parametric study. The effect of influence factors on the analysis and design in term of cost, time, and quality (FS and lateral movement) of the retaining wall types (SCC, SSCC and sheet pile with bracing) were studied. The stiffness of sheet pile is low, therefore the bracing is required to prevent the large lateral movement. The number of SCC rows can be reduced by inserting the steel pile to be SSCC Wall. The bracing also improves the FS. The SCC-2Row Wall, SSCC-1Row Wall with and without bracing system, and sheet pile wall were studied in this research (**Figure 4.6**). For SSCC Wall with bracing system, the steel piles were installed at the edge of SCC at

every other SCC to weld with the wale and strut system. The parameters of soil and pile structures for FEM analyses were presented in **Tables 4.1, 4.2, and 4.3.**

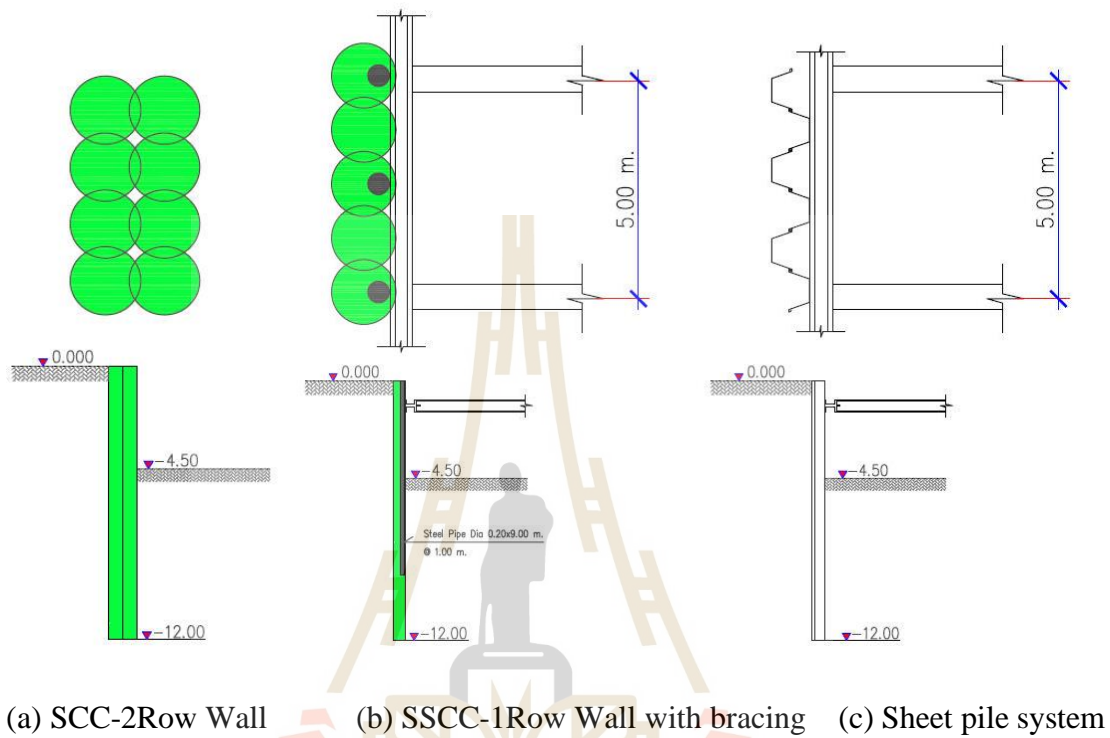


Figure 4.6. Layout and section of retaining wall: a) SCC-2Row, b) SSCC-1Row with bracing, and c) sheet pile.

Table 4.3. Parameter of strut (Anchor) for finite element analysis.

Type of wall	Type of behaviour	Normal Stiffness EA (kN/m)	Spacing out of plan Ls (m)	Maximum force (kN)
SSCC with bracing system	Elastic	2.0E6	5.00	1.0E15
Sheet Pile	Elastic	2.0E6	5.00	1.0E15

Figure 4.7 shows the FE model and FE mesh of SCC-2Row Wall, SSCC-1Row Wall with bracing system, and sheet pile wall. The phi-c reduction method based FS analyses were also carried out to investigate the stability and lateral movement of various types of SCC and SSCC Walls and compared with those of the sheet pile wall system. In this parametric study, the final depth of excavation was fixed at 4.5 m depth as it is common for the recycled water tank project. The thickness of soft Bangkok clay was fixed at 10 m, which is typical for central Bangkok area (Horpibulsuk et al., 2007).

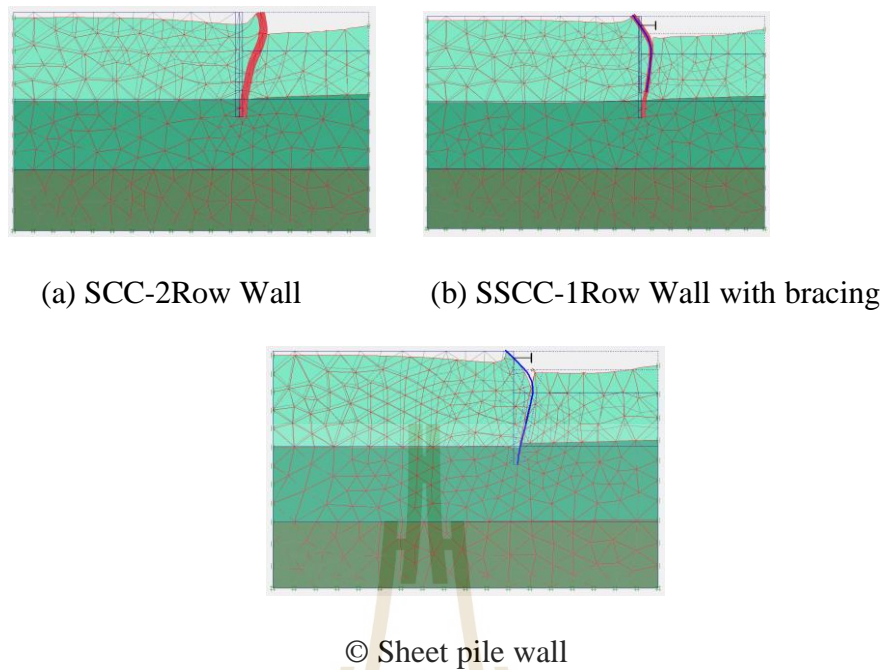


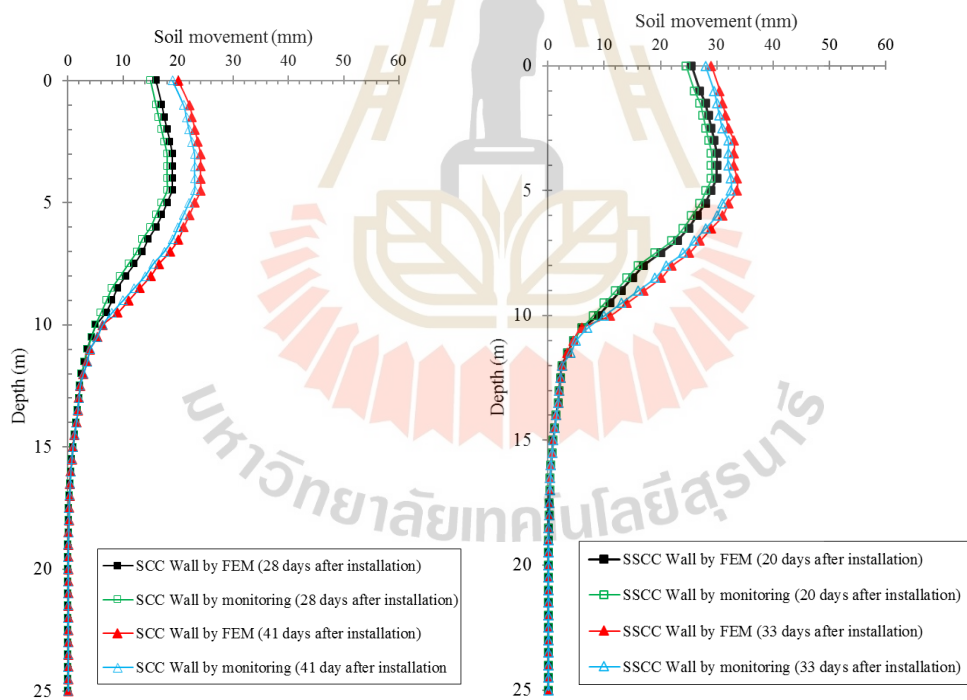
Figure 4.7. FE mesh: a) SCC-2Row wall, b) SSCC-1Row Wall with bracing, and c) Sheet pile wall.

4.4 Finite Element Analysis Results

The first and foremost important consideration in retaining wall design is the stability as unstable excavation might lead to catastrophic failure. The stability of the SCC and SSCC Walls can be examined by the FS. Typical FS of retaining structure can be varied based on international or local standards. In this research, the minimum required FS for a temporary structure of 1.30 specified by the Department of Public Works and Town & Country Planning, Thailand was used as a benchmark.

Figure 4.8 presents the simulated lateral movements compared with the field measurements at 28 days and 20 days after SCC-3Row Wall and SSCC-1Row Wall installation, respectively and after the installation of recycled water tanks (41 days and 33 days after SCC-3Row Wall and SSCC-1Row Wall installation, respectively).

The maximum lateral movement (δ_{max}) approximately occurred at the final excavation depth of 4.5 m for both simulation times. The measured field lateral movements during the excavation and after the installation of recycled water tanks were in good agreement with the FE results for SCC-3Row Wall and SSCC-1Row Wall. As such, the selected soil model could be used for the parametric studies. The FE estimation results indicated that FS of the SCC-3Row Wall and SSCC-1Row Wall were 2.05 and 1.45. With higher FS, the SCC-3Row Wall exhibited lower lateral movement than the SSCC-1Row Wall; the maximum lateral movement of SCC-3Row Wall was about 24 mm at 41 days while it was about 34 mm for the SSCC-1Row Wall at 33 days.



(a) SCC-3Row Wall

(b) SSCC-1Row Wall

Figure 4.8. Soil movement a) SCC-3Row Wall and b) SSCC-1Row Wall.

4.5 Results of Parametric Study

Jamsawang et al. (2015) revealed that maximum lateral movement, δ_{max} for a SCC retaining structure was directly related to FS. **Figure 9** demonstrates the relationship between the δ_{max} and FS of various types of SCC and SSCC Walls. It was evident that the relationship was different and depended on the type of retaining structures. For instance, the SCC-2Row Wall exhibited higher δ_{max} when compared to the SCC-3Row Wall at the same FS. This indicated that the higher stiffness of retaining wall led to the lower lateral movement at the same FS. The SSCC-1Row Wall exhibited the lowest δ_{max} at the same FS. This implies that the δ_{max} of retaining wall can be reduced by increasing the number of SCC rows or enhancing the stiffness of the SCC by inserting the rigid pile. Furthermore, adding bracing to the SSCC-1Row Wall could significantly reduce the δ_{max} at the same FS.

Note that the FS of all studied types of walls can also be enhanced by increasing length of pile (L).

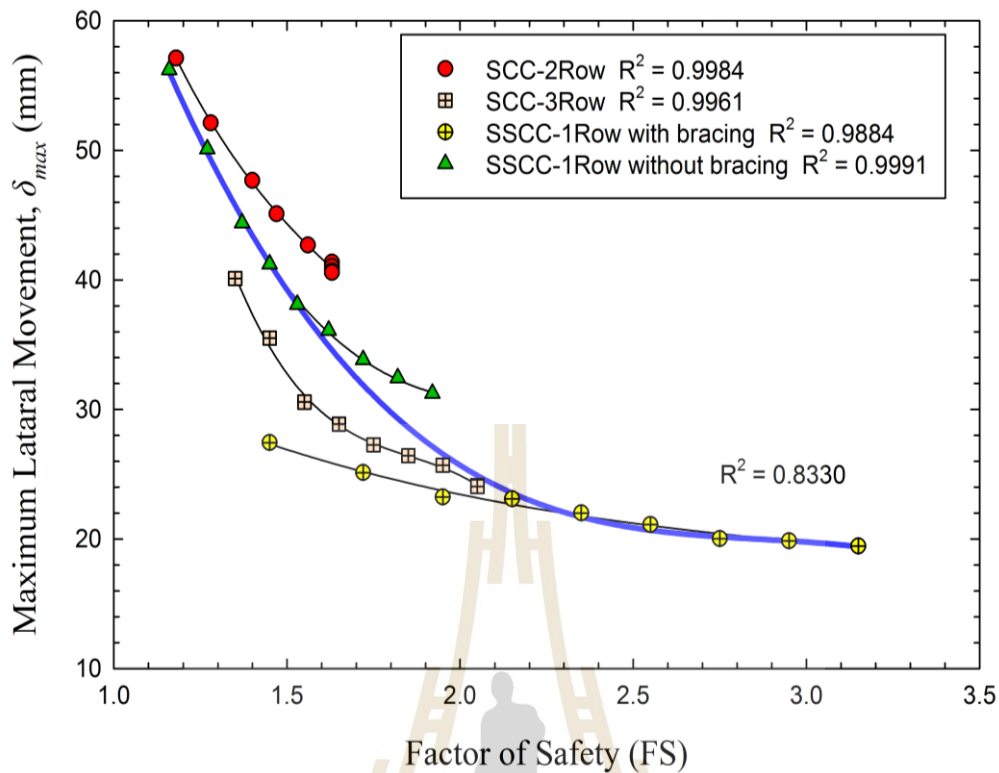
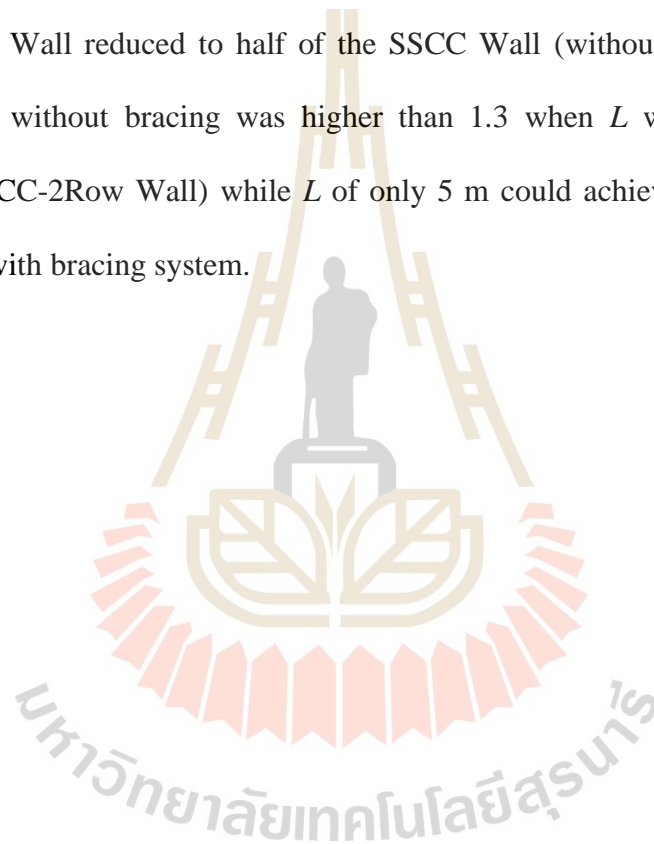


Figure 4.9. Correlation between maximum lateral movement and factor of safety of various walls.

Figure 4.10 shows the relationship between δ_{max} and FS of all different types of walls with various lengths of pile ($L = 5$ to 13 m). It was noted that FS increased while δ_{max} decreased with L up to the maximum FS and minimum δ_{max} at the critical L . The FS and δ_{max} of SCC-3Row Wall were approximately constant when $L > 12$ m, while its FS and δ_{max} gradually decreased and increased, respectively when $L < 12$ m (the critical $L = 12$ m). The critical L of SCC-2Row Wall was found to be lower of 10 m (the stiff clay layer). Although the FS of SCC-2Row Wall was lower than that of SCC-3Row Wall, the FS value of SCC-2Row Wall at $L = 7$ m was greater than the minimum requirement ($FS > 1.3$). This indicates that the temporary retaining wall with two rows of SCC and $L = 7$ m can be used for the narrow excavation in soft

Bangkok clay in term of FS. However, its $\delta_{max} = 48$ mm was slightly high compared with the SCC-3Row Wall.

Similarly, the FS and δ_{max} of both SSCC Walls with and without bracing increased and decreased, respectively with increasing L . The bracing system significantly increased FS and reduced δ_{max} of SSCC Wall compared with the SSCC Wall without bracing (**Figure 10**). With this bracing system, the number of steel piles in the SSCC Wall reduced to half of the SSCC Wall (without bracing). The FS of SSCC-1Row without bracing was higher than 1.3 when L was greater than 7 m (similar to SCC-2Row Wall) while L of only 5 m could achieve FS > 1.3 for SCC-1Row Wall with bracing system.



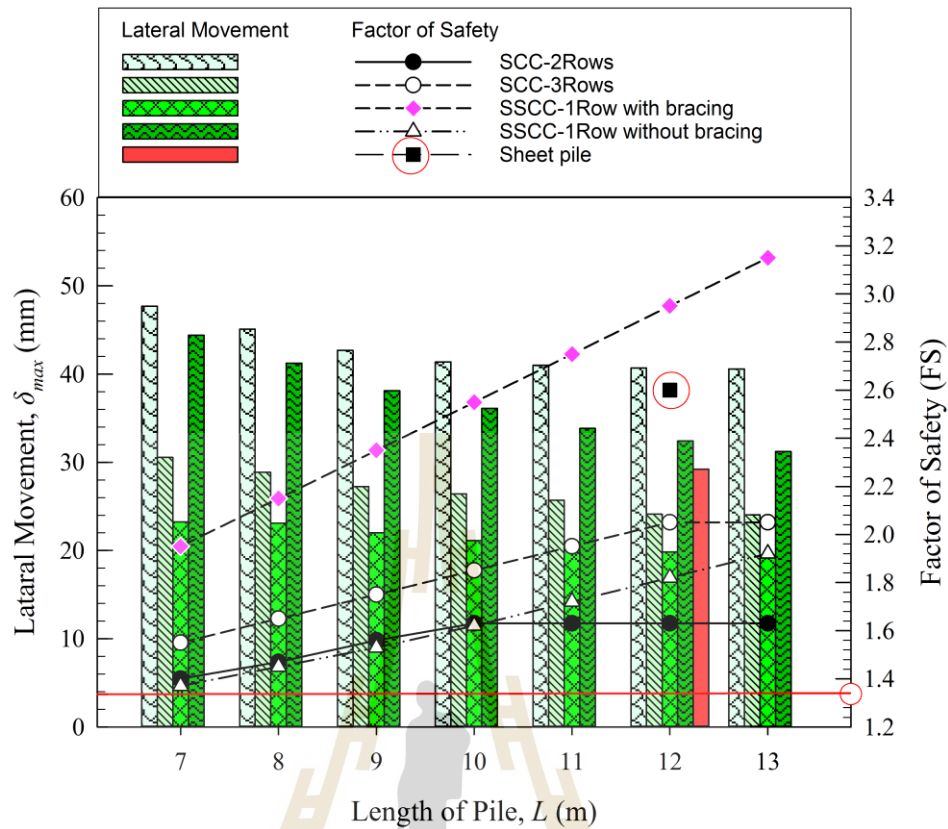


Figure 4.10. The relationship between factor of safety and lateral movement varied with lengths of piles.

Figure 4.11 shows the relationship between the FS and cost of construction at various L of different types of retaining walls. The cost of construction was estimated based on the cost of material and labor in 2020. Execution cost of SCC was 10.95 USD/m (material cost = 5.50 USD/m and labor cost = 5.45 USD/m), while the execution cost of steel pipe was 34 UDS/m (material cost = 17 USD/m and labor cost = 17 USD/m) (1 USD = 32 baht). The cost of construction was estimated per 1-m length of retaining wall, where there were 4 SCCs and 6 SCCs per 1-m length for SCC-2Row Wall and SCC-3Row Wall, respectively. Practically in Thailand, the execution cost of sheet pile is 14 USD/m, which includes labor cost and rental cost

per one month. As such, the sheet pile wall system is not economic for a long-term project due to the increased rental cost.

The construction cost of all types of SCC Walls gradually increased with increasing L (**Figure 4.11**) due to the increased construction material and time. At a particular L , the SSCC-1Row Wall without bracing had the highest cost, while the SCC-2Row Wall had the least followed by SSCC-1Row with bracing and SCC-3Row Wall. Comparing the SCC-2Row Wall with the conventional sheet pile, the construction cost of SCC-2Row Wall was lower when $L < 10$ m. Besides the stability enhancement, the bracing system could reduce the construction cost of SSCC Wall. It was found that the construction cost of SCC-1Row with bracing was lower than that of SCC-1Row without bracing for all L while FS was much higher. When compared with SCC-3Row Wall, the SSCC-1Row with bracing had higher FS and lower construction cost. For FS > 1.3 criterion, the construction cost of SCC-2Row with $L = 7$ to 10 m, SCC-3Row with $L = 7$ m and SSCC-1Row with bracing with $L = 7$ to 8 m were comparable with that of the conventional sheet pile. The FS of the SSCC-1Row with bracing with $L = 7$ to 8 m was between 1.95 and 2.15 while the FS of conventional sheet pile was 2.60 with $L = 12$ m.

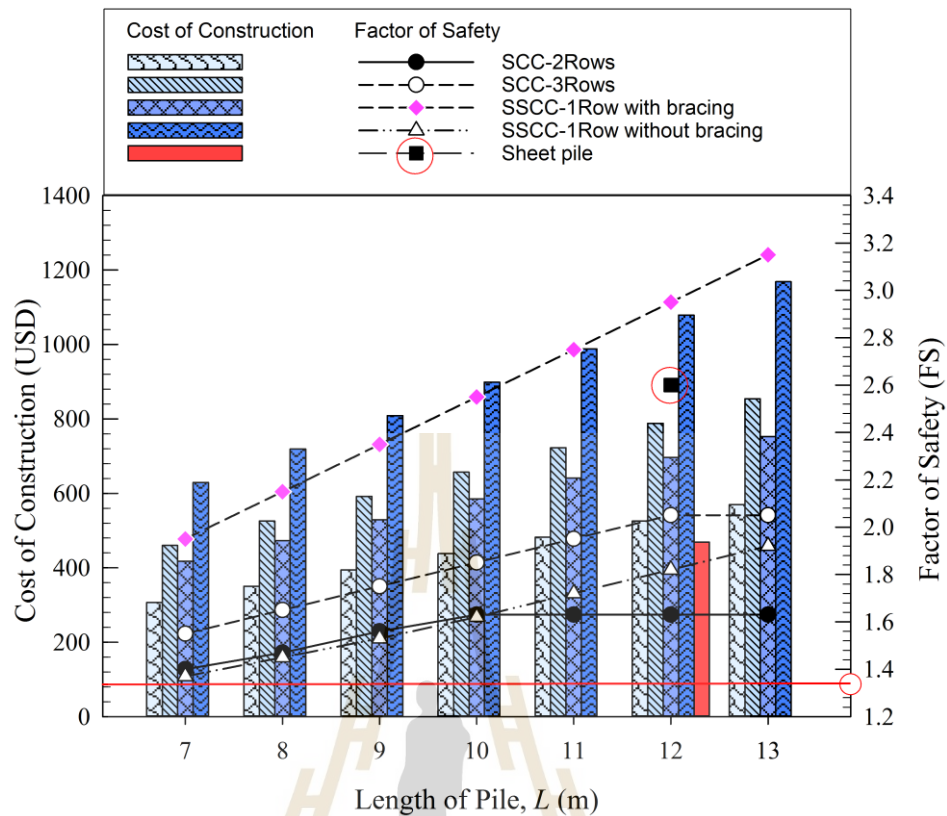


Figure 4.11. The relationship between factor of safety and cost of construction varied with lengths of piles.

Figure 4.12 shows the relationship between time and cost of construction for all types of walls with various L . The time of the construction was presented in hours per 1-m length of retaining wall. **Figure 4.12** indicated that the number of rows and L of SCC Wall notably influenced the construction time (i.e., for the same L , the construction time of SCC-3Row Wall was significantly longer than that of SCC-2Row Wall). The construction time of SSCC-1Row Wall without bracing was the shortest although its construction cost was the most expensive. The SCC-2Row Wall was the cheapest and the construction was fast (just after SSCC-1Row without bracing). Compared the SCC-2Row Wall and the SCC-3Row Wall, the slope of the

construction time versus L relationship was steeper for SCC-3Row Wall because the number of SCC rows controlled the construction time. Even the construction time of SSCC-1Row with bracing was higher than that of SSCC-1Row without bracing for L between 5 and 13 m, the slope of the construction time versus L relationship was gentler. As such, the difference in construction time was smaller with longer L . For $L < 7$ m, the SSCC-1Row with bracing had the longest construction time and followed by the SCC-3Row. However, for $L > 7$ m, the SCC-3Row had the longest construction time and followed by the SSCC-1Row with bracing.

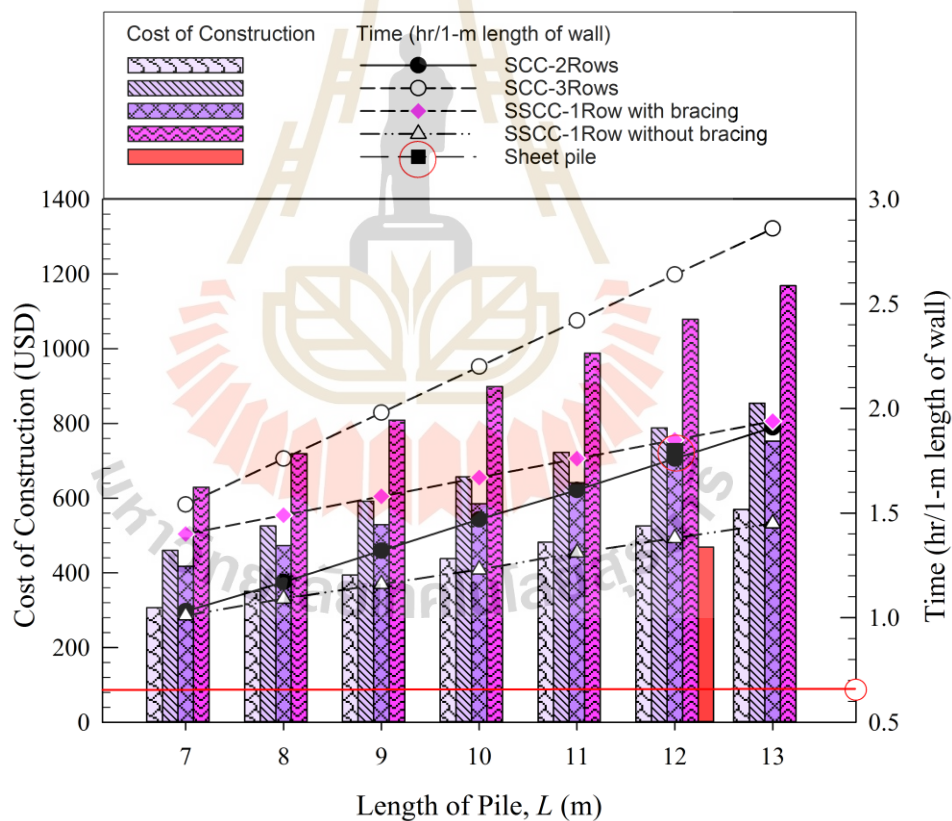


Figure 4.12. The relationship between time and cost of construction varied with lengths of piles.

Based on **Figures 4.11** and **4.12**, the comparison of construction time and cost and FS of all types of SCC Wall were investigated. The FS of SCC-3Row Wall and SSCC-1Row with bracing were greater than 1.3 when $L > 5$ m while SCC-2Row Wall and SSCC-1Row without bracing with $L > 7$ to 13 m had $FS > 1.3$. Compared SCC-2Row with SCC-3Row when $FS > 1.3$, the construction cost and time of SCC-2Row were lower than SCC-3Row when L was between 7 and 13 m. Similarly, when compared SSCC-1Row with and without bracing for $FS > 1.3$, although the construction time of SSCC-1Row with bracing was higher than that without bracing when L was between 7 and 13 m, the slope of the construction time versus L relationship indicated that the construction time of bracing wall was smaller for very long L . On the other hand, the construction cost of SSCC-1Row without bracing was significantly higher than that with bracing at all L .

When $L > 7$ m, the FS of SCC-2Row and SSCC-1Row without bracing were similar while the construction time and the slope of construction time versus L relationship of SCC-2Row were lightly higher. However, the construction cost of SSCC-1Row without bracing was significantly higher than that of SCC-2Row due to the material cost. The FS of SCC-2Row was found to be constant when $L > 10$ m while FS of SSCC-1Row was linearly increased. As such, for $FS > 1.3$ criterion, SCC-2Row had an advantage than SSCC-1Row without bracing at the critical $L < 10$ m in term of construction cost but disadvantage in term of construction time. The stability of these two types of wall can be increased by increasing its stiffness by either bracing system or increased number of SCC rows.

When compared SCC-3Row with SSCC-1Row with bracing, although the construction cost of SSCC-1Row with bracing was slightly lower than that of SCC-

3Row, its FS was remarkably higher than SCC-3Row at all L . It implies that the SSCC-1Row with bracing had benefits than SCC-3Row in term of stability and construction time. For this application, $L = 5$ m is recommended for both types of retaining wall.

When compared SCC-3Row and SSCC-1Row with bracing at $L = 5$ m with SCC-2Row at 7 m (these had $FS > 1.3$), the construction cost of SCC-2Row (306.6 USD) was the lowest followed by SSCC-1Row with bracing (361.4 USD) and SCC-3Row (394.2 USD). The construction time of SCC-2Row (1.03 hr/m) was the shortest and followed by SCC-3Row (1.54 hr/m) and SSCC-1Row with bracing (1.56 hr/m). In other words, the SCC-2Row at 7 m was the most effective in term of time and cost at the same $FS > 1.3$ criterion when compared with other type of SCC and SSCC walls.

4.6 Advantages and Disadvantages of the Studied Walls

4.6.1 For an accessible construction site

The standard 12-m long steel sheet pile with bracing system is commonly used as a temporary retaining structure for underground excavation. When comparing the FS of various studied walls at $L = 12$ m, the sheet pile wall with bracing had higher FS than SCC-3Row Wall, SCC-2Row Wall, and SSCC-1Row without bracing, but lower than SSCC-1Row with bracing (**Figure 4.11**). At same $L = 12$ m, sheet pile wall had the cheapest cost of construction and followed by SCC-2Row Wall, SSCC-1Row with bracing, SCC-3Row Wall, and SSCC-1Row without bracing, respectively. The time of construction of sheet pile wall was similar to that SCC-2Row Wall while it was higher than SSCC-1Row without bracing and lower

than SSCC-1Row with bracing and SCC-3Row Wall. It can be seen that at the standard $L = 12$ m, sheet pile had advantage in term of construction cost, while it had comparable benefits of FS and time of construction when compared with other types of walls. In general, the advantages of SCC and SSCC Walls over the conventional sheet pile is the designed length of pile can be varied to meet the required $FS > 1.3$ (for temporary retaining wall) while minimize the construction cost and time of retaining wall.

4.6.2 For a confined construction site

The 12-m standard length of sheet pile and the bracing system are considered as a constraint for the confined construction area such as Bangkok city. Consequently, the sheet pile wall and SSCC Wall with bracing are not suitable for such a condition. SCC Wall is a good alternative choice for a shallow and narrow excavation in soft Bangkok clay whereby the stability, lateral movement, cost and time of construction of SCC Wall can be flexibly designed at various desired length of pile. The length and number of SCC rows as well as its stiffness significantly controlled the stability and the construction cost and time of the SCC Walls. The construction cost and time analyses in this research revealed that the SCC-2Row at 7 m (about 1.5 times longer than excavation depth) was found to be the most effective when compared with other type of SCC walls at the same $FS > 1.3$ (see, **Figure 4.11** and **4.12**). Even though SCC-3Row at 5 m can be used as a temporary retaining wall as its $FS > 1.3$, the construction cost and time were slightly higher than that SCC-2Row at 7 m. It implies that the reduction L of SCC-3Row Wall exhibits no advantages in terms of construction cost and time over SCC-2Row Wall. However,

increasing row number of SCC can enhance the stiffness of the wall and resulted in reducing δ_{\max} (see **Figure 4.10**).

4.6.3 Summary and Recommendation

Based on the minimum requirement of $FS = 1.3$ for temporary retaining wall, the cost and time of construction of the case study can be reduced with effective wall design. The advantage of SSCC and SCC Wall system is the selectability of L whereas the L of sheet pile is fixed at 12 m and the FS is much higher the minimum requirement for temporary support. The construction cost of sheet pile system is mainly from the rental cost of sheet pile. The mobilization of long sheet pile and bracing system is disadvantageous for confined construction site.

Therefore, to maximize the performance of the SCC as a temporary retaining wall for the narrow excavation project in soft soil, some influence factors including types of wall, length of pile, FS , lateral movement, cost and time of construction should be considered in the analysis and design procedure. The procedures for the design of SCC Wall are summarized as follows: (1) carry out the in-situ soil investigation and geotechnical laboratory testing to obtain the required soil parameters, (2) design and select the SCC Wall properties, (3) design and select option of retaining structures, (4) variation of pile embedment depth and wall thickness (stiffness), (5) consider construction sequences and constraints, and (6) calculate wall stability and soil movement by FE method, and finally study the cost and time of construction as summarized in **Figures 4.10, 4.11 and 4.12**.

4.7 Conclusion

This research work performed the comparison studies of SCC and SCCC walls with the conventional sheet pile wall system in term of execution time and cost and stability (factor of safety and lateral movement), which is useful in selection of the suitable retaining structures for different constraints such as site accessibility to attain the target stability with reasonable construction cost.

The case study of the narrow deep excavation construction in soft Bangkok clay using SCC and SCCC walls as temporary retaining wall was studied and compared with the conventional sheet pile wall system. The model calibration was carried out using finite element method (FEM) in computer program, PLAXIS 2D to fit the FEM results with the field measurement data. The parametric studies including types of retaining structures, embedment depths, and bracing system were then performed to investigate the advantages and disadvantages between the SCC, SCCC, and sheet pile wall in term of stability (FS and lateral movement), effective economic analysis (construction cost and time) in the different site conditions.

The results indicated that the performance of retaining wall in term of cost and time of construction and FS and lateral movement can be achieved by the variation of the parametric studies. The simplicity and low construction cost of sheet pile wall were advantageous for the project in the accessible construction site when compared with other types of SCC and SCCC walls at only standard length of pile ($L = 12$ m). However, the rental cost of sheet piles during construction and their removal cost after the completion of construction were disadvantages for the long-run construction project. In addition, due to the low stiffness of sheet pile, bracing system was required to prevent the failure from the large lateral movement, or it might cause the problem

to the neighboring infrastructures. The variation of sheet pile length or the requirement of bracing system was not suitable for the narrow and shallow to medium depth excavation. As such, the SCC and SSCC Walls can be designed to maximize the stability performance (FS and lateral movement) while minimize the construction cost and time, which have more advantages than that conventional sheet pile system. In this research, SCC-2Row at 7 m, where the length of pile was about 1.5 times longer than the excavation depth was found to be the most effective wall in term of time and cost at the same $FS > 1.3$ criterion when compared with other type of SCC and SSCC walls in both accessible construction site and confined construction site.

The outcomes from this research can be used as a guideline to facilitate an effective analysis and design as well as selection of SCC Wall as a temporary retaining wall for excavation in the soft Bangkok clay. The knowledge gained from this research can be also applied to the similar excavation in soft soils.

4.8 References

- Abusharar, S. W., Zheng, J. J., & Chen, B. G. (2009). **Finite element modeling of the consolidation behavior of multi-column supported road embankment.** *Computers and Geotechnics*, 36(4), 676-685.
- Bergado, D.T, Ruenkairergsa, T., Taesiri, Y., & Balasubramaniam, A.S. (1999). **Deep soil mixing used to reduce embankment settlement, Ground Improvement**, 3, 145-162.
- Chen, C.H. (1990), **Behavior of the improved ground by deep cement mixing method under embankment loading**, M. Eng. Thesis, Asian Institute of Technology, Thailand.

- Chen, R. P., Chen, Y. M., & Xu, Z. Z. (2006). **Interaction of rigid pile-supported embankment on soft soil.** In *Advances in Earth Structures: Research to Practice* (pp. 231-238).
- Finno, R. J., Blackburn, J. T., & Roboski, J. F. (2007). **Three-dimensional effects for supported excavations in clay.** *Journal of Geotechnical and Geoenvironmental Engineering*, 133(1), 30-36.
- Han, J., Huang, J., & Porbaha, A. (2005). **2D numerical modeling of a constructed geosynthetic-reinforced embankment over deep mixed columns.** In *Contemporary issues in foundation engineering* (pp. 1-11).
- Han, J., Oztoprak, S., Parsons, R. L., & Huang, J. (2007). **Numerical analysis of foundation columns to support widening of embankments.** *Computers and Geotechnics*, 34(6), 435-448.
- Horpibulsuk, S., Shibuya, S., Fuenkajorn, K. and Katkan, W. (2007). **Assessment of Engineering Properties of Bangkok clay.** *Canadian Geotechnical Journal*, 44(2), 173-187.
- Hossain, M. S., Haque, M. A., & Rao, K. N. (2006). **Embankment over soft soil improved with chemico pile—a numerical study.** In *Advances in Earth Structures: Research to Practice* (pp. 239-246).
- Huang, J., & Han, J. (2009). **3D coupled mechanical and hydraulic modeling of a geosynthetic-reinforced deep mixed column-supported embankment.** *Geotextiles and Geomembranes*, 27(4), 272-280.
- Huang, J., Han, J., & Porbaha, A. (2006). **Two and three-dimensional modeling of DM columns under embankments [C].** ASCE, Geocongress. Atlanta.

- Jamsawang, P., Bergado, D.T., & Voottipruex, P. (2010). **Field behaviour of stiffened deep cement mixing piles**. Proceedings of the Institution of Civil Engineers, 164, 33-49.
- Jamsawang, P., Voottipruex, P., Boathong, P., Mairaing, W., & Horpibulsuk, S. (2015). **Three-dimensional numerical investigation on lateral movement and factor of safety of slopes stabilized with deep cement mixing column rows**. Engineering Geology, 188, 159-167.
- Lai, Y.P., Bergado, D. T., Lorenzo, G. A. & Duangchan, T. (2006), **Full-scale reinforced embankment on deep jet mixing improved ground**, Ground improvement Journal, 10(4), 153-164.
- Lin, K. Q., & Wong, I. H. (1999), **Use of deep mixing to reduce settlement at bridge approaches**, ASCE Journal of geotechnical and Geoenvironmental Engineering, 125(4), 309-320.
- Madhyannapu, R. S., Puppala, A. J., Hossain, S., Han, J., & Porbaha, A. (2006). **Analysis of geotextile reinforced embankment over deep mixed soil columns: using numerical and analytical tools**. In GeoCongress 2006: geotechnical engineering in the information technology age (pp. 1-6).
- Mun, B., Kim, T., Moon, T., & Oh, J. (2012). **SCM wall in sand: Numerical simulation and design implications**. Engineering geology, 151, 15-23.
- Neher, H. P., Wehnert, M., & Bonnier, P. G. (2000). **An evaluation of soft soil models based on trial embankments**. C. Desai, Computer Methods and Advances in Geomechanics. AA Balkema, Roterdão, 373-379.

- Rukdeechai, T., Jongpradist, P., Wonglert, A., & Kaewsri, T. (2009). **Influence of soil models on numerical simulation of geotechnical works in Bangkok subsoil.** Engineering Journal of Research and Development, 20(3), 17-28.
- Shen, S. L., Han, J., & Du, Y. J. (2008). **Deep mixing induced property changes in surrounding sensitive marine clays.** Journal of Geotechnical and Geoenvironmental Engineering, 134(6), 845-854.
- Shen, S. L., Kim, Y. H., Hong, Z. S., & Bai, Y. (2008). **Equipments for rapid solidification of soft ground through jet-grouting using two types of binders.** China Patent, Patent number: ZL200810033981, 4.
- Shen, S. L., Luo, C. Y., Bai, Y., Kim, Y. H., & Peng, S. J. (2009). **Instant solidification of soft ground horizontally using jet-grouting.** In Contemporary topics in ground modification, problem soils, and geo-support (pp. 257-264).
- Shen, S. L., Miura, N., & Koga, H. (2003). **Interaction mechanism between deep mixing column and surrounding clay during installation.** Canadian Geotechnical Journal, 40(2), 293-307.
- Shen, S. L., Wang, Z. F., Horpibulsuk, S., & Kim, Y. H. (2013). **Jet grouting with a newly developed technology: the twin-jet method.** Engineering Geology, 152(1), 87-95.
- Surarak, C., Likitlersuang, S., Wanatowski, D., Balasubramaniam, A., Oh, E., & Guan, H. (2012). **Stiffness and strength parameters for hardening soil model of soft and stiff Bangkok clays.** Soils and foundations, 52(4), 682-697.

- Tanseng, P. (2011). **Soil-Cement Wall without Bracing for Mat Foundation Construction in Bangkok Sub-Soils**. In ATC18 Mega Foundations 5th Workshop. Hong Kong.
- Tanseng, P. (2012). **Soil-cement column wall with wall-strut to minimize ground movement for a road tunnel construction in Bangkok subsoil**. In Proc. 38th Int. Conf. At World Tunnel Congress.
- Tanseng, P., & Namwiset, V. (2015, February). **Performance of soil-cement column retaining wall used with top-down construction method for basement construction in Bangkok subsoil**. In Soil-Structure Interaction, Underground Structures and Retaining Walls: Proceedings of the ISSMGE Technical Committee 207 International Conference on Geotechnical Engineering (Vol. 4, p. 359). IOS Press.
- Vaziri, H. H. (1996). **Numerical study of parameters influencing the response of flexible retaining walls**. Canadian geotechnical journal, 33(2), 290-308.
- Voottipruex, P., Bergado, D. T., Suksawat, T., Jamsawang, P., & Cheang, W. (2011a). **Behavior and simulation of deep cement mixing (DCM) and stiffened deep cement mixing (SDCM) piles under full scale loading**, Soil and foundations, 5(2), 307-320.
- Voottipruex, P., Suksawat, T., Bergado, D. T., & Jamsawang, P. (2011b). **Numerical simulations and parametric study of SDCM and DCM piles under full scale axial and lateral loads**. Computers and Geotechnics, 38(3), 318-329.
- Wang, J. H., Xu, Z. H., & Wang, W. D. (2010). **Wall and ground movements due to deep excavations in Shanghai soft soils**. Journal of Geotechnical and Geoenvironmental Engineering, 136(7), 985-994.

Wang, Z. F., Shen, S. L., Modoni, G., & Zhou, A. (2020). **Excess pore water pressure caused by the installation of jet grouting columns in clay.** Computers and Geotechnics, 125, 103667.



CHAPTER V

CONCLUSION

5.1 Conclusion

The significance of this research in field investigation and finite element analysis of soil cement columns in foundation and excavation applications in soft Bangkok clay can be concluded as follows.

The cost and time of executing SCSP were compared with those of traditional dry-process bored pile to illustrate the advantage of SCSP. The ultimate load capacity of the piles studied was examined by the field static load test and compared with the conventional design methods. The ultimate load capacity of SP was significantly enhanced by the SCC. The full SCSP provided the highest ultimate load capacity comparing to SCC, SP, and partial SCSP at the same pile length. The conventional individual bearing method could be used to estimate the ultimate load capacity of SP. The load capacity predictive equations for both partial and full SCSP due to soil failure were proposed and validated based on the field static pile load test results. The equations are applicable for soft Bangkok clay and were successfully used for some construction projects in Thailand.

In Thailand, the application of the full SCSP can save on the installation cost when compared to SP and partial SCSP at the same required ultimate load. The execution (raw material and labor) cost of SP was 4.2 times higher than that of SCC for the same pile length. In other words, the execution cost of partial and full SCSP is governed by the SCC length; the longer the SCC length results in the cheaper

execution cost. The execution time was 0.03, 0.05 and 0.08 hour/m length for SP, SCC and full SCSP; the execution time of the full SCSP was approximately 2.5 times longer than that of the SP. The execution time of SCSP increased with the increase in the SCC length. The unit cost of SP was found to be the highest while the unit cost of SCSP was found to be the lowest for the same target ultimate load. As a result, the application of the full SCSP had more economical benefits than both partial SCSP and SP. But the partial SCSP and SP had more advantage in term of construction time and was suitable for a time-constrained project. When comparing SCSP with the traditional dry-process bored pile at the same target ultimate load capacity, the SCSP had higher efficiency and productivity than the bored pile.

The case study of the narrow deep excavation construction in soft Bangkok clay using SCC and SSCC walls as temporary retaining wall was studied and compared with the conventional sheet pile wall system. The model calibration was carried out using finite element method (FEM) in computer program, PLAXIS 2D to fit the FEM results with the field measurement data. The parametric studies including types of retaining structures, embedment depths, and bracing system were then performed to investigate the advantages and disadvantages between the SCC, SSCC, and sheet pile wall in term of stability (FS and lateral movement), effective economic analysis (construction cost and time) in the different site conditions.

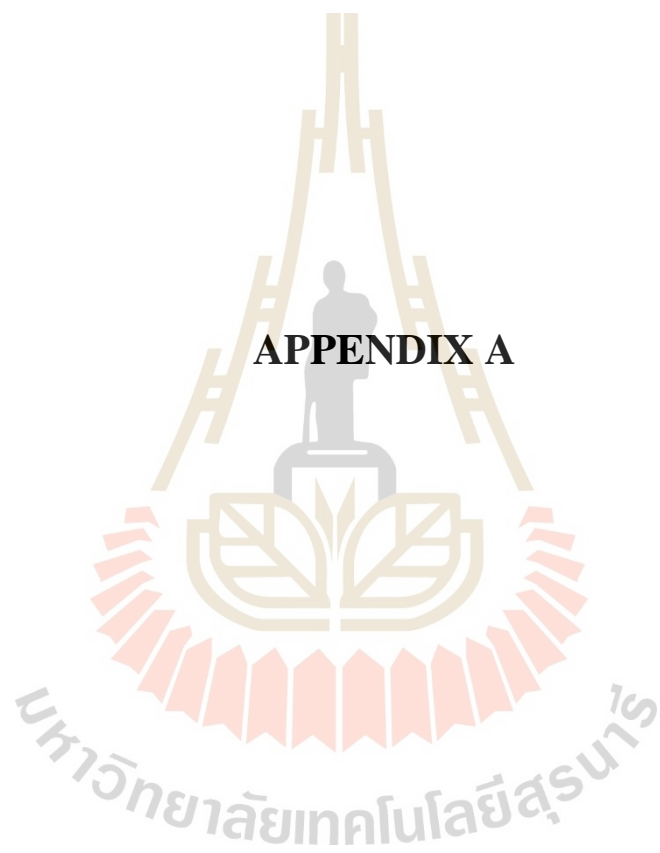
The results indicated that the performance of retaining wall in term of cost and time of construction and FS and lateral movement can be achieved by the variation of the parametric studies. The simplicity and low construction cost of sheet pile wall were advantageous for the project in the accessible construction site when compared with other types of SCC and SSCC walls at only standard length of pile ($L = 12$ m).

However, the rental cost of sheet piles during construction and their removal cost after the completion of construction were disadvantages for the long-run construction project. In addition, due to the low stiffness of sheet pile, bracing system was required to prevent the failure from the large lateral movement, or it might cause the problem to the neighboring infrastructures. The variation of sheet pile length or the requirement of bracing system was not suitable for the narrow and shallow to medium depth excavation. As such, the SCC and SSCC Walls can be designed to maximize the stability performance (FS and lateral movement) while minimize the construction cost and time, which have more advantages than that conventional sheet pile system. In this research, SCC-2Row at 7 m, where the length of pile was about 1.5 times longer than the excavation depth was found to be the most effective wall in term of time and cost at the same $FS > 1.3$ criterion when compared with other type of SCC and SSCC walls in both accessible construction site and confined construction site.

5.2 Recommendation

The outcome of this research will lead to the development of a guideline and code of practice of SCSP in soft clay, which useful for construction industry particularly pertaining to the scheduling and cost performance of SCSP in contemporary construction projects. The knowledge gained from study of SCC wall, SSCC wall and sheet pile system in excavation can be applied to the similar excavation in soft soils. However, in this research were studied only in soft Bangkok clay. Therefore, the study of apply SCC in different soils such as sand is recommended for further research for benefit of geotechnical works.

APPENDIX A



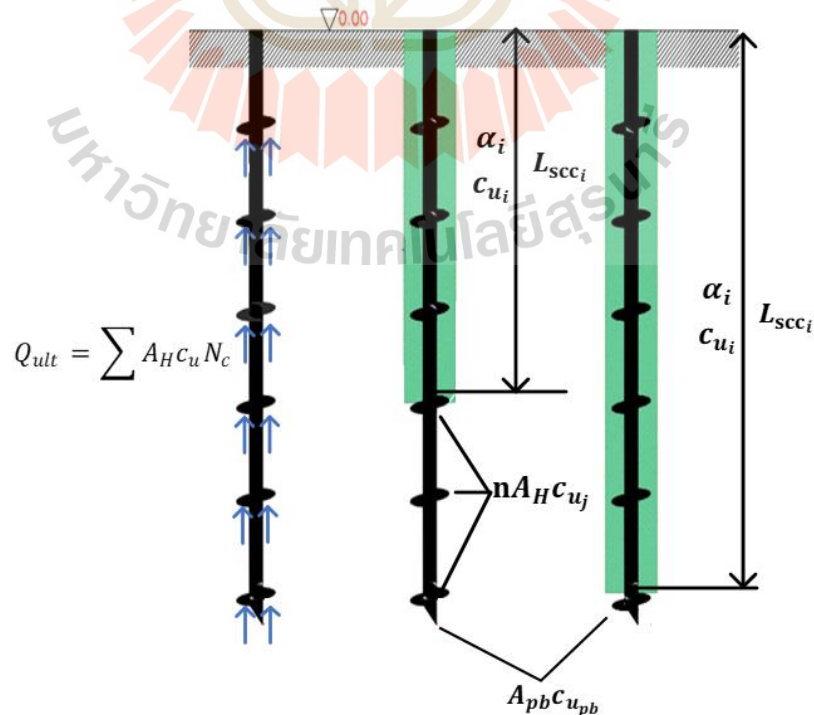
The estimation of the ultimate load capacity of the SP (Eq.3.6), partial and full SCSP (Eqs.3.10 and 3.11) and bored pile (Eq.3.12) presented in Table 3.2 is presented as follows:

$$Q_{ult} = \sum A_H c_u N_c \quad (3.6)$$

$$Q_{ult} = \pi d(\alpha_i L_{scc_i} c_{u_i}) + 9nA_H c_{u_j} + 9A_{pb} c_{u_{pb}} \quad (3.10)$$

$$Q_{ult} = \pi d(\alpha_i L_{scc_i} c_{u_i}) + 9A_{ph} c_{u_{pb}} \quad (3.11)$$

$$Q_{ult} = 0.45S_u A_s + 9wA_b S_u \text{ where, } w = 0.80 \text{ based on Skempton (1966)} \quad (3.12)$$



where d = diameter of SCC; α = adhesion factor; L_{SCC_i} = length of SCC; c_{u_i} = undrained shear strength of soil surrounding SCC; c_{u_j} = undrained shear strength of soil below SCC; $c_{u_{pb}}$ = undrained shear strength of soil layer at pile base; n = number of the helix below SCC; A_H = area of the helix (without filled concrete); and A_{pb} = combined area of the helix and shaft at pile base, and N_c = bearing capacity factor for cohesive soils .

Calculation of SP Using Eq. (6)

$$\text{For } L = 17 \text{ m, } Q_{ult} = 9(8)\pi(0.4^2-0.2^2)/4(20) + 9(1)\pi(0.4^2-0.2^2)/4(75) + 9(2)\pi(0.4^2-0.2^2)/4(125) + 9\pi(0.4^2)/4(125) = 553 \text{ kN}$$

Partially SCSP Using Eq. (10)

$$\text{For } SCC = 3 \text{ m, } Q_{ult} = \pi(0.60)(1)(3)(20) + 9(6) \pi(0.4^2-0.2^2)/4(20) + 9(1) \pi(0.4^2-0.2^2)/4(75) + 9(2) \pi(0.4^2-0.2^2)/4(125) + 9\pi(0.4^2)/4(125) = 632 \text{ kN}$$

$$\text{For } SCC = 5 \text{ m, } Q_{ult} = \pi(0.60)(1)(5)(20) + 9(5) \pi(0.4^2-0.2^2)/4(20) + 9(1) \pi(0.4^2-0.2^2)/4(75) + 9(2) \pi(0.4^2-0.2^2)/4(125) + 9\pi(0.4^2)/4(125) = 691 \text{ kN}$$

$$\text{For } SCC = 7 \text{ m, } Q_{ult} = \pi(0.60)(1)(7)(20) + 9(3) \pi(0.4^2-0.2^2)/4(20) + 9(1) \pi(0.4^2-0.2^2)/4(75) + 9(2) \pi(0.4^2-0.2^2)/4(125) + 9\pi(0.4^2)/4(125) = 732 \text{ kN}$$

$$\text{For } SCC = 9 \text{ m, } Q_{ult} = \pi(0.60)(1)(9)(20) + 9(2) \pi(0.4^2-0.2^2)/4(20) + 9(1) \pi(0.4^2-0.2^2)/4(75) + 9(2) \pi(0.4^2-0.2^2)/4(125) + 9\pi(0.4^2)/4(125) = 732 \text{ kN}$$

For SCC = 11 m, $Q_{ult} = \pi(0.60)(1)(11)(20) + 9(1) \pi(0.4^2-0.2^2)/4(20) + 9(1) \pi(0.4^2-0.2^2)/4(75) + 9(2) \pi(0.4^2-0.2^2)/4(125) + 9\pi(0.4^2)/4(125) = 851$
kN

For SCC = 13 m, $Q_{ult} = \pi(0.60)(1)(12)(20) + \pi(0.60)(0.50)(1)(75) + 9(2) \pi(0.4^2-0.2^2)/4(125) + 9\pi(0.4^2)/4(125) = 877$ kN

For SCC = 15 m, $Q_{ult} = \pi(0.60)(1)(12)(20) + \pi(0.60)(0.50)(2)(75) + \pi(0.60)(0.50)(1)(125) + 9(1) \pi(0.4^2-0.2^2)/4(125) + 9\pi(0.4^2)/4(125) = 959$ kN

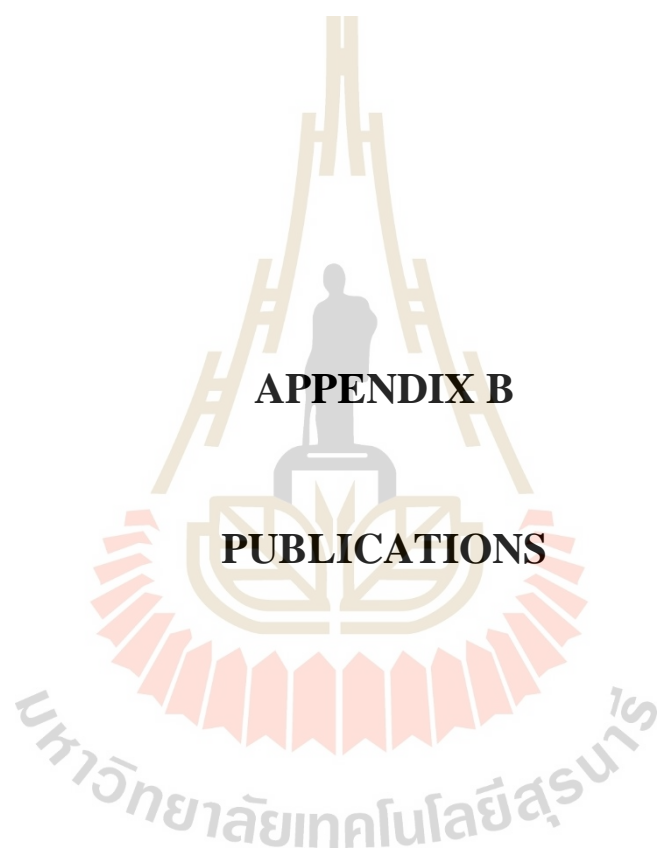
Fully SCSP Using Eq. (11)

For SCC = 17 m, $Q_{ult} = \pi(0.60)(1)(12)(20) + \pi(0.60)(0.50)(2)(75) + \pi(0.60)(0.50)(3)(125) + 9\pi(0.4^2)/4(125) = 1089$ kN

For SCC = 18.8 m, $Q_{ult} = \pi(0.60)(1)(12)(20) + \pi(0.60)(0.50)(2)(75) + \pi(0.60)(0.50)(4.8)(125) + 9\pi(0.4^2)/4(125) = 1300$ kN

Calculation of Bored Pile (Dia. 0.60 x 21.0 m)

$Q_{ult} = 0.45\pi(0.60)(20 \times 12 + 75 \times 2 + 7 \times 125) + 9(0.80)\pi(0.62)/4(125) = 1327$ kN ≈ 1300
kN.



List of Publications

Chayanon Srijaroen, Menglim Hoy, Suksun Horpibulsuk, Runglawan Rachan and Arul

Arulrajah (2021) **Soil-Cement Screw Pile: Alternative Pile for Low-and Medium-Rise Buildings in Soft Bangkok Clay**. Journal of Construction Engineering and Management. Volume 147 Issue 2 - February 2021.




ASCE

Soil–Cement Screw Pile: Alternative Pile for Low- and Medium-Rise Buildings in Soft Bangkok Clay

Chayanon Srijaroen¹; Menglim Hoy, Ph.D.²; Suksun Horpibulsuk, Ph.D.³;
Runglawan Rachan, Ph.D.⁴; and Arul Arulrajah, Ph.D.⁵

Abstract: Bangkok clay is a soft marine clay with high water content and low bearing capacity. Bored piles installed by the dry process commonly are used for low- to medium-rise buildings in the metropolis. However, the installation of bored piles is time consuming and labor intensive, and requires skillful supervision, quality control, and the disposal of excavated spoils. The soil–cement screw pile (SCSP), a composite piling system which incorporates a soil–cement column (SCC) and a screw pile (SP), is an innovative alternative piling solution. This paper presents the ultimate load, time and cost analysis, and suggested effective design method for this piling system in soft Bangkok clay. The load capacity predictive equations for the SCSP were proposed and validated based on the field static pile load test results. These equations were used successfully for the installation of this piling system in construction projects on soft Bangkok clay. The unit cost of the SP was found to be the highest, and the unit cost of the SCSP and bored pile was found to be the lowest and almost similar. As a result, the application of the full SCSP and bored pile is more economical than the partial SCSP and SP under the same ultimate load design. However, the partial SCSP and SP have more advantages in terms of construction time and are suitable for a time-constrained project. The SCSP has higher efficiency, productivity, and competitiveness than the traditional dry-process bored pile. The outcome of this research will lead to the development of guidelines and a code of practice for SCSP in soft clay, which will be useful for the construction industry, particularly pertaining to the scheduling and cost performance of SCSPs in construction projects. DOI: 10.1061/(ASCE)CO.1943-7862.0001988. © 2020 American Society of Civil Engineers.

Author keywords: Soil cement column; Screw pile; Soil–cement screw pile; Piled foundation; Soft Bangkok clay; Ground improvement.

Introduction

The foundation is a medium through which building loads are transferred from the superstructure to the ground (Poulos and Davis 1980). The foundation can be classified into two predominant types, namely shallow foundation and deep foundations. The selection of the foundation system depends mainly upon several factors, which include location, type of structure, ground condition, access for construction equipment, effect of installation on adjacent

foundations, local construction practice, and availability of construction material and relative cost.

The shallow foundation system is used where the soil has high bearing capacity and can carry superstructure loads with small settlement, such as that in the Northeast region of Thailand. On the other hand, in some areas, the ground conditions are unsuitable for a shallow foundation system to support heavy-load buildings where the vertical and lateral loadings imposed on the foundation are significant. In these circumstances, a deep foundation system, particularly with the use of piled foundations, is more applicable. The use of piled foundations is a method of overcoming the difficulties of foundation on soft soil which has low shear strength and high compressibility, such as soft Bangkok clay.

Based on the construction method, piled foundations can be classified into two predominant types, driven piles and cast-in-situ piles. Driven pile foundations can be made from concrete, steel, or timber. RC driven piles are prefabricated before placing at the construction site, and are driven into the ground using a pile hammer. The driven pile is easy to install, so it is a common foundation construction in many projects. In addition, transportation of the driven piles from the manufacturer to the construction site is more convenient and cost-effective than the cast-in-situ pile method. However, the construction method of driven piles produces noise, vibration, and soil movement, which might cause damage to neighboring buildings.

A cast-in-situ or bored pile consist of a RC pile which is constructed at the construction site by drilling a hole into the ground to the required depth, placing the reinforcement, and then filling the steel tube with concrete. The installation of a cast-in-situ pile has two methods, namely the dry and the wet processes. The suitable installation process used at the construction site depends on the nature of the soil and the superstructure loads. For soft Bangkok clay, dry-process bored piles commonly are used for low- to

¹Ph.D. Scholar, School of Civil Engineering, Suranaree Univ. of Technology, Nakhon Ratchasima 30000, Thailand; Senior Civil Engineer, Thai Pile Rig Co. Ltd., Prachantit Rd., Samsenok, Huay Kwang, Bangkok 10310, Thailand. Email: sr_chayanon@yahoo.com

²Lecturer and Research Fellow, School of Civil Engineering, Center of Excellence in Innovation for Sustainable Infrastructure Development, Suranaree Univ. of Technology, Nakhon Ratchasima 30000, Thailand. Email: menglim@g.sut.ac.th

³Professor and Director, School of Civil Engineering, Center of Excellence in Innovation for Sustainable Infrastructure Development, Suranaree Univ. of Technology, Nakhon Ratchasima 30000, Thailand; Associate Fellow, Academy of Science, The Royal Society of Thailand, Bangkok 10300, Thailand (corresponding author). ORCID: <https://orcid.org/0000-0003-1965-8972>. Email: suksun@g.sut.ac.th

⁴Assistant Professor, Dept. of Civil Engineering, Mahanakorn Univ. of Technology, Nong Chok, Bangkok 10530, Thailand. Email: runglawa@mut.ac.th

⁵Professor, Dept. of Civil and Construction Engineering, Swinburne Univ. of Technology, Melbourne, P.O. Box 218, Hawthorn, VIC 3122, Australia. Email: arulrajah@swin.edu.au

Note. This manuscript was submitted on May 3, 2020; approved on September 15, 2020; published online on December 10, 2020. Discussion period open until May 10, 2021; separate discussions must be submitted for individual papers. This paper is part of the *Journal of Construction Engineering and Management*, © ASCE, ISSN 0733-9364.

medium-rise buildings. However, dry-process bored piles have two main disadvantages—low productivity, and low load capacity—compared with driven piles of the same diameter and length. The ultimate bearing capacity of dry-process bored piles at a construction site in central Bangkok was investigated by Poonlappanish and Buasri (2017). Static pile load tests were conducted on 42 bored piles with diameters of 0.5–0.60 m and lengths of 19–21 m. Using Mazurkiewicz's method, the average factor of safety was found to be over 2.0. Monkaew and Nawalerspunya (2013) investigated the installation productivity of 172 bored piles (0.50-m diameter and 24-m length) at a construction site in Bangkok was by. The approximate rate of productivity was 275.31 min/pile.

Soft Bangkok clay has a thickness of about 15–30 m with high water content and low shear strength (Horpibulsuk et al. 2007); consequently, the installation of bored piles requires steel casing. The driving and extraction of the steel casing is time-consuming and requires great labor. The low load capacity of dry-process bored piles is due to the soil disturbance caused by driving and removal of the steel casing, which reduces soil friction around the pile (Skenpton 1966). Furthermore, the installation of cast-in-situ piles requires skillful supervision and quality control of all piling construction materials. This method also needs sufficient space for storage of materials used in the construction, which is not suitable for the limited space of some construction sites.

To overcome these problems of using bored piles in Bangkok area, an alternative piling solution, designated soil–cement screw piles (SCSPs), has been introduced in Thailand. The SCSP is a combination of a screw pile (SP) and a soil–cement column (SCC), in which the SP is inserted in a previously installed SCC. The SCC can be installed rapidly in soft Bangkok clay as a friction pile, without the requirement for a steel casing. Because the strength of SCCs is relatively low, the inserted SP is used to stiffen and strengthen the SCC to prevent pile failure. Previous researchers have demonstrated the successful use of SCCs to support low-rise buildings and road embankments (Shen et al. 2013a, b, 2017; Wang et al. 2018, 2019).

The SCSP construction method provides many advantages, including easy and quick installation, minimal dewatering, and minimal equipment requirements. It also provides high-tensile and acceptable compressive capacities and produces minimal noise and vibration during installation (Zhang et al. 1998; Livneh and El Nagggar 2008; Sakr 2009, 2011). SCSPs successfully have been used by Thai Pile Rig in piled foundations in two important projects: The Royal Chitralada Pasteurized Milk Factory and The Royal Chitralada Rice Mill of Chitralada Palace, Bangkok Thailand, which required significantly low noise, clean and rapid construction.

SCSPs were introduced to the Thailand market by Thai Pile Rig in early 2018, and this piling system is expected to be very popular due to its many advantages over conventional driven and bored piles. The success of construction projects using SCSPs depends mainly on three indicators of performance—construction schedule, cost, and quality (Kim et al. 2020; McKim et al. 2000; Moon et al. 2020)—which were the focus of this research. Quality performance is the precise determination of the ultimate load capacity of SCSPs at a construction site using a simple and rational closed-form calculation and/or pile load test. This precise determination leads to the best selection of the SCSP section properties and length suitable for cost and time conditions.

To the best of the authors' knowledge, a complete research study to determine the load capacity and the analysis of economic decisions of SCSPs in term of construction cost and time, which is the key to successful construction management, has not been undertaken previously. Therefore, this research is an innovative study of construction engineering and management of SCSP systems. The outcomes of this research will result in the development of

guidelines for the effective design of SCSPs, in terms of their load capacity calculation, construction time, and installation cost in soft clays, such as Bangkok clay.

Methodology

To investigate the effectiveness of the SCSP, the ultimate load capacity and execution cost and time of the SCSP were compared with those of soil–cement columns and SPs. The ultimate load capacity of a SP and a SCSP were measured by static load tests. The results of load tests on the SCSP were compared with the available load-predictive methods, including the cylindrical method proposed by Rao and Prasad (1993), the individual bearing method of Sakr (2009), and the soil–cement column method of Bergado et al. (1996). The undrained shear strength (c_u) of SCCs, which is one of the most important parameters in the estimation of the ultimate load capacity of SCSPs, is determined from the unconfined compressive strength of the field cored samples.

Detail of Studied Piles

Fig. 1 shows a schematic of the studied SP. The SP was made of circular hollow steel pipe with helices every 1.5 m, and the pipe was filled with concrete. The hollow steel pipe [JIS G 3444-2010 (JSA 2010)] had a diameter of 0.20 m, thickness of 4.5 mm, cross-sectional area (A_s) of 29.94 cm², and tensile strength (f_s) of 240 MPa. The helix was a hot-rolled steel plate with a diameter of 0.40 m and a thickness of 5 mm. The filled concrete had a cross-sectional area (A_c) of 337.51 cm² and compressive strength (f_c) of 18 MPa. The SPs were galvanized to prevent the rust and corrosion in accordance with ASTM A123 (ASTM 2017).

Four different types of studied piles are shown in Fig. 2. All piles were installed at a fixed depth of 17.0 m. Pile 1 [Fig. 2(a)] was a SCC with a diameter of 0.6 m (without a screw pile), and Pile 2 [Fig. 2(b)] was a SP. Piles 3 and 4 [Figs. 2(c and d)] were a partial SCSP and a full SCSP, respectively, in which a SP was installed in a SCC. A partial SCSP is a combination of a SP (17.0-m length) and a SCC with a diameter of 0.6 m and a length of 13 m from the ground surface. A full SCSP comprises a SP (17.0-m length) and a SCC with a diameter of 0.6 m and a length of 17.0 m.

The construction site was located in Nongchok District, Bangkok, Thailand. The soil profile varied from a very soft to a stiff clay (Fig. 3). The SCC (Pile 1) was installed using the wet-mixing method. Cement content of 200 kg/m³ soil and a water to cement (w/c) ratio of 1.0 were used for SCC execution. The installation (for both penetration and withdrawal) rate was 1.0 m/min, which was recommended by Horpibulsuk et al. (2011) and Srijaroen et al. (2014) for soft Bangkok clay. The SP (Pile 2) was installed to a depth of 17.0 m using the installation machine shown in Fig. 4. The execution process of the partial SCSP (Pile 3) and the full SCSP (Pile 4) was similar. The SCC with 0.6 m diameter was installed using the wet-mixing method with a deep mixing machine to the designed depths of 13.0 and 17.0 m for Pile 3 and Pile 4, respectively. The 17.0-m length of the SP then immediately was installed at the center of the SCC for both the partial and the full SCSP. The hollow steel pile then was filled with concrete.

Determination of Ultimate Bearing Capacity

Static Load Test

The static load test was performed in accordance with ASTM D1143 (ASTM 2013); the loading was applied incrementally on

Downloaded from ascelibrary.org by Suksum Hospital on 12/10/20. Copyright ASCE. For personal use only; all rights reserved.

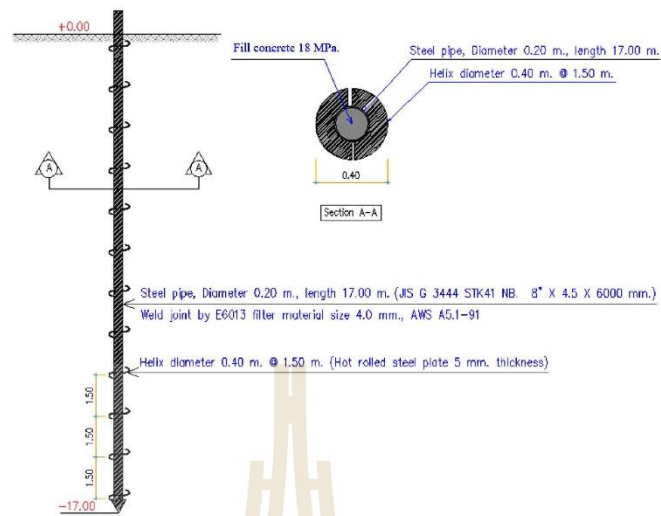


Fig. 1. Schematic of screw pile.

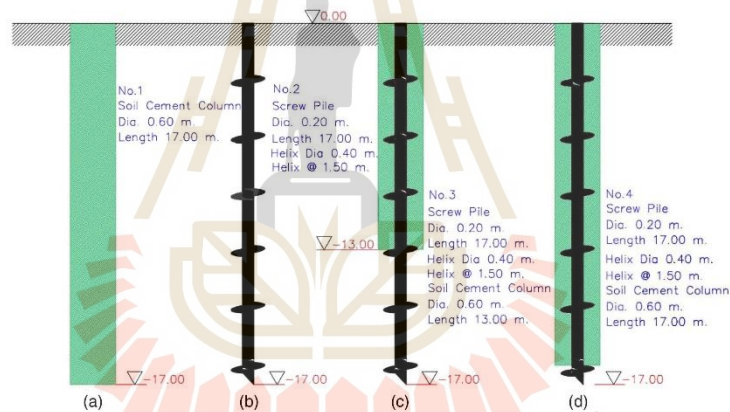


Fig. 2. Types of studied piles: (a) SCC; (b) SP; (c) partial SCSP; and (d) full SCSP.

the piles, and the corresponding settlement was measured to produce the load–settlement curves. For the partial and full SCSPs, the loading was applied on the SP via a concrete pile cap. The ultimate load capacity of the test piles was calculated using Butler and Hoy’s (1976) method, which defines the ultimate load as the load at the intersection of the tangent slope [0.127 mm/kN (0.05 in./t)] and the tangent to the initial straight portion of the curve, or to a line that is parallel to the rebound portion of the curve. The target design safe load for SPs and partial and full SCSPs (Piles 2, 3, and 4) was

400 kN for this study. For the SCC (Pile 1), the design safe load was 68 kN.

The static load testing apparatus (Fig. 5) was developed as follows:

- Reaction beams (steel girders) were laid across the test pile.
- Two reference beams (125 × 65 × 5 mm channels) were cross-connected and laid on the support, which was embedded firmly in the ground with one end fixed and the other end free.

Downloaded from ascelibrary.org by Suksum Horpibulsath on 12/10/20. Copyright ASCE. For personal use only; all rights reserved.

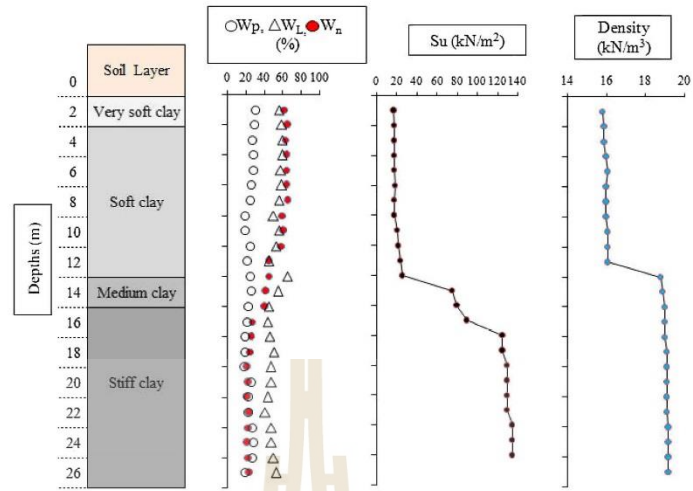


Fig. 3. Soil profile at the construction site, Nongchok District, Thailand.



Fig. 4. Installation machine for SPs and SCSPs.

Fig. 5. Static load test apparatus.

- A hydraulic jack with a capacity of 3,000 kN was used to apply the load on the pile head.
- A ball bearing was inserted between the reaction beam and the hydraulic jack to provide a noncentric load to the pile head.
- Four dial-gauge micrometers 0–50 mm with accuracy of 0.01 mm were mounted between the pile head and reference beam to monitor the pile movements.
- A leveling instrument with an accuracy of 0.01 mm was used to check the relative movements of the test pile head and reference beam. Readings were made on a fixed ruler scale at the reading

points (one point on the pile head and two points on the reference beam).

For Piles 2, 3, and 4, static load tests were carried out according to ASTM D1143 (ASTM 2013) using a standard loading procedure based on the design load at 400 kN. Two cycles of tests were performed.

Cycle 1 (Maximum 200% of Design Load)

1. The applied loads were increased gradually from 0% to 25%, 50%, 75%, 100%, 125%, 175%, and 200% of the design load.
2. The load increment was added only when the settlement was less than 0.25 mm/h or 2 h after the previous achieved load increment.
3. At each load increment, the load, settlement, and time were recorded at 1, 2, 4, 8, 15, 30, 60, 90, 120, and 240 min and then every 2 h with an accuracy of at least 0.01 mm.
4. The maximum load was kept constant for at least 24 h and then reduced to 150%, 100%, 50% and 0% of the design load. Each load was maintained until the rate of settlement was greater than 0.25 mm/h or for 2 h.
5. At the initial load, the rebound movements were recorded at 1, 2, 4, 8, 15, 30, 60 min and every 1 h thereafter until a constant settlement was reached.

Cycle 2 (Loading in Excess of Standard Test Load)

1. The applied loads were increased gradually from 0% to 25%, 50%, 75%, 100%, 125%, 175%, and 200% of the design load.
2. After each load increment was achieved, the next load increment was added after 20 min.
3. The load was added gradually by increasing 10% of the design load until pile failure.
4. For each load increment, the load, settlement, and time were recorded at 1, 2, 4, 8, 15, and 20 min with an accuracy of at least 0.01 mm.

For the SCC (Pile 1), the static load test was carried out in accordance with ASTM D1143 (ASTM 2013) using the quick load test method based on the design load at 68 kN. The test cycle was performed using the following procedure:

1. The load was added gradually in increments of 15% of the design load until pile failure.
2. For each load increment, the load, settlement, and time were recorded at 5 min with an accuracy of at least 0.01 mm.

Conventional Calculation Methods

The cylindrical shear method (Rao and Prasad 1993) and individual bearing method (Sakr 2009) were used to estimate the ultimate load capacities of the SP, whereas the soil-cement column method (Bergado et al. 1996) was used for the SCC and full SCSP, for which the undrained shear strength of the SCC at 28 days of curing was used for calculation.

Cylindrical Shear Method. The cylindrical shear method was pioneered by Mitsch and Clemence (1985) and Mooney et al. (1985) to estimate the axial capacity of SPs in sand and in clay/silt, respectively. Fig. 6 shows the cylindrical shear model assuming that the cylindrical shear failure is formed in the connection between the top and bottom helices. Nasr (2009) concluded that the ultimate load capacity is influenced by the number of helices, the pile geometry, the soil condition, and the helical spacing. The ultimate load capacity is the sum of the end-bearing resistance below the bottom helix, the shear resistance along the cylindrical shear surface, and the shaft friction above the top helix (Hawkins and Thorsten 2009; Livneh and El Naggar 2008; Sakr 2009, 2011; Tappenden et al. 2009; Zhang et al. 1998)

$$Q_{ult} = Q_{helix} + Q_{bearing} + Q_{shaft} \quad (1)$$

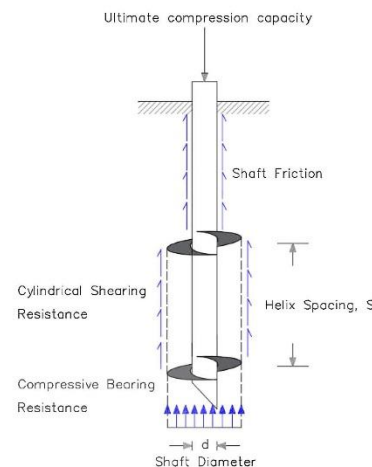


Fig. 6. Cylindrical shear model under compression load.

where Q_{ult} = ultimate load capacity; Q_{helix} = shearing resistance mobilized along the cylindrical failure surface; $Q_{bearing}$ = end bearing capacity; and Q_{shaft} = resistance developed along the steel shaft.

The ultimate load capacity of a SP in cohesive soil therefore is derived from Eq. (1) as follows (Mooney et al. 1985):

$$Q_{ult} = S_f(\pi DL_c)c_u + A_H c_u N_c + \pi d H_{eff} \alpha c_u \quad (2)$$

where S_f = spacing ratio factor; D = diameter of pile helix; L_c = distance between top and bottom helical plates; A_H = area of helix; c_u = undrained shear strength of soil; N_c = bearing capacity factor for cohesive soils; d = diameter of pile shaft; H_{eff} = effective length of pile above top helix; and α = adhesion factor.

Rao and Prasad (1993) reported that the spacing to diameter (S/D) ratio of a pile helix significantly affects the ultimate load capacity. Increasing the S/D ratio decreases the ultimate load capacity. Rao and Prasad (1993) proposed the following equations to determine the spacing ratio factor (S_f):

$$S_f = 1.00 \quad \text{for } S/D < 1.5 \quad (3)$$

$$S_f = 0.683 + 0.069(3.5 - S/D) \quad \text{for } 1.5 \leq S/D \leq 3.5 \quad (4)$$

$$S_f = 0.700 + 0.148(4.6 - S/D) \quad \text{for } 3.5 \leq S/D \leq 4.6 \quad (5)$$

Individual Bearing Method. Adams and Klym (1972) reported that the load capacity of SPs can be estimated individually if the spacing distance between each plate is large enough. Fig. 7 shows the individual bearing method. The parameters affecting the load capacity are the screw plate bearing area and the undisturbed surrounding soil. Furthermore, the equations for individual bearing method involve both the resistance from each individual helix and the shaft resistance. Therefore, the overall ultimate load capacity of the SP can be calculated by the sum of all the individual helical capacities along with the shaft resistance (Hawkins and Thorsten 2009; Livneh and El Naggar 2008; Sakr 2009, 2011; Zhang et al. 1998)

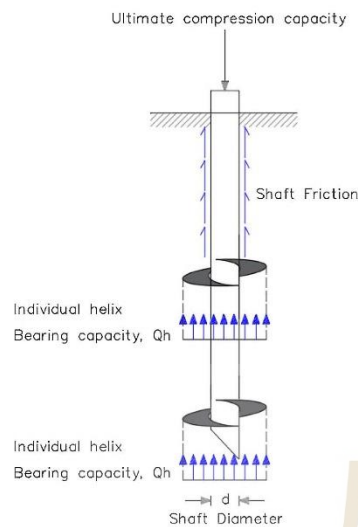


Fig. 7. Individual bearing model for screw pile under compressive load.

$$Q_{ult} = \sum A_H c_u N_c \quad (6)$$

where A_H = area of helix; c_u = undrained shear strength of soil; and N_c = bearing capacity factor for cohesive soils.

Load Capacity of SCC. The load capacity of a single SCC can be estimated based on the mode of failure by either soil failure or column failure. The ultimate load capacity of a SCC in soft clay for the soil failure mode can be calculated as (Bergado et al. 1996)

$$Q_{ult,soil} = (\pi dH + 2.25\pi d^2)c_u \quad (7)$$

where $Q_{ult,soil}$ = load capacity of single column due to soil failure; d = diameter of column; and H = column length. It is assumed that the skin resistance is equal to the undrained shear strength of the surrounding clay, and that the end resistance is $9c_u$.

Because the shear strength of the SCC is influenced insignificantly by the increase in column length (Horpibulsuk and Miura 2001; Horpibulsuk et al. 2011), the ultimate load capacity due to column failure is estimated by the following expression:

$$Q_{ult,col} = A_{col}q_{uf} \quad (8)$$

where $Q_{ult,col}$ = load capacity due to column failure; A_{col} = cross-sectional area of column; and q_{uf} = field strength of column.

Because no theoretical method is available for the soil–cement screw pile. Therefore, a theoretical method to predict the ultimate load capacity of a SCSP, which is useful for the geotechnical engineers and project managers, is presented in the following section. The development of this method was based on the field static load test. The cost analysis of a SCSP in terms of construction materials, labor, and time was studied to verify the SCSP performance using the proposed method.

Results

After 28 days of curing, core samples were collected using a coring machine from the middle of the SCC (Pile 1) at 1-m depth increments to determine the unconfined compressive strength of the SCC (q_u). The cored samples were trimmed to the required nominal dimension of 50-mm diameter and 100-mm height. Fig. 8 shows the relationship between the SCC length and q_u , indicating an average q_u of 730 kPa. Comparing the ultimate load capacity calculated from Eqs. (7) and (8), the SCC failed in the mode of pile failure with $Q_{ult,col} = 207$ kN. Fig. 9 shows the load–settlement curve of the SCC (Pile 1) obtained from the field static load test. The measured ultimate load capacity (200 kN) agreed with the predicted value (207 kN).

The ultimate load capacity of the SP (Pile 2) obtained from the static load test was 565 kN (Fig. 10). The ultimate load capacity of

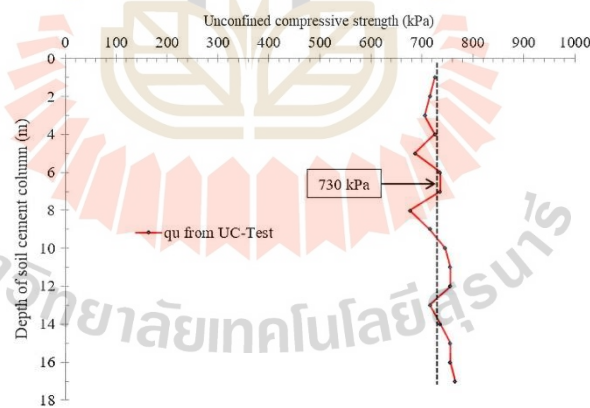


Fig. 8. Relationship between the depth of a SCC and its unconfined compressive strength.

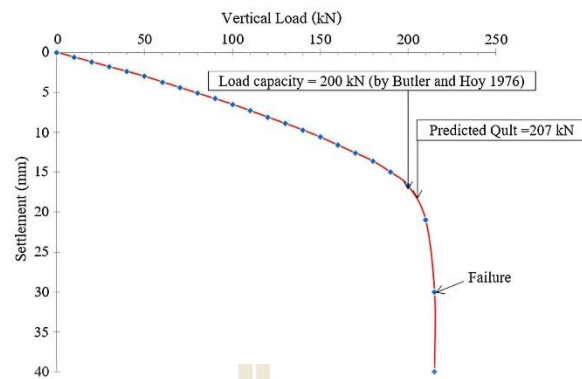


Fig. 9. Load-settlement curve of a SCC (Pile 1).

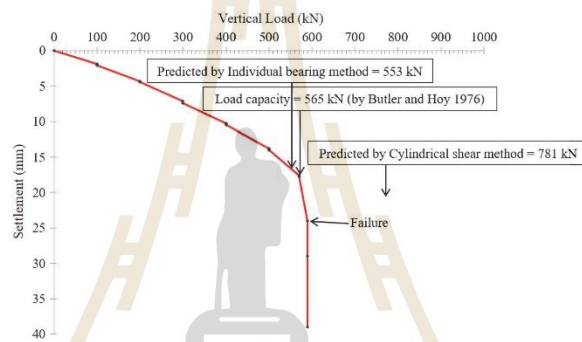


Fig. 10. Load-settlement curve of a SP (Pile 2).

the SP was notably higher than that of the SCC for the same length and soil condition. This indicates that the shear strength of the SCC controls the load capacity of the piles studied. The ultimate load capacity of the SP estimated by the cylindrical shear method and the individual bearing method was 781 and 553 kN, respectively. The ultimate load capacity of the SP (Pile 2) estimated by the individual bearing method had better agreement with the static load test than did that estimated by the cylindrical shear method.

The ultimate load capacity of a partial SCSP (Pile 3) can be obtained from the static load test results (Fig. 11). The failure occurred in Cycle 2 of the loading test (factor of safety = 2), in which the load was maintained at about 900 kN while the pile continued to move downward. The ultimate load capacity of a partial SCSP (Pile 3) was estimated to be 860 kN using Butler and Hoy's (1976) method. The ultimate load capacity of the partial SCSP (Pile 3) was higher than that of the SCC (Pile 1) and the SP (Pile 2). In other words, the ultimate load capacity of a SP can be improved significantly by a SCC. The ultimate load capacity is contributed

by the individual bearing of the SP and the load capacity of the SCC (due to either soil failure or pile failure). Assuming that the pile material was strong enough to resist pile failure, the predicted ultimate load capacity was 870 kN, which is close to the measured value. It thus is evident that the partial SCSP behave as a rigid composite pile, which failed in soil failure mode.

The measured ultimate load capacity of the full SCSP (Pile 4) was 1,030 kN (Fig. 12). The full SCC enhanced the ultimate load capacity of the SP significantly; it had the highest ultimate load capacity compared with the other studied piles. Similar to Pile 3, assuming that the pile material is strong enough against the pile failure, the ultimate load capacity can be estimated from Eq. (7), which is controlled by the shear strength of surrounding clay. The predicted ultimate load capacity was 1,089 kN, which is in good agreement with the measured value from the field test result. Assuming high interface shear strength between the SP and the SCC, the calculated ultimate load capacity of the test SCSP (Pile 4) using the individual bearing method and shear strength of the SCC [Eq. (6)], was 3,406 kN. This confirms that the failure of a SCSP

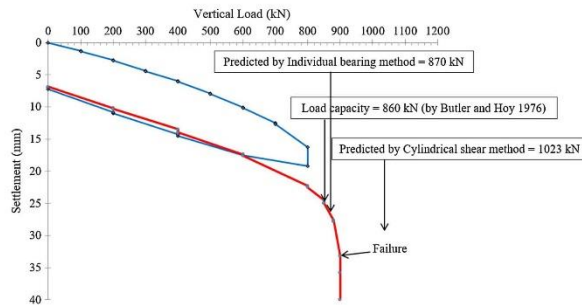


Fig. 11. Load-settlement curve of a partial SCSP (Pile 3).

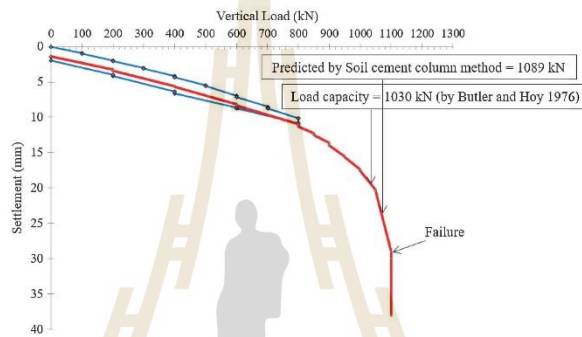


Fig. 12. Load-settlement curve of a full SCSP (Pile 4).

is governed by the strength of surrounding clay without failure at the interface; the SCC and the SP together act as a rigid composite SCSP. Table 1 summarizes the predicted and measured ultimate load capacities of all studied piles. The ultimate load capacity of all studied piles can be predicted satisfactorily by the proposed methods.

Ultimate Load, Time, and Cost Analysis

It is evident from the previous section that the ultimate load capacity of all studied piles was estimated based on the soil failure mode. Ideally, a cost-effective design exists when the ultimate load capacity is mobilized from the full capacity of both pile material and surrounding soil equally. The ultimate load capacity of a SP due to the material failure is determined by the following expression:

$$Q_{ult} = f_c(A_c) + f_s(A_s) \tag{9}$$

Thus, the ultimate load capacity of the SP (Fig. 1) due to material failure [Eq. (9)] was 1,300 kN ($f_c A_c = 595$ kN and $f_s A_s = 705$ kN), which is higher than that of all the studied piles (due to soil failure) (Table 1). This indicates uneconomical use of the SP and SCSP. Therefore, it is important, in terms of cost

effectiveness, to analyze the ultimate load capacity of a SP and a SCSP, taking the value of 1,300 kN (material failure) as a benchmark.

Screw Pile

For a particular diameter, the ultimate load capacity of a SP is dependent on the length of the SP. The diameter of the studied SP was fixed at 0.20 m, because this commonly is available on the market. Based on the soil profile in Fig. 3, the relationship between the ultimate load and length of the SP is shown in Fig. 13. Using the individual bearing method, the calculated ultimate load of SP increased linearly with increasing length, and the ultimate load capacity of 1,300 kN was reached at 27.5-m length (10 m longer than the test pile).

Soil-Cement Screw Pile

To investigate the influence of the SCC and SP on the ultimate load capacity of a SCSP, the length of the SCC was varied at 3, 5, 7, 9, 11, 13, 15, and 17 m, and the length of the SP was varied from 17 m to reach the ultimate load capacity of 1,300 kN. The diameter of the SCC was fixed at 0.6 m. Eqs. (10) and (11) are proposed to

Downloaded from ascelibrary.org by Suksum Hospital on 12/10/20. Copyright ASCE. For personal use only; all rights reserved.

Table 1. Summary of ultimate bearing capacity of all types of studied piles

Type of piles	SCC length, diameter = 0.6 m (m)	SP length, diameter = 0.2 m (m)	Ultimate bearing capacity (kN)					
			Cylindrical shear method	Individual bearing method	Soil cement column method	Cylindrical shear and soil cement column method	Individual bearing and soil cement column method	Static load test
Pile 1	17.0	—	—	—	207	—	—	200
Pile 2	—	17.0	781	553	—	—	—	565
Pile 3	13.0	17.0	4,584	3,190	—	1,023	870	860
Pile 4	17.0	17.0	5,248	3,406	1,089	—	—	1,030

estimate the ultimate load capacity of partial and full SCSPs, respectively. The ultimate load capacity of partial SCSP is the sum of the ultimate load capacity of the SCC, the shaft resistance of SP, the bearing capacity of helix, and the end bearing of SP. When calculating the ultimate load of the full SCSP, Eq. (10) becomes Eq. (11), in which the individual helical capacity is not considered

$$Q_{ult} = \pi d(\alpha_s L_{SCC} c_{u_s}) + 9nA_H c_{u_b} + 9A_{pb} c_{u_{pb}} \quad (10)$$

$$Q_{ult} = \pi d(\alpha_s L_{SCC} c_{u_s}) + 9A_{pb} c_{u_{pb}} \quad (11)$$

where d = diameter of SCC; α = adhesion factor; L_{SCC} = length of SCC; c_{u_s} = undrained shear strength of soil surrounding SCC; c_{u_b} = undrained shear strength of soil below SCC; $c_{u_{pb}}$ = undrained shear strength of soil layer at pile base; n = number of helices below SCC; A_H = area of helix (with out filled concrete); and A_{pb} = combined area of helix and shaft at pile base.

The ultimate load capacity was estimated based on the soil profile in Fig. 3. Fig. 14 shows the SP length versus ultimate load capacity of the SCSP with various SCC lengths. The ultimate load capacity of a SCSP increases with increasing SP length. At a particular length of the SP, for example, $SP = 18.80$ m, the ultimate load capacity of a partial SCSP slightly increased with increasing SCC length (from 3.0 to 15.0 m). At a particular ultimate load of a partial SCSP, the length of the SP can be reduced by increasing the length of the SCC, and a SCSP always has a higher ultimate load capacity than a SP at the same pile length. For instance, to reach the

benchmark ultimate load capacity of 1,300 kN, the SP lengths for a partial SCSP with SCC = 3.0 and 15.0 m are 26.5 and 21.5 m, respectively, whereas the length of the SP for a full SCSP is only 18.8 m. In other words, for a partial SCSP with SCC = 3.00 m and $SP = 26.50$ m (SP about 9 times SCC), the SP length must increase about 55.9% to reach the benchmark ultimate load capacity. For a partial SCSP with SCC = 15.00 m and $SP = 21.50$ m (SP about 1.5 times SCC), the SP length must increase about 26.5%, whereas for a full SCSP, the SP length must increase only about 10.6% to reach the benchmark ultimate load capacity. This indicates the economic advantage of the full SCSP application in terms of raw material cost, because the SCC material is cheaper than the SP material for the same length.

The undrained shear strength of soil mobilized by the helical anchor affects the load capacity of a SP (Ruberti 2015). Hence, the q_u of the SCC must be studied to confirm the stability of the SCSP. There are two conditions for the calculation of ultimate load capacity for a SCSP: failure at the interface of the SCC and the SP, and the failure in the surrounding soil. To confirm that no failure at the interface of the SCC and the SP occurred, Q_{ult} first was calculated using Eqs. (10) and (11) for partial and full SCSPs and with undrained shear strengths (c_u) of the surrounding clay. The calculated Q_{ult} values were used to back-calculate the required

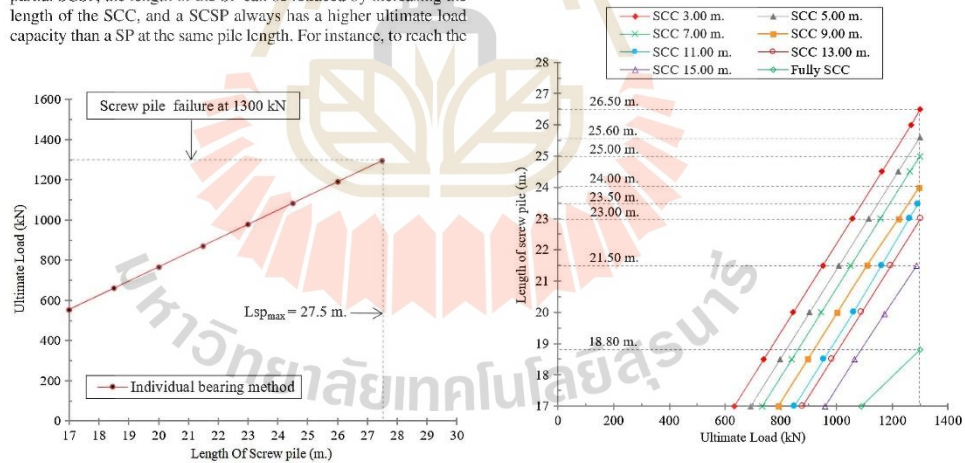


Fig. 13. Ultimate load versus length of screw pile.

Fig. 14. Length of screw pile versus ultimate load of SCSP at various lengths of SCC.

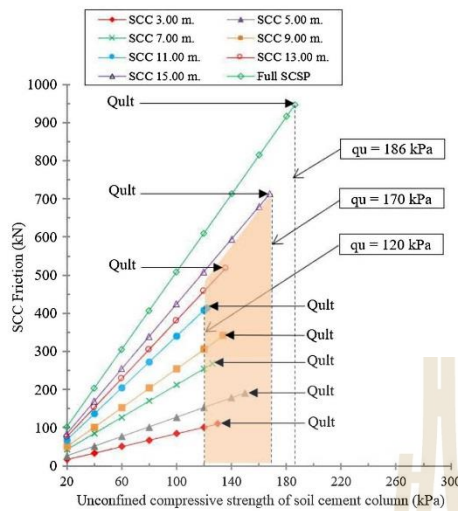


Fig. 15. SCC friction versus undrained shear strength of SCC.

minimum q_u value, which causes the interface failures between the SCC and the SP by taking $c_{ul} = q_u/2$. A relationship between the SCC friction and q_u is shown in Fig. 15. The SCC friction is defined as the maximum force that results in the interface failure between a SCC and a SP. The required minimum q_u for various SCC frictions was calculated to be in a range of 120–170 kPa for the partial SCSP, whereas it was 186 kPa for the full SCSP. However, the typical q_u value of about 600 kPa at 28 days of curing was used for the SCC in soft Bangkok clay, which was significantly higher than the required minimum q_u values. This confirms the excellent bonding between the SP and the SCC (no interface failure between the SCC and the SP). In other words, it is possible to utilize field $q_u < 600$ kPa for economic purposes.

The cost of SCSP execution also was studied to illustrate the economic advantage of its application in soft Bangkok clay. The execution costs included those of raw materials for the SCC and SP, as well as labor costs based on the local construction rates in Thailand for 2018. The calculated cost versus ultimate load relationships of the SP, partial SCSP, and full SCSP are plotted in Fig. 16, and the corresponding execution time and unit cost are listed Table 2. The execution cost including material and labor expenses was USD 37.5/m length for the SP and USD 8.85/m length for the SCC. It is evident that the execution cost of the SP is 4.2 times higher than that of the SCC for the same pile length. For a particular ultimate load, the execution cost of the SP is the highest, whereas the execution cost of the SCSP is the lowest (Fig. 16). The longer SCC length in partial and full SCSPs can reduce the SP length for the same target ultimate load capacity. In other words, the execution cost of partial and full SCSPs is governed by the SCC length; a longer SCC length results in a cheaper execution cost. For example, at the benchmark ultimate load of 1,300 kN, the execution cost was only USD 871 for the full SCSP with 18.8-m pile length, whereas it was USD 1,030 for the SP with 26.50-m pile length (Figs. 14 and 16). Overall, the execution cost of a full SCSP

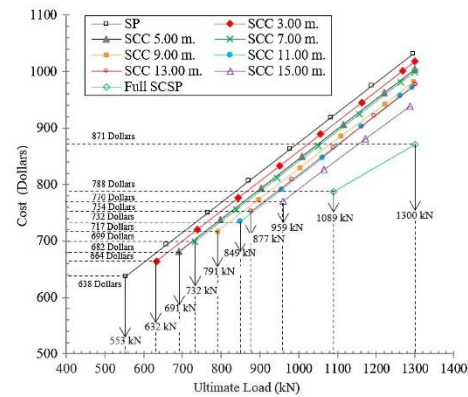


Fig. 16. Cost versus ultimate load of SP and SCSP.

is approximately 15% lower than that of a SP. This 15% reduction of the execution cost is significant for large-scale projects. In addition, the shorter length of the SP in a full SCSP compared with a SP alone is another advantage in confined construction areas.

Compared with the dry-process bored pile commonly used in Thailand, the execution cost of both the full SCSP and the bored pile essentially is similar for the same target ultimate load (Table 2). The required pile length of a bored pile is slightly longer than that of a full SCSP because the friction between the pile and the surrounding soil is lower due to the soil removal for installation of reinforcement and filling of concrete.

The execution time for a SP is the lowest, 0.5 h/pile, whereas the execution time for a full SCSP is the highest, 1.3 h/pile (the execution time for a SCC is approximately 0.8 h/pile) at the same pile length of 17 m (Table 2). In other words, the execution time is 0.03, 0.05, and 0.08 h/m length for a SP, SCC, and full SCSP; the execution time of a full SCSP is approximately 2.5 times longer than that of a SP. It is evident that the execution time of a SCC governs the execution time of partial and full SCSPs. The execution time of a SCSP increases with the increase in the SCC length. In addition, the execution time of a dry-process bored pile is 2.5 times longer than that of a full SCSP.

The unit cost of a SP, partial and full SCSPs, and a dry-process bored pile at various pile lengths also is presented in Table 2. The unit cost of a SP is the highest, USD 2.88/kN, whereas the unit cost of a full SCSP and a bored pile is approximately the same and is the lowest, approximately USD 1.62–1.80/kN. As a result, the application of a full SCSP and a bored pile is more economical than both a partial SCSP and a SP under the same ultimate load design. However, a partial SCSP and a SP have more advantages in term of construction time, and are suitable for a time-constrained project. At the same target ultimate load capacity, the full SCSP has higher efficiency and productivity than the traditional dry-process bored pile.

A stepwise procedure for designing the ultimate bearing capacity of a SCSP at optimal time and cost based on the critical analysis of the test results is suggested as follows:

1. Conduct the in situ soil investigation at the construction site and laboratory test the soil samples to obtain soil profiles and undrained shear strength (c_u).

Table 2. Cost and time analysis of SP and SCSP execution

Pile type	Pattern	Soil cement column diameter (m)	Soil cement column length (m)	Screw pile length, diameter = 20 cm (m)	Ultimate capacity (kN)	Allowable capacity (kN) ^a	Time of installation (h)	Total cost (USD)	Unit cost (USD/kN)
SP	Pattern 1	—	—	17.00	553	221	0.50	637.50	2.88
Partial SCSP	Pattern 2	0.60	3.00	17.00	632	253	0.60	664.05	2.62
	Pattern 3	0.60	5.00	17.00	691	273	0.70	681.75	2.50
	Pattern 4	0.60	7.00	17.00	732	293	0.80	699.45	2.39
	Pattern 5	0.60	9.00	17.00	791	317	0.90	717.15	2.26
	Pattern 6	0.60	11.00	17.00	851	340	1.00	734.85	2.16
	Pattern 7	0.60	13.00	17.00	877	351	1.10	752.55	2.14
	Pattern 8	0.60	15.00	17.00	959	384	1.20	770.25	2.00
	Pattern 9	0.60	17.00	17.00	1,089	436	1.30	787.95	1.80
Full SCSP	Pattern 10	0.60	18.80	18.80	1,300	520	1.40	871.38	1.68
	Pattern 11	—	—	—	1,300	520	3.50	843.75	1.62
Bored pile (Diameter 0.60 × 21.00)									

Note: Execution cost of SCC with 0.6-m diameter = USD 8.85/m (material cost = USD 3.40/m, and labor cost = USD 5.45/m); execution cost of SP = USD 37.5/m (material cost = USD 18/m, and labor cost = USD 19.5/m); execution cost of dry-process bored pile = USD 40.18/m (material cost = USD 24.60/m, and labor cost = 1 USD 5.58/m); and USD 1 = 32 baht.

^aFactor of safety = 2.50.

- Determine the relationship between ultimate load capacity of the SCSP versus the SCC and the SP lengths (Fig. 14). From the target ultimate load, determine the SP and the SCC lengths from the developed relationship.
- Determine the required q_{u_s} of the SCC to have sufficient SCC friction for each set of calculated SPs and SCCs (Fig. 15).
- Plot the relationship between execution cost and ultimate load capacity (Fig. 16), and determine the corresponding execution time.
- Select the SCC and SP lengths to meet the time and cost criteria of the construction project.

Conclusions

This research paper presented the ultimate load, time, and cost analysis and suggested effective design method for soft Bangkok clay. The cost and time of executing SCSPs were compared with those of traditional dry-process bored piles to illustrate the advantages of SCSPs. The ultimate load capacity of the piles studied was examined using field static load tests and was compared with the conventional design methods. The ultimate load capacity of SPs was enhanced significantly by the SCC. The full SCSP provided the highest ultimate load capacity compared with the SCC, SP, and partial SCSP at the same pile length. The conventional individual bearing method can be used to estimate the ultimate load capacity of SPs. The load capacity predictive equations for both partial and full SCSPs due to soil failure were proposed and validated based on the field static pile load test results. The equations are applicable for soft Bangkok clay and were used successfully for some construction projects in Thailand.

In Thailand, the application of the full SCSP can save installation cost compared with SPs and partial SCSPs at the same required ultimate load. The execution (raw material and labor) cost of SPs is 4.2 times higher than that of SCCs for the same pile length. In other words, the execution cost of partial and full SCSPs is governed by the SCC length; longer SCC length results in cheaper execution cost. The execution time was 0.03, 0.05, and 0.08 h/m length for SPs, SCCs, and full SCSPs; the execution time of the full SCSP was approximately 2.5 times longer than that of the SP. The execution time of SCSPs increased with the increase in the SCC length. The unit cost of SPs was the highest, whereas the unit cost of SCSPs was the lowest for the same target ultimate load. As a result,

the application of the full SCSP has more economical benefits than both partial SCSPs and SPs. However, the partial SCSP and SP have more advantages in terms of construction time, and are suitable for a time-constrained project. At the same target ultimate load capacity, the SCSP had higher efficiency and productivity than the traditional dry-process bored pile.

The construction process and construction cost are strongly dependent on the current cost of construction materials, which varies from country to country. The outcome of this research will lead to the development of guidelines and a code of practice of SCSPs in soft Bangkok clay and other similar soil conditions. It also can be used as fundamental knowledge for the use of SCSP in other countries which have different soil profiles and construction costs. This practice research highlights the critical elements for the design and construction management (cost and time), installation process, and load test results of SCSPs, which are useful for construction industry particularly pertaining to the scheduling and cost performance of SCSPs in construction projects. It provides recommendations

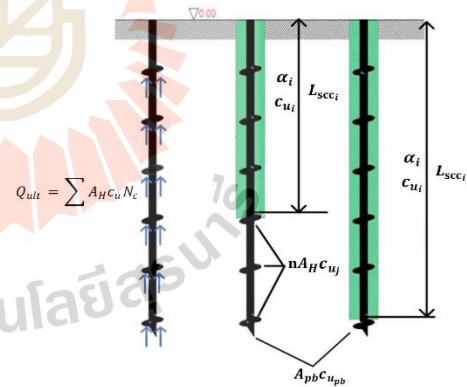


Fig. 17. Definitions of parameters in Eqs. (6) and (10)–(12).

Downloaded from ascelibrary.org by Suksum Horpibulsath on 12/10/20. Copyright ASCE. For personal use only; all rights reserved.

for good practice in Thailand, which can be used as a reference for project engineers, developers, contractors, local authorities, and other relevant end-users. Outcomes of this research also are applicable to other developed and developing countries.

$$Q_{ult} = \pi d(\alpha L_{scc} c_{u_i}) + 9A_{ph} c_{u_{pb}} \quad (14)$$

$$Q_{ult} = 0.45 S_u A_s + 9w A_b S_u \quad (15)$$

Appendix. Ultimate Load Capacity Calculation

The ultimate load capacities of the SP [Eq. (12)], partial and full SCSPs [Eqs. (13) and (14)], and bored pile [Eq. (15)] in Table 2 are estimated as follows:

$$Q_{ult} = \sum A_H c_u N_c \quad (12)$$

$$Q_{ult} = \pi d(\alpha L_{scc} c_{u_i}) + 9n A_H c_{u_i} + 9A_{pb} c_{u_{pb}} \quad (13)$$

where $w = 0.80$, based on Skempton (1966); d = diameter of SCC; α = adhesion factor; L_{scc} = length of SCC; c_{u_i} = undrained shear strength of soil surrounding SCC; c_{u_j} = undrained shear strength of soil below SCC; $c_{u_{pb}}$ = undrained shear strength of soil layer at pile base; n = number of helices below SCC; A_H = area of helix (with or without filled concrete); A_{pb} = combined area of helix and shaft at pile base; and N_c = bearing capacity factor for cohesive soils. The definition of each parameter is given in Fig. 17.

SP [Eq. (6)]

$$\text{For } L = 17 \text{ m, } Q_{ult} = 9(8)\pi(0.42 - 0.22)/4(20) + 9(1)\pi(0.42 - 0.22)/4(75) + 9(2)\pi(0.42 - 0.22)/4(125) + 9\pi(0.42)/4(125) = 553 \text{ kN}$$

Partial SCSP [Eq. (10)]

$$\text{For SCC} = 3 \text{ m, } Q_{ult} = \pi(0.60)(1)(3)(20) + 9(6)\pi(0.42 - 0.22)/4(20) + 9(1)\pi(0.42 - 0.22)/4(75) + 9(2)\pi(0.42 - 0.22)/4(125) + 9\pi(0.42)/4(125) = 632 \text{ kN}$$

$$\text{For SCC} = 5 \text{ m, } Q_{ult} = \pi(0.60)(1)(5)(20) + 9(5)\pi(0.42 - 0.22)/4(20) + 9(1)\pi(0.42 - 0.22)/4(75) + 9(2)\pi(0.42 - 0.22)/4(125) + 9\pi(0.42)/4(125) = 691 \text{ kN}$$

$$\text{For SCC} = 7 \text{ m, } Q_{ult} = \pi(0.60)(1)(7)(20) + 9(3)\pi(0.42 - 0.22)/4(20) + 9(1)\pi(0.42 - 0.22)/4(75) + 9(2)\pi(0.42 - 0.22)/4(125) + 9\pi(0.42)/4(125) = 732 \text{ kN}$$

$$\text{For SCC} = 9 \text{ m, } Q_{ult} = \pi(0.60)(1)(9)(20) + 9(2)\pi(0.42 - 0.22)/4(20) + 9(1)\pi(0.42 - 0.22)/4(75) + 9(2)\pi(0.42 - 0.22)/4(125) + 9\pi(0.42)/4(125) = 732 \text{ kN}$$

$$\text{For SCC} = 11 \text{ m, } Q_{ult} = \pi(0.60)(1)(11)(20) + 9(1)\pi(0.42 - 0.22)/4(20) + 9(1)\pi(0.42 - 0.22)/4(75) + 9(2)\pi(0.42 - 0.22)/4(125) + 9\pi(0.42)/4(125) = 851 \text{ kN}$$

$$\text{For SCC} = 13 \text{ m, } Q_{ult} = \pi(0.60)(1)(12)(20) + \pi(0.60)(0.50)(1)(75) + 9(2)\pi(0.42 - 0.22)/4(125) + 9\pi(0.42)/4(125) = 877 \text{ kN}$$

$$\text{For SCC} = 15 \text{ m, } Q_{ult} = \pi(0.60)(1)(12)(20) + \pi(0.60)(0.50)(2)(75) + \pi(0.60)(0.50)(1)(125) + 9(1)\pi(0.42 - 0.22)/4(125) + 9\pi(0.42)/4(125) = 959 \text{ kN}$$

Full SCSP [Eq. (11)]

$$\text{For SCC} = 17 \text{ m, } Q_{ult} = \pi(0.60)(1)(12)(20) + \pi(0.60)(0.50)(2)(75) + \pi(0.60)(0.50)(3)(125) + 9\pi(0.42)/4(125) = 1,089 \text{ kN}$$

$$\text{For SCC} = 18.8 \text{ m, } Q_{ult} = \pi(0.60)(1)(12)(20) + \pi(0.60)(0.50)(2)(75) + \pi(0.60)(0.50)(4.8)(125) + 9\pi(0.42)/4(125) = 1,300 \text{ kN}$$

Bored pile (diameter = 0.60 m and length = 21.0 m) [Eq. (12)]

$$Q_{ult} = 0.45\pi(0.60)(20 \times 12 + 75 \times 2 + 7 \times 125) + 9(0.80)\pi(0.62)/4(125) = 1,327 \text{ kN} \approx 1,300 \text{ kN}$$

Data Availability Statement

Data generated or analyzed during the study are available from the corresponding author by request. Information about the *Journal's* data-sharing policy can be found here: [http://ascelibrary.org/doi/10.1061/\(ASCE\)CO.1943-7862.0001263](http://ascelibrary.org/doi/10.1061/(ASCE)CO.1943-7862.0001263).

Acknowledgments

The installation and static load tests of the studied piles were conducted by Thai Pile Rig Co. The first author acknowledges the financial support from Suranaree University of Technology for his PhD studies. The authors acknowledge the support of the National Science and Technology Development Agency under the Chair Professor program (P-19-52303).

References

- Adams, J., and T. Klym. 1972. "A study of anchorages for transmission tower foundations." *Can. Geotech. J.* 9 (1): 89–104. <https://doi.org/10.1139/t72-007>.
- ASTM. 2013. *Standard test methods for deep foundations under static axial compressive load*. ASTM D1143. West Conshohocken, PA: ASTM.
- ASTM. 2017. *Standard specification for zinc (hot-dip galvanized) coatings on iron and steel products*. ASTM A123. West Conshohocken, PA: ASTM.
- Bergado, D., L. Anderson, N. Miura, and A. Balasubramaniam. 1996. *Soft ground improvement in lowland and other environments*. Reston, VA: ASCE.
- Butler, H., and H. E. Hoy. 1976. *The Texas quick-load method for foundation load testing, user's manual*. NASA STI/recon Technical Rep. No. 77. Washington, DC: National Aeronautics and Space Administration.
- Hawkins, K., and R. Thorsten. 2009. "Load test results—Large diameter helical pipe piles." In *In Proc., Int. Foundation Congress and Equipment Expo 2009*, 488–495. Reston, VA: ASCE. [https://doi.org/10.1061/41021\(335\)61](https://doi.org/10.1061/41021(335)61).
- Horpibulsuk, S., R. Rachan, A. Suddepong, and A. Chinkulkijniwat. 2011. "Strength development in cement admixed Bangkok clay: Laboratory and field investigations." *Soils Found.* 51 (2): 239–251. <https://doi.org/10.3208/sandf.51.239>.
- Horpibulsuk, S., and N. Miura. 2001. "A new approach for studying behavior of cement stabilized clays." In *Proc., Int. Conf. on Soil Mechanics and Geotechnical Engineering*. Rotterdam, Netherlands: A.A. Balkema.
- Horpibulsuk, S., S. Shibuya, K. Fuenkajom, and W. Katkan. 2007. "Assessment of engineering properties of Bangkok clay." *Can. Geotech. J.* 44 (2): 173–187. <https://doi.org/10.1139/t06-101>.
- JSA (Japanese Standards Association). 2010. *Standard specification for carbon steel tubes for general structure*. JIS G 3444. Tokyo: JSA.
- Kim, J. J., J. A. Miller, and S. Kim. 2020. "Cost impacts of change orders due to unforeseen existing conditions in building renovation projects." *J. Constr. Eng. Manage.* 146 (8): 04020094. [https://doi.org/10.1061/\(ASCE\)CO.1943-7862.0001888](https://doi.org/10.1061/(ASCE)CO.1943-7862.0001888).
- Livneh, B., and M. H. El Naggar. 2008. "Axial testing and numerical modeling of square shaft helical piles under compressive and tensile loading." *Can. Geotech. J.* 45 (8): 1142–1155. <https://doi.org/10.1139/T08-044>.
- McKim, R., T. Hegazy, and M. Attalla. 2000. "Project performance control in reconstruction projects." *J. Constr. Eng. Manage.* 126 (2): 137–141. [https://doi.org/10.1061/\(ASCE\)0733-9364\(2000\)126:2\(137\)](https://doi.org/10.1061/(ASCE)0733-9364(2000)126:2(137)).
- Mitsch, M. P., and S. P. Clemence. 1985. *Uplift capacity of helix anchors in sand*, 26–47. New York: ASCE.
- Monkaew, S., and T. Nawalerspunya. 2013. *Productivity of bored pile dry process*. [In Thai.] Bangkok, Thailand: Faculty of Engineering, Rajamangla Univ. of Technology Phra Nakhon.
- Moon, H., K. Kim, H.-S. Lee, M. Park, T. P. Williams, B. Son, and J.-Y. Chun. 2020. "Cost performance comparison of design-build and design-bid-build for building and civil projects using mediation analysis." *J. Constr. Eng. Manage.* 146 (9): 04020113. [https://doi.org/10.1061/\(ASCE\)CO.1943-7862.0001873](https://doi.org/10.1061/(ASCE)CO.1943-7862.0001873).
- Mooney, J. S., S. Adamczak, and S. P. Clemence. 1985. *Uplift capacity of helical anchors in clay and silt*, 48–72. New York: ASCE.
- Nasr, M. 2009. "Performance-based design for helical piles." In *Proc., Int. Foundation Congress and Equipment Expo 2009*, 496–503. Reston, VA: ASCE. [https://doi.org/10.1061/41021\(335\)62](https://doi.org/10.1061/41021(335)62).
- Poonlappanish, C., and P. Buasri. 2017. "Capacity of dry-process bored piles in Bangkok." In *Proc., 22nd National Convention on Civil Engineering*. Pak Chong, Nakhon Ratchasima, Thailand: Khao Yai Convention Center.
- Poulos, H. G., and E. H. Davis. 1980. *Pile foundation analysis and design*. New York: Wiley.
- Rao, S. N., and Y. Prasad. 1993. "Estimation of uplift capacity of helical anchors in clays." *J. Geotech. Eng.* 119 (2): 352–357. [https://doi.org/10.1061/\(ASCE\)0733-9410\(1993\)119:2\(352\)](https://doi.org/10.1061/(ASCE)0733-9410(1993)119:2(352)).
- Ruberli, M. 2015. *Investigation of installation torque and torque-to-capacity relationship of screw-piles and helical anchors*. Springfield, MA: Univ. of Massachusetts. <https://doi.org/10.7275/xqch-7b54>.
- Sakr, M. 2009. "Performance of helical piles in oil sand." *Can. Geotech. J.* 46 (9): 1046–1061. <https://doi.org/10.1139/T09-044>.
- Sakr, M. 2011. "Installation and performance characteristics of high capacity helical piles in cohesionless soils." *J. Deep Found. Inst.* 5 (1): 39–57. <https://doi.org/10.1179/dfi.2011.004>.
- Shen, S. L., Z. F. Wang, and W. C. Cheng. 2017. "Estimation of lateral displacement induced by jet grouting in clayey soils." *Geotechnique* 67 (7): 621–630.
- Shen, S. L., Z. F. Wang, S. Horpibulsuk, and Y. H. Kim. 2013a. "Jet-grouting with a newly developed technology: The twin-jet method." *Eng. Geol.* 152 (1): 87–95. <https://doi.org/10.1016/j.enggeo.2012>.
- Shen, S. L., Z. F. Wang, W. J. Sun, L. B. Wang, and S. Horpibulsuk. 2013b. "A field trial of horizontal jet grouting with composite-pipe method in soft deposit of Shanghai." *Tunnelling Underground Space Technol.* 35: 142–151.
- Skempton, A. 1966. *Summing up large bored piles*, 155–157. London: Thomas Telford.
- Srijaroen, C., R. Rachan, and S. Horpibulsuk. 2014. "Strength development in soil cement column and soil fly ash-cement column in soft bangkok-clay deposit." *KMUTT Res. Dev. J.* 37 (2): 151–164.
- Tappenden, K., D. Segó, and P. Robertson. 2009. "Load transfer behavior of full-scale instrumented screw anchors." In *Proc., Int. Foundation Congress and Equipment Expo 2009*, 472–479. Reston, VA: ASCE. [https://doi.org/10.1061/41021\(335\)59](https://doi.org/10.1061/41021(335)59).
- Wang, Z. F., J. S. Shen, and W. C. Cheng. 2018. "Simple method to predict ground displacements caused by installing horizontal jet-grouting columns." *Math. Prob. Eng.* 2018: 1–11. <https://doi.org/10.1155/2018/1897394>.
- Wang, Z. F., S. L. Shen, and G. Modoni. 2019. "Enhancing discharge of spoil to mitigate disturbance induced by horizontal jet grouting in clayey soil: Theoretical model and application." *Comput. Geotech.* 111: 222–228.
- Zhang, D., R. Chalatumyk, P. Robertson, D. Segó, and G. Cyre. 1998. "Screw anchor test program. Part I: Instrumentation, site characterization and installation." In *Proc., 51st Canadian Geotechnical Conf.* Ottawa: Canadian Geotechnical Society.

BIOGRAPHY

Name : Chayanon Srijaroen

Date of Birth : 22 August 1977

Education :

- Bachelor degree of Civil Engineering, Khonkaen University (KKU), Thailand, (1999).
- Master degree of Civil Engineering in Geotechnical Engineering, Mahanakorn University of Technology (MUT), Thailand, (2013).

Work Experience :

- Civil Engineer, Thai Piling Rig Co. Ltd., (2000-2021)
- Senior Civil Engineer, Thai Piling Rig Co. Ltd., Prachautit Rd., Samseannok, Huay Kwang, Bangkok 10310, Thailand.

Email: sr_chayanon@yahoo.com, sr.chayanon@gmail.com

มหาวิทยาลัยเทคโนโลยีสุรนารี